



MASTER'S THESIS

PRECISION CALCULATION OF THE EFFECTIVE
NUMBER OF NEUTRINO SPECIES

Adrian Finke

University of Münster

Institute of Theoretical Physics

First Examiner: Prof. Dr. Michael Klasen

Second Examiner: Prof. Dr. Yvonne Wong

Münster, 20. July 2025

Contents

1	Introduction	1
2	Effective number of neutrino species	3
2.1	Entropy conservation	4
2.2	Generalized neutrino Boltzmann equations and continuity equation	5
2.3	A brief thermal history of the universe	8
3	Finite temperature field theory	10
3.1	Scalar fields	11
3.2	Equilibrium density matrix as time evolution operator	12
3.3	Generating functional	13
3.4	Free scalar propagators	15
3.5	Remaining propagators and Feynman rules	18
3.6	Dyson-Schwinger and Kadanoff-Baym equations	18
4	Neutrino interaction rates – Leading Order	22
4.1	LO neutrino self-energy	23
4.2	The integral	24
5	Neutrino Interaction Rates – Next to leading order	26
5.1	Frog	27
5.2	Cancellation of infrared divergences	29
5.2.1	Phase-space slicing & soft photon approximation	29
5.2.2	Vacuum infrared divergences	30
5.2.3	Thermal infrared divergences	34
5.3	Baseball	36
5.3.1	Real emission diagrams	38
5.3.2	Vacuum virtual correction	42
5.3.3	Thermal virtual correction - Photon cut	42
5.3.4	Thermal virtual correction - Electron cut	43

5.3.5	Thermal virtual correction - Two cuts	45
5.4	Donut and Ladybug overview	45
5.5	Thermal integrals for the photon cut	47
5.5.1	Scalar integral L	47
5.5.2	Vector integral L^μ	50
5.5.3	Tensor integral $L^{\mu\nu}$	50
5.6	Connection to the Boltzmann formalism	51
6	Numerical evaluation	55
6.1	Energy cut off independence	55
6.2	Numerical results	57
7	Conclusion and outlook	60
A	Loop calculations	61
A.1	Dimensional regularization	61
A.2	Passarino-Veltman reduction	63
A.3	Counter term	64
A.4	The integral I_{ab}	65
A.5	Formfactors	66
A.5.1	Vector current	67
A.5.2	Axial current	70
B	Further Details	71
B.1	Use of AI tools	71
B.2	Useful integrals	72
B.3	KMS relation	72
B.4	Lagrangian in Fermi theory	73
B.5	Finite temperature self-energy of the photon and resummed photon propagator	74
B.6	Connection of rates with different CPT indices	77
	References	79

Chapter 1

Introduction

In recent years, interest in a precise calculation of the effective number of neutrinos (N_{eff}) has grown. Defined by the energy density of free-streaming, ultra relativistic particles relative to the energy density in photons (approximately 3 in the Standard Model for the three neutrinos), N_{eff} provides an important parameter for hot Big Bang cosmology, as it determines the expansion rate at temperatures below 1 MeV (after neutrino decoupling). As a result, N_{eff} influences many areas, such as the primordial light element abundances [1, 2, 3], the correlation statistics of the CMB [4, 5], and the large-scale matter distribution [6]. This makes experimental determination possible and increases interest in a theoretical calculation. Furthermore a lot of beyond the standard model scenarios include N_{eff} changing effects. Examples are light sterile neutrinos [7, 8] or axions [9], but there are also many more.

The state of the art calculation for N_{eff} solves the fully momentum-dependent transport equations using `FortEPiano` [10], the calculation takes into account finite temperature corrections to the EoS, neutrino oscillations and also a first estimate of NLO contributions in the weak interaction rate [11, 12, 13, 14] (see table 1). And yields a result of $N_{\text{eff}}^{\text{th}} = 3.0440 \pm 0.002$, which is in perfect agreement with the measured value of $N_{\text{eff}}^{\text{exp}} = 2.99 \pm 0.34$ [15] nevertheless, a discussion about the third decimal place remains [16].

Table 1.1: Standard-model corrections to $N_{\text{eff}}^{\text{SM}}$ and their leading-digit contributions [13, 17].

Standard-model corrections to $N_{\text{eff}}^{\text{SM}}$	Leading-digit contribution
m_e/T_d correction	+0.04
$\mathcal{O}(e^2)$ FTQED correction to the QED EoS	+0.01
Non-instantaneous decoupling + spectral distortion	-0.006
$\mathcal{O}(e^3)$ FTQED correction to the QED EoS	-0.001
Flavor oscillations	+0.0005
FTQED corrections to the weak rates	$\lesssim 10^{-4}$

Numerous calculations have already been performed on N_{eff} . In [18, 19] the energy transfer into the neutrinos was calculated up to NLO in the imaginary time path formalism with the approximation that $m_e = 0$. Also, the deviation that arises because of the finite electron mass on LO was quantified. In [16] the NLO contributions in the real time formalism were calculated for $e^-e^+ \rightarrow \nu_\alpha\bar{\nu}_\alpha$, but in fact they took the interaction rates originally calculated for energy loss in stellar plasma [20]. Where scattering contributions and the NLO diagram that was calculated in [13] were neglected. The diagram that was neglected is enhanced by a t-channel and should therefore at first glance yield the biggest contribution. In general, there is a need for clarification of the influence of the NLO contributions with $m_e \neq 0$ and all diagrams included. This is what this work aims for, at least to contribute to the full NLO calculation.

The structure of this thesis is organized as follows. In chapter 2 we will introduce N_{eff} and see how ΔN_{eff} effects can be calculated via entropy conservation and by solving the generalized neutrino Boltzmann equations and the continuity equation. After that in chapter 3 we will introduce thermal field theory. As the neutrino decoupling happens at rather high temperatures compared to today's time, it is important to also include thermal effects to the rate, which is done by using thermal field theory. In addition, it is possible to deduce a first-principle kinetic equation from thermal field theory, which can be used instead of using the Boltzmann formalism, since the Boltzmann formalism has multiple problems [21]. With the foundations, we will calculate the LO rate in chapter 4. After that we will focus on the NLO (chapter 5). On NLO, there are multiple infrared divergences that appear. In addition to the well-known infrared divergences from vacuum theory, there are also thermal infrared divergences appearing, with which we will deal in section 5.2. After we canceled all divergences we will go over to the calculation of the neutrino interaction rates. The results we get for the neutrino interaction rates will then finally be evaluated numerically in chapter 6.

Chapter 2

Effective number of neutrino species

The energy density of radiation in the SM consists of the energy density of photons ρ_γ and neutrinos ρ_ν . If one also looks at BSM physics that contribute to the radiation energy density, we could also include an energy density for that ρ_{BSM} . This in general would stand for light-sterile neutrinos, axions, gravitational waves, etc. With that we can write the radiation energy density as $\rho_R = \rho_\gamma + \rho_\nu + \rho_{\text{BSM}}$. Under the strongest approximations, namely:

- **Ideal gas approximation:** the QED plasma and the neutrino sector are described by an ideal gas
- **Instantaneous decoupling:** generally decoupling is a process, which has to be described by kinetic equations. In this approximation the system changes, at temperature T_d from a state of thermal contact in an instant into a state of no thermal contact
- **Ultra-relativistic approximation:** the decoupling of the neutrinos occurs at temperature, where all particles are still relativistic, therefore $\frac{T_d}{m_e} \rightarrow \infty$

and also the assumption that there is no BSM physics that would contribute to the radiation, we get that (see [22])

$$\rho_R = \rho_\gamma \left[1 + \frac{7}{8} \left(\frac{4}{11} \right)^{\frac{4}{3}} \cdot 3 \right], \quad (2.1)$$

where the factors of $\frac{7}{8}$ come in due to different relativistic degrees of freedom of fermions and bosons and the factor of $\left(\frac{4}{11}\right)^{\frac{4}{3}}$ accounts for the cooling of photons relative to neutrinos after electron-positron annihilation. Now, if we have deviation from that, for example due to loosening the approximations or postulating new particles, we could exchange the 3 by the parameter N_{eff} to account for these deviations. This parameter will then, of course, differ slightly from 3. For this work we will drop ρ_{BSM} , as this thesis focuses only on the SM, but here you can see how also BSM physics can in principle on N_{eff} . We therefore can write the following as the definition

of the effective number of neutrino species:

$$\frac{\rho_\nu}{\rho_\gamma} = \frac{7}{8} \left(\frac{4}{11} \right)^{\frac{4}{3}} \cdot N_{\text{eff}} . \quad (2.2)$$

2.1 Entropy conservation

The complete calculation for a change in N_{eff} would mean evolving the distribution function for neutrinos f_ν . This is a calculation that takes a lot of computation time, but in general it would eliminate all approximations. As you can see in table 1 the biggest contribution of the approximations comes from not setting $T_d/m_e \rightarrow \infty$. It is believed that the universe is expanding adiabatically; therefore, entropy is conserved in a comoving volume. We assume that our QED plasma and the neutrino sector is to a good approximation an ideal gas, and we also think of the decoupling as an instantaneous process. Therefore, we only loosen the ultra-relativistic approximation. Because of entropy conservation, we have that:

$$s_{e+\gamma}(a_1)a_1^3 = s_{e+\gamma}(a_2)a_2^3 , \quad (2.3)$$

$$s_\nu(a_1)a_1^3 = s_\nu(a_2)a_2^3 , \quad (2.4)$$

where $s_{e+\gamma}$ is the entropy density of the QED plasma and $s_\nu(a_1)$ is the entropy of the neutrinos. We take a_1 to be at the epoch of neutrino decoupling, then the temperature of the neutrinos is just their decoupling temperature $T_\nu(a_1) = T_d = T(a_1)$ with T being the photon temperature. Then we choose a_2 to be a long time after neutrino decoupling. The entropy density of a relativistic particle is given by [22]

$$s_R = g_s \frac{2\pi^2}{45} T^3 , \quad (2.5)$$

$$g_s = \sum_{i,\text{boson}} g_i \left(\frac{T_i}{T} \right)^3 + \frac{7}{8} \sum_{j,\text{fermion}} g_j \left(\frac{T_j}{T} \right)^3 , \quad (2.6)$$

where g_s is the degree of freedom of the entire particle gas, while g_i and g_j are the degrees of freedom of bosons or fermions, respectively. With that, the entropy of neutrinos can be written as follows

$$s_\nu = 3 \frac{7}{8} \frac{2\pi^2}{45} g_\nu T_\nu^3(a) . \quad (2.7)$$

Therefore, by using equation (2.4) we get that

$$T_\nu(a_2) = \frac{a_1}{a_2} T_\nu(a_1) = \frac{a_1}{a_2} T_d . \quad (2.8)$$

Now the entropy for the QED-Plasma in the ideal gas approximation can be written as:

$$s(a) = \frac{2\pi^2}{45} \tilde{g}_s(a) T^3(a) , \quad (2.9)$$

with the effective degrees of freedom of an ideal gas

$$\tilde{g}_s = g_\gamma + \frac{45}{4\pi^4} \frac{g_e}{T^4(a)} \int_0^\infty dp p^2 \left(E_e + \frac{p^2}{3E_e} \right) f_F(E_e, T(a)) + \frac{7}{8} \sum_{\beta \neq \alpha} g_{\nu_\beta} . \quad (2.10)$$

Now by using equation (2.3) and (2.8) we get the following relation between the neutrino and the photon temperature:

$$\frac{T_{\nu_\alpha}(a_2)}{T(a_2)} = \left[\frac{\tilde{g}_s(a_2)}{\tilde{g}_s(a_d)} \right]^{\frac{1}{3}} . \quad (2.11)$$

In general, now the decoupling temperature of ν_e would differ from ν_τ, μ . However, because of the large mixing in the neutrino sector, it can be argued that all neutrinos effectively decouple at the same temperature. Further we take a_2 to be long after e^\pm annihilation, it therefore holds that $\tilde{g}_s(a_2) = g_\gamma = 2$, while for a_1 that we choose to be around the decoupling time $\tilde{g}_s(a_1)$ can be written as:

$$\tilde{g}_s(a_d) = g_\gamma + \frac{45}{\pi^4 T_{d(e)}^4} \int_0^\infty dp p \left(E_e + \frac{p^2}{3E_e} \right) f_F(E_e, T_{d(e)}) \quad (2.12)$$

Now we translate the temperature ratio (2.11) into an energy density ratio. For that we use $\rho_\gamma \propto g_\gamma T^4$ and $\rho_{\nu_\alpha} \propto \frac{7}{8} g_{\nu_\alpha} T_\nu^4$ giving

$$\frac{\rho_\nu}{\rho_\gamma} \Big|_{\frac{T}{m_e} \rightarrow 0} = \sum_\alpha \frac{\rho_{\nu_\alpha}(a_2)}{\rho_\gamma(a_2)} = 3 \times \frac{7}{8} \left[\frac{2}{\tilde{g}_s(a_d)} \right]^{\frac{4}{3}} . \quad (2.13)$$

After using the definition for N_{eff} (2.2) we get:

$$N_{\text{eff}} = 3 \times \left[\frac{11}{4} \frac{2}{\tilde{g}_s(a_d)} \right]^{\frac{4}{3}} . \quad (2.14)$$

2.2 Generalized neutrino Boltzmann equations and continuity equation

A more involved way to calculate the change in N_{eff} would be to solve the generalized neutrino Boltzmann equations that are derived from non-equilibrium thermal field theory (see section

3.6)

$$\frac{df_\alpha}{dt} = [1 - f_\alpha]\Gamma_\alpha^< - f_\alpha\Gamma_\alpha^>. \quad (2.15)$$

Also, one has to solve the continuity equation to get an evolution of the temperature of the QED plasma. With the total energy density ρ , the pressure P and the Hubble constant H [22].

$$\dot{\rho} + 3H(\rho + P) = 0 \quad (2.16)$$

For the full calculation, one could use `FortEPiANO` [10], a precision neutrino decoupling code. Apart from that, it is also possible to make the damping approximation. There, it is assumed that the thermal distribution functions of the neutrinos $f_\alpha(p)$ only differ slightly from the equilibrium distributions $f_D(p)$ (see also [17]). Then it is possible to write $f_\alpha(p) = f_D(p) + \delta f_\alpha(p)$. Expanding equation 2.15 up to linear order in $\delta f_\alpha(p)$ we get:

$$\frac{df_\alpha}{dt} \approx -\Gamma_\alpha \delta f_\alpha. \quad (2.17)$$

Here, $\Gamma_\alpha = \Gamma_\alpha^< + \Gamma_\alpha^>$ is the mode-dependent interaction rate. We follow the discussion in [23, 17], where comoving quantities $x = am_e$, $y = ap$ and $z = aT$ were introduced. In these quantities x can be thought of as a comoving time, y corresponds to the comoving momentum and z to the comoving temperature. With that, the continuity equation can be written as:

$$\frac{dz}{dx} = \frac{\frac{x}{z}J(\frac{x}{z}) - \frac{1}{2z^2}\frac{d\bar{\rho}}{dx} + G_1(\frac{x}{z})}{\frac{x^2}{z^2}J(\frac{x}{z}) + Y(\frac{x}{z}) + \frac{2\pi^2}{15} + G_2(\frac{x}{z})}. \quad (2.18)$$

The new introduced functions have different purposes. The ideal-gas behavior of the QED plasma is given by the two functions

$$J(u) = \frac{1}{\pi^2} \int_0^\infty dw w^2 \frac{e^{\sqrt{w^2+u^2}}}{1 + e^{\sqrt{w^2+u^2}}} \quad (2.19)$$

$$Y(u) = \frac{1}{\pi^2} \int_0^\infty dw w^4 \frac{e^{\sqrt{w^2+u^2}}}{1 + e^{\sqrt{w^2+u^2}}}. \quad (2.20)$$

Finite-temperature corrections up to order $\mathcal{O}(e^2)$ are encoded in

$$G_1(u) = 2\pi\alpha_{\text{em}} \left[\frac{1}{u} \left(\frac{K(u)}{3} + 2K^2(u) - \frac{J(u)}{6} - K(u)J(u) \right) + \left(\frac{K'(u)}{6} - K(u)K'(u) + \frac{J'(u)}{6} + J'(u)K(u) + J(u)K'(u) \right) \right] \quad (2.21)$$

$$G_2(u) = 2\pi\alpha_{\text{em}} \left[-4 \left(\frac{K(u)}{6} - \frac{1}{2}K^2(u) + \frac{J(u)}{6} + K(u)J(u) \right) + \left(\frac{K'(u)}{6} - K(u)K'(u) + \frac{J'(u)}{6} + J'(u)K(u) + J(u)K'(u) \right) \right] \quad (2.22)$$

Further, the function $K(u)$ is determined via:

$$K(u) = \frac{1}{\pi^2} \int_0^\infty dw \frac{w^2}{\sqrt{w^2 + u^2}} \frac{1}{e^{\sqrt{w^2 + u^2}} + 1} . \quad (2.23)$$

The derivative of the comoving neutrino energy density $\bar{\rho}_\nu = \rho_\nu a^4$ can be calculated by looking at the integral, weighted by the energy over the distribution function. Generally, this would be $\rho(t) = \frac{g}{(2\pi)^3} \int d^3\mathbf{p} E(\mathbf{p}) f(\mathbf{p}, t)$. In this case, with the comoving variables, we get:

$$\frac{d\bar{\rho}_\nu}{dx} = \frac{1}{\pi^2} \int dy y^3 \sum_\alpha \frac{df_\alpha(x, y)}{dx} , \quad (2.24)$$

where the derivative of the distribution function is given by the approximated generalized neutrino Boltzmann functions of equation (2.17) now written in comoving variables

$$\frac{df_\alpha(x, y)}{dx} \approx -\frac{\Gamma_\alpha(x, y)}{xH(x)} \delta f_\alpha(x, y) . \quad (2.25)$$

One could now solve equation (2.25) and the continuity equation (2.18) for a set of neutrino momenta that would cover almost all of the neutrino distribution. This method is called the full-momentum approach and is obviously very expensive. It is also possible to only look at the mean momentum mode, which is typically set to $\langle y \rangle = 3.15z(T_0)$, where T_0 is the photon initialization temperature. In the mean-momentum approach we would then only change the number of total neutrinos, but we would assume that the distribution function has the shape of the equilibrium function

$$f_\alpha(y) = \frac{f_\alpha(\langle y \rangle)}{f_D(\langle y \rangle T)} f_D(yT) . \quad (2.26)$$

In the mean-momentum approach we get

$$\frac{d\bar{\rho}_\nu}{dx} = -\frac{7\pi^2}{120xH(x)} \sum_\alpha \Gamma_\alpha(\langle y \rangle) \left(\frac{f_\alpha(x, \langle y \rangle)}{f_D(\langle y \rangle T)} - z^3(x) \right) . \quad (2.27)$$

After calculating $\bar{\rho}_\nu$ and z in the full-momentum or mean-momentum approach, we can use the definition of N_{eff} of equation (2.2), which can be written in terms of comoving variables as

$$N_{\text{eff}} = \frac{8}{7} \left(\frac{11}{4} \right)^{\frac{4}{3}} \frac{30}{2\pi^2} \left(\frac{z(T_0)}{z(x)} \right)^4 \bar{\rho}_\nu(x) \Big|_{x \rightarrow \infty} \quad (2.28)$$

In fact, it turns out that the mean momentum approach and the full momentum approach only differ very slightly in the end. This is discussed further in [13].

2.3 A brief thermal history of the universe

The impact of N_{eff} on cosmological phenomena, such as the CMB and BBN, arises from its contribution to the radiation energy density during the radiation-dominated era of the universe. During this phase, the Hubble rate is proportional to the total radiation energy density, $H^2 \propto \rho_{\text{rad}}$, to which N_{eff} contributes. Therefore, increasing N_{eff} directly increases the expansion rate H .

To understand the effects on N_{eff} one has to understand neutrino decoupling. We now want to discuss the thermal history of the universe. This will allow us to see neutrino decoupling in the broader spectrum of the whole history of the universe. A more detailed discussion of this can be found in [24, 25, 26].

- **10¹⁹ GeV – 10 TeV** (10^{-43} s – 10^{-14} s) Our universe undergoes an hypothetical inflationary phase. It is believed that this **inflationary phase** exists because it can explain the flatness of the universe, the homogeneity of the CMB and the monopole problem that would otherwise occur. It is also believed that baryon asymmetry creating processes, called **Baryogenesis** happen in this area.
- **~ 160 GeV** ($\sim 10^{-11}$ s) At this scale the Standard Model undergoes the hypothetical **Electroweak Phase Transition**. The $SU(2)_L \times U(1)_Y$ gauge symmetry gets broken into the $U(1)_{\text{em}}$ gauge symmetry. This process gives mass to almost all particles.
- **~ 150 MeV** ($\sim 10^{-5}$ s) Quarks and gluons that were previously free become confined in baryons and mesons. This transition is called **QCD Phase Transition**.
- **~ 1 MeV** (~ 1 s) The temperature is now so low that the Hubble rate is of the same order as the interaction rate between neutrinos and the QED plasma $H \sim \Gamma$, which means that **neutrinos decouple**.
- **~ 0.5 MeV** (~ 6 s) The typical energy of the universe now corresponds to the mass of the electron. At this energy, the process $\gamma\gamma \rightarrow e^+e^-$ becomes energetically suppressed. Therefore, **electron-positron annihilation** is favored over pair production. This transfers energy from the electrons and positrons into photons. The transfer of energy increases ρ_γ . At this point, the highly energetic neutrinos are still in thermal equilibrium with the QED plasma, meaning they are also affected by the energy flowing into the photon energy density.

- $\sim 0.1 \text{ MeV}$ ($\sim 3 \text{ min}$) Light elements, in general ${}^2\text{H}$, ${}^4\text{He}$ and ${}^3\text{Li}$ are formed in a process that is called **Big Bang Nucleosynthesis**. Also, at around this temperature **positronium** formation is possible. This has an impact on N_{eff} through modifications of the QED EoS [14].
- $\sim 0.3 \text{ eV}$ ($\sim 300 \text{ kyr}$) The temperature is now below the ionization energy of hydrogen, which means that there are now only a few free electrons left that can scatter with the photons. At around this temperature the **CMB** got released.
- $\sim 5 \text{ meV}$ ($\sim 300 \text{ Myr}$) **Stars and galaxies** are formed in the universe.

Chapter 3

Finite temperature field theory

An assumption we make in “normal” (vacuum) quantum field theory is that our fields have well-defined asymptotic states. By that we mean that the states after the scattering are free states, which do not interact anymore. And when we calculate expectation values of an operator we would just write

$$\langle \hat{\mathcal{O}} \rangle = \langle \psi | \hat{\mathcal{O}} | \psi \rangle . \quad (3.1)$$

This is a really good approximation for collider physics because our particles scatter in a prepared vacuum. This obviously does not hold for early universe kinematics. The particles constantly interact with each other and never are “free”. Therefore, we cannot make this approximation anymore. We now have to specify our system in terms of a density matrix $\hat{\rho}$. In this case, we would write our expectation value as

$$\langle \hat{\mathcal{O}} \rangle_{\text{thermal}} = \frac{\sum_{\psi} \langle \psi | \hat{\rho} \hat{\mathcal{O}} | \psi \rangle}{\sum_{\psi} \langle \psi | \hat{\rho} | \psi \rangle} = \frac{\text{Tr} [\hat{\rho} \hat{\mathcal{O}}]}{Z(\beta)} , \quad (3.2)$$

where now $Z(\beta)$ is our well-known partition function with $\beta = \frac{1}{T}$.

To evaluate the thermal expectation value, there are different methods. The first method was developed by Matsubara [27]. He used the similarity of the statistical density matrix $\hat{\rho} = \exp(-\beta \hat{H})$ to the time-evolution operator $\exp(-it \hat{H})$. If one only allows imaginary times $t = -i\beta$, it is possible to treat the density matrix as a time evolution into imaginary time, hence the name: **Imaginary time** (Matsubara) formalism. In this formalism, one gets a sum over the so-called Matsubara modes. This is very useful for phase transitions where only long-range interactions, which are described by the zeroth Matsubara mode, are needed [28]. The problem is that first of all we assume that our density matrix has the form $\hat{\rho} = \exp(-\beta \hat{H})$ which only is the case in equilibrium. We also restrict ourselves to an imaginary time evolution, which means that we are not able to treat dynamical systems with this method.

To circumvent these problems, Keldysh and Schwinger worked out a formalism where also real time values are allowed, its called: **Real time** (Keldysh-Schwinger) formalism ([29],[30]). This method can then be used for non-equilibrium and dynamical systems. But due to the more complicated contour that we have to choose later in this chapter, we get a doubling of the degrees of freedom, which makes the calculations more involved.

In this chapter, we are focusing on the real-time formalism and mainly look at it for the equilibrium case. We will deduce the generating functional Z_C for scalar particles, give the new Feynman rules, and calculate the thermal propagators. This chapter follows the discussions in [17],[31],[32][33][34][35].

3.1 Scalar fields

To construct the formalism, we use a real scalar field ϕ . Later, one also has to calculate the propagators for fermions and gauge bosons. But these calculations are much more involved and, therefore, not that pedagogical. The scalar field has the following Lagrangian:

$$\mathcal{L} = \frac{1}{2}\partial_\mu\phi\partial^\mu\phi - \frac{1}{2}m^2\phi^2 . \quad (3.3)$$

We will find that the thermal averages $\langle\hat{\mathcal{O}}\rangle_\beta(t) = \text{Tr} [\hat{\rho}(t)\hat{\mathcal{O}}] / Z(\beta)$, where the density matrix can in general be time-dependent, can be calculated by a generating functional. For this functional the time arguments are not restricted to lie on the real-axis but can be, and will be complex. We therefore choose a contour C that starts at $t_i^+ = t_i + i\epsilon$ with an infinitesimal small step ϵ in the imaginary direction. The Contour then turns over to $t_f + i\epsilon$, performs a semicircle and goes back to $t_i^- = t_i - i\epsilon$. We then send $t_f \rightarrow \infty$ to allow arbitrarily large times. With that we get the contour shown in figure 3.1.

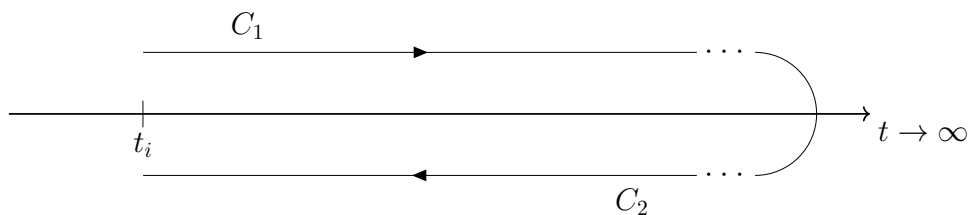


Figure 3.1: Real-time Closed Time Path

Choosing this contour also is the reason for the doubling of degrees of freedom, as we will treat the fields ϕ_1 on C_1 to be a different field as the field ϕ_2 on C_2 . It will then be important for the

later discussion to define an appropriate step function Θ_C on this contour:

$$\Theta_C(x^0, y^0) = \begin{cases} \Theta(x^0 - y^0) & \text{if } x^0, y^0 \in C_1 \\ \Theta(y^0 - x^0) & \text{if } x^0, y^0 \in C_2 \\ 1 & \text{if } x^0 \in C_2, y^0 \in C_1 \\ 0 & \text{if } x^0 \in C_1, y^0 \in C_2. \end{cases} \quad (3.4)$$

From this definition via $\delta_C(x^0, y^0) = \frac{d\Theta(x^0, y^0)}{dx^0}$ we directly get the definition for the δ -distribution as:

$$\delta_C = \begin{cases} \delta(x^0 - y^0) & \text{if } x^0, y^0 \in C_1 \\ -\delta(y^0 - x^0) & \text{if } x^0, y^0 \in C_2 \\ 0 & \text{otherwise} \end{cases}. \quad (3.5)$$

3.2 Equilibrium density matrix as time evolution operator

In general, the density matrix can have an arbitrary form. But in equilibrium, we know that the density matrix has the following form:

$$\hat{\rho}(\beta) = \frac{\exp(-\beta\hat{H})}{\text{Tr} [\exp(-\beta\hat{H})]}. \quad (3.6)$$

We realize that the density matrix can be written as a time evolution $U(t_i - i\beta, t_i)$. With that we can write $\hat{\rho}(t)$ as:

$$\hat{\rho}(t) = \frac{U(t, 0)U(t_i - i\beta, t_i)U(0, t)}{\text{Tr} [U(t_i - i\beta, t_i)]}. \quad (3.7)$$

Here it does not matter how we choose the time t_i . Now when we calculate the thermal expectation value of an operator \mathcal{O} we can write the density matrix in terms of evolution operators and get the following:

$$\begin{aligned} \langle \hat{\mathcal{O}} \rangle_\beta(t) &= \text{Tr} [\hat{\rho}(t)\hat{\mathcal{O}}] \\ &= \frac{\text{Tr} [U(t, 0)U(t_i - i\beta, t_i)U(0, t)\mathcal{O}]}{\text{Tr} [U(t_i - i\beta, t_i)]} \\ &= \frac{\text{Tr} [U(t_i - i\beta, t_i)U(t_i, t)\mathcal{O}U(t, t_i)]}{\text{Tr} [U(t_i - i\beta, t_i)]}, \end{aligned} \quad (3.8)$$

where we have used the cyclic property of the trace and that the two evolution operators $U(t_i - i\beta, t_i)$ and $U(t_i, 0)$ commute. Now we insert another time evolution $U(t_i, t_f)U(t_f, t_i)$. It might seem redundant to insert this time evolution. But in the end, when we are working out the generating functional this will be important to include fields with an arbitrary time. If we

would only look at the imaginary time path formalism we would not have to insert this. With this insertion, we get:

$$\langle \mathcal{O} \rangle_\beta(t) = \frac{\text{Tr} \left[U(t_i - i\beta, t_i) U(t_i, t_f) U(t_f, t) \hat{\mathcal{O}} U(t, t_i) \right]}{\text{Tr} \left[U(t_i - i\beta, t_i) U(t_i, t_f) U(t_f, t_i) \right]} . \quad (3.9)$$

The physical interpretation of this is that the field evolves from $t_i \rightarrow t$ it then interacts with the Operator \mathcal{O} after that it evolves until t_f , which we will send to ∞ in the end. After that, the field evolves back to t_i and then evolves into imaginary time until $t_i - i\beta$. As you can see here, this is the contour that we will use later but with an additional part from $t_i \rightarrow t_i - i\beta$ (see figure 3.2). In the end, the integral over this piece will only be a multiplicative constant and therefore will be included into the normalization constant.

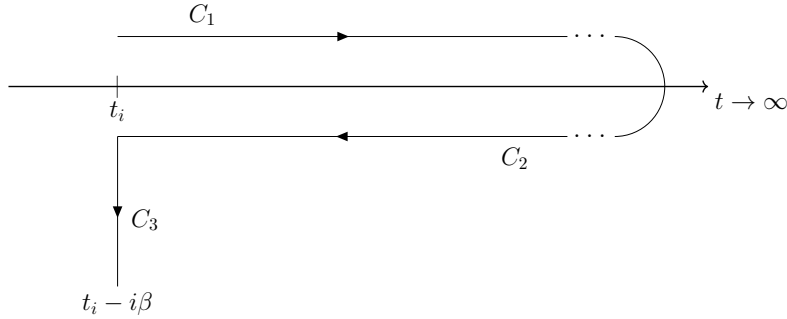


Figure 3.2: Real time path that also includes the contour from t_i to $t_i - i\beta$

3.3 Generating functional

In vacuum theory, we were interested in finding a generating functional for expectation values of the form:

$$\langle T[\hat{\phi}(x_1) \dots \hat{\phi}(x_N)] \rangle . \quad (3.10)$$

In the end we find [36, 37]

$$Z(J) = \int \mathcal{D}\phi \exp \left(i \int_{-\infty}^{\infty} dt \int d^3x (\mathcal{L} + J\phi) \right) . \quad (3.11)$$

Here we integrate over t from $-\infty$ up to ∞ , because our time evolution starts at $t_i = -\infty$ and ends at $t_f = \infty$. The difference now in the real time path formalism is that our time evolution starts at t_i to $t \rightarrow \infty$ then back to t_i and then down to $t_i - i\beta$ due to the density operator. We therefore in the end integrate over this more complicated contour instead from $-\infty$ to ∞ . But there are some more steps we have to take.

We are going to follow the deviation for the generating functional in [37] for vacuum theory but include the thermal density matrix. We therefore first look at an expectation value with

no extra fields added. In vacuum theory, this corresponds to $\langle 0, t_f | 0, t_i \rangle$. We can then write the trace using a path integral:

$$\text{Tr} [\hat{\rho}] = \int \mathcal{D}\phi \langle \phi; t_f | \hat{\rho} | \phi, t_i \rangle . \quad (3.12)$$

Let us for now only look at the matrix element $\langle \phi; t_f | \hat{\rho} | \phi, t_i \rangle$, the path integral only gives a normalization constant in the end. Similarly to the vacuum path integral derivation, we now insert a time quantization into the matrix element to get the following:

$$\begin{aligned} \langle \phi; t_f | \hat{\rho} | \phi, t_i \rangle &= \int \mathcal{D}\phi_1 \cdots \mathcal{D}\phi_l \cdots \mathcal{D}\phi_m \cdots \mathcal{D}\phi_n \\ &\times \underbrace{\langle \phi | e^{\delta t \hat{H}(t_i - i\beta + i\delta t)} | \phi_n \rangle \langle \phi_n | \cdots | \phi_{m+1} \rangle \langle \phi_{m+1} | e^{+\delta t \hat{H}(t_i)} | \phi_m \rangle}_{\text{Time evolution } t_i \rightarrow t_i - i\beta} \\ &\times \underbrace{\langle \phi_m | e^{i\delta t \hat{H}(t_i + \delta t)} | \phi_{m-1} \rangle \langle \phi_{m-1} | \cdots | \phi_{l+1} \rangle \langle \phi_{l+1} | e^{+i\delta t \hat{H}(t_f)} | \phi_l \rangle}_{\text{Time evolution } t_f \rightarrow t_i} \\ &\times \underbrace{\langle \phi_l | e^{-i\delta t \hat{H}(t_f - \delta t)} | \phi_{l-1} \rangle \langle \phi_{l-1} | \cdots | \phi_1 \rangle \langle \phi_1 | e^{-i\delta t \hat{H}(t_i)} | \phi \rangle}_{\text{Time evolution } t_i \rightarrow t_f} . \end{aligned} \quad (3.13)$$

Now each of the pieces $\langle \phi_{j+1} | e^{-i\delta t \hat{H}(t)} | \phi_j \rangle$ can be evaluated by inserting $\int \mathcal{D}\Pi |\Pi\rangle \langle \Pi| = \mathbb{1}$ and then finding a Gaussian integral. But first we should talk about the Hamiltonian. In general, the Hamiltonian can be written as $H = \frac{1}{2}(\delta_t \hat{\phi})^2 + \frac{1}{2}(\nabla \hat{\phi})^2 + \frac{1}{2}m^2 \hat{\phi} + V(\hat{\phi})$. The interactions of the field lie in the potential $V(\hat{\phi})$. We then introduce $\delta_t \hat{\phi} = \hat{\pi}$. The states $|\Pi\rangle$ that we insert are the eigenstates of $\hat{\pi}$. Also for the scalar product, it holds $\langle \Pi | \phi \rangle = \exp(-i \int d^3x \Pi(\vec{x}) \phi(\vec{x}))$. With that we can write:

$$\begin{aligned} \langle \phi_{j+1} | e^{-i\delta t \hat{H}(t)} | \phi_j \rangle &= \int \mathcal{D}\Pi_j \langle \phi_{j+1} | \Pi_j \rangle \\ &\times \langle \Pi_j | \exp \left(-i\delta t \int d^3x \left[\frac{1}{2} \hat{\pi}^2 + \frac{1}{2} (\nabla \hat{\phi})^2 + \frac{1}{2} m^2 \hat{\phi} + V(\hat{\phi}) \right] \right) | \phi_j \rangle \\ &= \int \mathcal{D}\Pi_j \exp \left(i \int d^3x \Pi_j(\vec{x}) [\phi_{j+1}(\vec{x}) - \phi_j(\vec{x})] \right) \\ &\times \exp \left(-i\delta t \int d^3x \left[\frac{1}{2} \Pi_j^2 + \frac{1}{2} (\nabla \phi_j)^2 + \frac{1}{2} m^2 \phi_j + V(\phi_j) \right] \right) . \end{aligned} \quad (3.14)$$

To perform the Gaussian integral over Π we have to complete the square

$$-\frac{1}{2}[\delta t \Pi^2 - 2\Pi(\phi_{j+1} - \phi_j)] = -\frac{1}{2} \left(\sqrt{\delta t} \Pi - \frac{(\phi_{j+1} - \phi_j)}{\sqrt{\delta t}} \right)^2 - \frac{1}{2} \frac{(\phi_{j+1} - \phi_j)^2}{\delta t} . \quad (3.15)$$

After shifting $\sqrt{\delta t} \Pi - \frac{(\phi_{j+1} - \phi_j)}{\sqrt{\delta t}} \rightarrow \sqrt{\delta t} \Pi'$ we perform the Gaussian integral, which just gives

some constant N . We therefore can write:

$$\begin{aligned} \langle \phi_{j+1} | e^{-i\delta t \hat{H}(t)} | \phi_j \rangle &= N \exp \left(-i\delta t \int d^3x \left[-\frac{1}{2} \left(\frac{\phi_{j+1} - \phi_j}{\delta t} \right)^2 + \frac{1}{2} (\nabla\phi)^2 + \frac{1}{2} m^2 \phi^2 + V(\phi_j) \right] \right) \\ &= N \exp \left(-i\delta t \int d^3x \mathcal{L}(\phi_j, \partial_t \phi_j) \right) \end{aligned} \quad (3.16)$$

When we put this back into equation (3.13) and piece together the integration path that goes from $t_i \rightarrow t_f \rightarrow t_i \rightarrow t_i - i\beta$ instead of just $t_i \rightarrow t_f$ as it was in vacuum theory. We get the following result

$$\langle \phi; t_f | \hat{\rho} | \phi, t_i \rangle = N \int \mathcal{D}\psi(\vec{x}, t) e^{i \int_C d^4x \mathcal{L}}, \quad (3.17)$$

which is the same as in vacuum theory besides the contour that we integrate over. The dependence on ϕ' can be absorbed into N . Putting this back into equation (3.12) and integrating the integral over $\mathcal{D}\phi$ and absorbing this into the normalization constant, we get:

$$\text{Tr} [\hat{\rho}] = N' \int \mathcal{D}\psi(\vec{x}, t) e^{i \int_C d^4x \mathcal{L}}. \quad (3.18)$$

If we want to have field insertions into our Green's function we have to include the same source term as in vacuum theory; we therefore get for the generating functional:

$$Z(\beta, J) = \int \mathcal{D}\phi e^{i \int_C d^4x (\mathcal{L} + J\phi)}. \quad (3.19)$$

It should be noted that the generating functional, for $t_f \rightarrow \infty$, factorizes into the parts $Z_{C_\beta} = Z_{C_1 \cup C_2} \times Z_{C_3}$. Here Z_{C_3} just gives some constant that in the end does not matter. We are therefore safe by restricting our integration contour on $C_1 \cup C_2$. We can then generate our thermal Green's function by functional differentiation of the generating functional, for example:

$$\begin{aligned} G_C(t - t') &= \langle T_C(\phi(t)\phi(t')) \rangle_\beta \\ &= \frac{1}{Z(\beta, J)} \frac{\delta^2 Z(\beta, J)}{i\delta J(t) i\delta J(t')}. \end{aligned} \quad (3.20)$$

3.4 Free scalar propagators

The propagator of a field is given by the two-point function:

$$\langle T_C[\hat{\phi}(x_1)\hat{\phi}(x_2)] \rangle_\beta = i\Delta(x_1 - x_2). \quad (3.21)$$

Suppose there exists a function $G_C(x_1, x_2)$ such that the generating functional can be expressed as:

$$Z[\beta, J] = N \exp \left(-\frac{i}{2} \int_C d^4x d^4x' J(x) G_C(x, x') J(x') \right), \quad (3.22)$$

where N is a normalization constant. To extract the two-point function from this generating functional, we take functional derivatives with respect to the source $J(x)$:

$$\begin{aligned} \langle T_C[\hat{\phi}(x_1)\hat{\phi}(x_2)] \rangle_\beta &= \frac{(-i)^2}{Z(\beta)} \frac{\delta^2 Z(\beta, J)}{\delta J(x_1)\delta J(x_2)} \Big|_{J=0} \\ &= iG_C(x_1 - x_2). \end{aligned} \quad (3.23)$$

You can then see that the function $G_C(x_1 - x_2)$ we introduced is the two-point function that we want to calculate. We now start with the generating functional of equation (3.19) and use the Lagrangian of equation (3.3). We then get for the generating functional:

$$Z(\beta, J) = Z(\beta) \int \mathcal{D}\phi \exp \left(-i \int_C d^4x \frac{1}{2} \phi(\partial_\mu \partial^\mu + m^2)\phi - J(x)\phi \right) \quad (3.24)$$

The field ϕ is understood to satisfy $\lim_{\mathbf{x} \rightarrow \infty} \phi(\mathbf{x}, t) = 0$. Also, the discussion for the $i\epsilon$ prescription is rather involved; we will therefore not go into detail here. But you can read about this in [32].

We can then introduce a substitution:

$$\tilde{\phi}(x) = \phi(x) + \int_C d^4x' G_C(x - x') J(x'). \quad (3.25)$$

With the substitution it is possible to write

$$\begin{aligned} \int_C d^4x \frac{1}{2} \tilde{\phi}(\partial_\mu \partial^\mu + m^2)\tilde{\phi} &= \int_C d^4x \frac{1}{2} \left(\phi(x) + \int_C d^4x' G_C(x - x') J(x') \right) \\ &\quad \times (\partial_\mu \partial^\mu + m^2) \left(\phi(x) + \int_C d^4x'' G_C(x - x'') J(x'') \right). \end{aligned} \quad (3.26)$$

We now force $G_C(x_1 - x_2)$ to satisfy $(\partial_\mu \partial^\mu + m^2)G_C(x_1 - x_2) = -\delta_C(x_1 - x_2)$. For now we will use this to bring the generating functional into the form of equation (3.22), but later this will be the condition that we have to solve to get the propagator.

$$\begin{aligned} \int_C d^4x \frac{1}{2} \tilde{\phi}(\partial_\mu \partial^\mu + m^2)\tilde{\phi} &= \int_C d^4x \left[\frac{1}{2} \phi(x)(\partial_\mu \partial^\mu + m^2)\phi(x) - J(x)\phi(x) \right. \\ &\quad \left. - \frac{1}{2} \int_C d^4x' J(x) G_C(x - x') J(x') \right] \end{aligned} \quad (3.27)$$

Putting this back into the generating functional we get:

$$Z_C(\beta, J) = Z(\beta) \exp\left(-\frac{i}{2} \int_C \int_C d^4x d^4x' J(x) G_C(x-x') J(x')\right) \quad (3.28)$$

$$\times \int \mathcal{D}\phi \exp\left(-\frac{i}{2} \int_C d^4x \frac{1}{2} \phi(x) (\partial_\mu \partial^\mu + m^2) \phi(x)\right) .$$

Now we can use the identity:

$$\int \mathcal{D}\phi \exp\left(i \int dt \phi(t) \mathcal{O}\phi(t)\right) = N[\det \mathcal{O}(t)]^{-\frac{1}{2}} , \quad (3.29)$$

where N is just a normalization constant. With this identity the path integral part of equation (3.28) only changes the constant in front, which does not matter for the propagator. We finally get:

$$Z_C(\beta, J) = \tilde{Z}(\beta) \exp\left(-\frac{i}{2} \int_C \int_C d^4x d^4x' J(x) G_C(x-x') J(x')\right) . \quad (3.30)$$

Now we have to find a solution to the equation we forced G_C to satisfy

$$(\partial_\mu \partial^\mu + m^2) G_C(x_1 - x_2) = -\delta_C(x_1 - x_2) . \quad (3.31)$$

First we Fourier transform the equation. With $E = \sqrt{\mathbf{p}^2 + m^2}$ we get

$$\left(\frac{\partial^2}{\partial x_0^2} + E^2\right) G_C(x^0 - y^0, E) = -\delta_C(x^0, y^0) . \quad (3.32)$$

A solution to this equation that also holds for the periodic boundary conditions from the KMS-relation $\langle \hat{\mathcal{O}}_1(t) \hat{\mathcal{O}}_2(t') \rangle_\beta = \langle \hat{\mathcal{O}}_2(t') \hat{\mathcal{O}}_1(t + i\beta) \rangle_\beta$ (see also section B.3) is given by:

$$iG_C(x^0 - y^0, E) = \frac{f_B(E)}{2E} \left(\Theta_C(x^0, y^0) \left[e^{\beta E - iE(x^0 - y^0)} + e^{iE(x^0 - y^0)} \right] \right. \\ \left. + \Theta_C(y^0, x^0) \left[e^{\beta E - iE(y^0 - x^0)} + e^{iE(y^0 - x^0)} \right] \right) . \quad (3.33)$$

This actually reduces to the vacuum solution for $\beta \rightarrow \infty$. Evaluating the Θ -functions in the four different areas, the four options arise because the fields ϕ_1 or ϕ_2 can either lie on C_1 or C_2 .

This yields the propagators:

$$i\Delta^{11}(p) = \frac{i}{p^2 - m^2 + i\epsilon} + 2\pi\delta(p^2 - m^2) f_B(|p^0|) = (i\Delta^{22})^* , \quad (3.34)$$

$$i\Delta^{12}(p) = 2\pi\delta(p^2 - m^2) [f_B(|p^0|) + \Theta(-p^0)] , \quad (3.35)$$

$$i\Delta^{21}(p) = 2\pi\delta(p^2 - m^2) [f_B(|p^0|) + \Theta(p^0)] . \quad (3.36)$$

3.5 Remaining propagators and Feynman rules

The calculation for the free Dirac fermion propagator is analogous to the free scalar propagator. With the Fermi-Dirac distribution f_D we get:

$$iS^{11}(p) = \frac{i(\not{p} + m)}{p^2 - m^2 + i\epsilon} - 2\pi(\not{p} + m)\delta(p^2 - m^2)f_D(|p^0|) = \gamma^0(iS^{22})^\dagger\gamma^0, \quad (3.37)$$

$$iS^{12}(p) = -2\pi(\not{p} + m)\delta(p^2 - m^2)[f_D(|p^0|) - \Theta(-p^0)], \quad (3.38)$$

$$iS^{21}(p) = -2\pi(\not{p} + m)\delta(p^2 - m^2)[f_D(|p^0|) - \Theta(p^0)]. \quad (3.39)$$

The photon propagators are given by:

$$iD_{\mu\nu}^{ab}(p) = \left(-g_{\mu\nu} + (1 - \xi)\frac{p_\mu p_\nu}{p^2} \right) i\Delta^{ab}(p)\Big|_{m=0}, \quad (3.40)$$

where $i\Delta^{ab}(p)\Big|_{m=0}$ is the scalar propagator with zero mass. You can see that the propagators are composed of different parts. The so-called vacuum part lies in the 11 and 22 propagators. This part is the same as the propagators in vacuum theory and is also not temperature dependent. The other parts are in a sense the temperature-dependent correction the vacuum propagators.

The Feynman rules in thermal field theory are similar to the vacuum Feynman rules. But remember that because of the two branches C_1 and C_2 we have essentially doubled our degrees of freedom. Therefore, we now have Type-1 and Type-2 vertices. Also denoted by a Closed-Time-Path index (CTP index) '1' or '2' at the vertex. The Type-2 vertices get an additional minus and we have to sum over all CTP indices. Also a vertex with CTP index a is connected to a vertex with CTP index b via an Δ^{ab} propagator.

3.6 Dyson-Schwinger and Kadanoff-Baym equations

The aim of this section is to find an evolution equation for the propagator. There are different methods to do this, but both of them include one particle irreducible graphs (1PI), these are graphs which stay connected if you cut only one particle line. In the first method, one can find a generating functional for 1PI correlation functions and deduce the evolution equation from that. This is the more rigorous ansatz, but its not that insightful. The more insightful way is to think of the full propagator as a sum over the 1PI graphs (see figure 3.3).



Figure 3.3: Schematic representation of the Dyson-Schwinger equation for fermions.

This can be written as an infinite sum in the following way ([38]):

$$\begin{aligned}
 i\Delta_{\text{Full}}^{ab}(x, y) &= i\Delta_{\text{Free}}^{ab}(x, y) - \int_C d^4x' d^4y' i\Delta_{\text{Free}}^{ac}(x, x') i\Pi^{cd}(x', y') i\Delta_{\text{Free}}^{db}(y', y) \\
 &+ \int_C d^4x' d^4y' d^4x'' d^4y'' i\Delta_{\text{Free}}^{ac}(x, x') i\Pi^{cd}(x', y') i\Delta_{\text{Free}}^{de}(y', x'') i\Pi^{ef}(x'', y'') i\Delta_{\text{Free}}^{fb}(y'', y) \\
 &+ \dots \\
 &= i\Delta_{\text{Free}}^{ab}(x, y) + \int_C d^4x' d^4y' i\Delta_{\text{Free}}^{ac}(x, x') i\Pi^{cd}(x', y') \left[i\Delta_{\text{Free}}^{db}(y', y) \right. \\
 &\quad \left. - \int_C d^4x'' d^4y'' i\Delta_{\text{Free}}^{de}(x, x'') i\Pi^{ef}(x'', y'') i\Delta_{\text{Free}}^{fb}(y'', y) + \dots \right] \\
 &= i\Delta_{\text{Free}}^{ab}(x, y) - \int_C d^4x' d^4y' i\Delta_{\text{Free}}^{ac}(x, x') i\Pi^{cd}(x', y') i\Delta_{\text{Full}}^{db}(y', y) .
 \end{aligned} \tag{3.41}$$

In a sense these are self-consistent integral equations for the full propagator. But the problem is the still remaining free propagator. To remove these, we act with $(\square_x + m^2)$ on the equation. Recall that the free propagator solves $(\partial_\mu \partial^\mu + m^2)G_{\text{Free}}(x, y) = -\delta_C(x - y)$.

$$(\partial_\mu \partial^\mu + m^2)G_{\text{Full}}(x, y) + i \int_C d^4y' \Pi^{cd}(x, y') G_{\text{Full}}^{db}(y', y) = -\delta_C^{(4)}(x - y) \tag{3.42}$$

This is known as the Dyson-Schwinger equation in position space, where the self-energy on the contour can be written as:

$$\Pi(x, y) = \theta_C(x, y)\Pi^>(x, y) + \theta_C(y, x)\Pi^<(x, y) . \tag{3.43}$$

Now we define the advanced and retarded propagators and self-energies in this manner:

$$\begin{aligned}
 \mathcal{O}^R(x, y) &= \theta(x^0 - y^0)(\mathcal{O}^>(x, y) - \mathcal{O}^<(x, y)) \\
 &= \mathcal{O}^{11}(x, y) - \mathcal{O}^{12}(x, y) = \mathcal{O}^{21}(x, y) - \mathcal{O}^{22}(x, y)
 \end{aligned} \tag{3.44}$$

$$\begin{aligned}
 \mathcal{O}^A(x, y) &= \theta(y^0 - x^0)(\mathcal{O}^<(x, y) - \mathcal{O}^>(x, y)) \\
 &= \mathcal{O}^{11}(x, y) - \mathcal{O}^{21}(x, y) = \mathcal{O}^{12}(x, y) - \mathcal{O}^{22}(x, y) .
 \end{aligned} \tag{3.45}$$

In general, the Dyson-Schwinger equations are four equations, one for each combinations of thermal indices. But the equations are not linearly independent. We can therefore write the four Dyson-Schwinger equations into two sets of equations for the advanced and retarded propagator and for the ($<$) and ($>$) propagator:

$$(-\square_x - m^2)\Delta^{R/A}(x, y) = (\Delta^{R/A} \odot \Pi^{R/A})(x, y) + \delta^{(4)}(x - y) \tag{3.46}$$

$$(-\square_x - m^2)\Delta^{\cong}(x, y) = (\Pi^{\cong} \odot \Delta^A)(x, y) + (\Pi^R \odot \Delta^{\cong})(x, y) , \tag{3.47}$$

where we have defined the product \odot as the integration over the intermediate variable of the two functions $(f \odot g)(x, y) = \int d^4z f(x, z)g(z, y)$. We then introduce yet another set of functions, the

Hermitian and anti-Hermitian, which are defined by:

$$\Delta^{\mathcal{H}} = \frac{1}{2}(\Delta^R + \Delta^A) \quad (3.48)$$

$$\Delta^{\mathcal{A}} = \frac{i}{2}(\Delta^R - \Delta^A) . \quad (3.49)$$

With them we get the final form of the Kadanoff-Baym equations for the scalar propagators:

$$(-\square_x - m^2)\Delta^{\cong} - \Pi^{\cong} \odot \Delta^{\mathcal{H}} - \Pi^{\mathcal{H}} \odot \Delta^{\cong} = \frac{1}{2}(\Pi^> \odot \Delta^< - \Pi^< \odot \Delta^>) . \quad (3.50)$$

When transforming this into momentum space we have to be careful because the functions in non-equilibrium are not only dependent on the relative coordinate $r = x - y$ but also on the average coordinate $z = \frac{x+y}{2}$. One could now think that, as we look on everything in equilibrium we can also suppose equilibrium now and reduce the functions on the relative coordinate r . The problem is that we are calculating the evolution of the propagators and in equilibrium there is obviously no evolution. We therefore have to think of the system on a large scale to not be in equilibrium while on small scales the system is in equilibrium. We can then use equilibrium thermal field theory to calculate the scatterings that happen on small scales but we can also use the non equilibrium equations for the evolution of the propagators.

Because the functions are now also dependent on the average coordinate z we can not just Fourier transform the equation, but we have to introduce the Wigner transformation:

$$f(p, z) = \int d^4r e^{ipr} f\left(z + \frac{r}{2}, z - \frac{r}{2}\right) . \quad (3.51)$$

Now we also have to define the moyal product \diamond [39], which is important to write the integration over the intermediate variable $f \odot g$ in Wignerspace. In equilibrium $f \odot g$ would just be a convolution $f * g$ but we have to be more rigorous now.

$$\diamond\{f(p, z)\}\{g(p, z)\} = \frac{1}{2}(\partial_z f \partial_p g - \partial_p f \partial_z g) \quad (3.52)$$

$$\int d^4r e^{ipr} (f \odot g) = e^{-i\odot} (f(p, z))(g(p, z)) \quad (3.53)$$

where $e^{-i\odot}$ acts as a series expansion on $\{f(p, z)\}\{g(p, z)\}$. After partial integration, we get $(-\square - m^2)\Delta(x, y) \rightarrow (p^2 - m^2 - \frac{1}{4}\partial_z^2 + ip\partial_z)$. We then get in Wignerspace:

$$\begin{aligned} (p^2 - m^2 - \frac{1}{4}\partial_z^2 + ip\partial_z)\Delta^{\cong} - e^{-i\odot} [\{\Pi^{\cong}\}\{\Delta^{\mathcal{H}}\} + \{\Pi^{\mathcal{H}}\}\{\Delta^{\cong}\}] \\ = -\frac{1}{2}e^{-i\odot} [\{\Pi^>\}\{\Delta^<\} - \{\Pi^<\}\{\Delta^>\}] . \end{aligned} \quad (3.54)$$

Now we can use the gradient expansion that assumes $\partial_z \ll p$. This means that the average coordinate changes rather small compared to the the momentum. We can then expand $e^{-i\odot}$ only to a given order. We then also can assume homogeneity and isotropy, which means that all

spatial derivatives drop out. Furthermore, it should be noted that $\Pi^{\mathcal{H}}$ and $\Delta^{\mathcal{H}}$ are intrinsically real objects while Π^{\lessgtr} and Δ^{\lessgtr} are purely imaginary. The real part of equation (3.54) then becomes:

$$p_0 \partial_t (i\Delta^{\lessgtr}) = -\frac{1}{2} (i\Pi^> i\Delta^< - i\Pi^< i\Delta^>) . \quad (3.55)$$

That is, the Kadanoff-Baym equation in Wignerspace for scalar particles. In the same way, we would get the following for fermions:

$$\gamma^0 \partial_t (-iS^{\lessgtr}) = i\Sigma^> iS^< - i\Sigma^< iS^> . \quad (3.56)$$

You can already see that if we put in the (<) or (>) free propagators we would get an evolution equation for the distribution function f_D of the particle. This is what we will use later.

Chapter 4

Neutrino interaction rates – Leading Order

From the Kadanoff-Baym equation for fermions (3.56) of the Keldysh-Schwinger formalism we can derive a quantum kinetic equation for the neutrino distribution functions

$$\frac{df_\alpha(p)}{dt} = [1 - f_\alpha(p)]\Gamma_\alpha^<(p) - f_\alpha(p)\Gamma_\alpha^>(p) . \quad (4.1)$$

There is a high similarity to the Boltzmann formalism as you can see in section 5.6. This similarity will lead to some names of the rates that would otherwise be not directly obvious. Neutrino oscillations are not included in the kinetic equation (4.1). Therefore, we only have to calculate the production and destruction rates, which are given by:

$$\Gamma_\alpha^\gtrless(p) = \mp \frac{1}{2p_0} \text{Tr} \left[-i\not{p}\Sigma_\alpha^\gtrless \right] \Big|_{p_0=\mathbf{p}} . \quad (4.2)$$

The total neutrino interaction rate is the sum of the production and destruction rates. We can use the KMS relation to express the total rate solely in terms of the production rate

$$\Gamma_\alpha(p) = \frac{1}{2p_0} \text{Tr} \left[-i\not{p}(\Sigma_\alpha^< - \Sigma_\alpha^>) \right] \Big|_{p_0=\mathbf{p}} \quad (4.3)$$

$$= \frac{1}{2p_0} \text{Tr} \left[-i\not{p}(\Sigma_\alpha^< - e^{\beta p_0} \Sigma_\alpha^<) \right] \Big|_{p_0=\mathbf{p}} \quad (4.4)$$

$$= \frac{1}{2p_0 f_D(p_0)} \text{Tr} \left[-i\not{p}\Sigma_\alpha^< \right] \Big|_{p_0=\mathbf{p}} . \quad (4.5)$$

4.1 LO neutrino self-energy

The leading order diagram for the neutrino self-energy has all propagating fermions put on shell (figure 4.1). We therefore can think of it as a cut through the whole diagram, which in the end would give the squared tree-level matrix element of the $2 \rightarrow 2$ processes. This is also a way to connect to the Boltzmann formalism. Indeed in the end it turns out that on leading order the Keldysh-Schwinger formalism and the Boltzmann formalism give the exact same result. Thermal corrections appear only on the NLO.

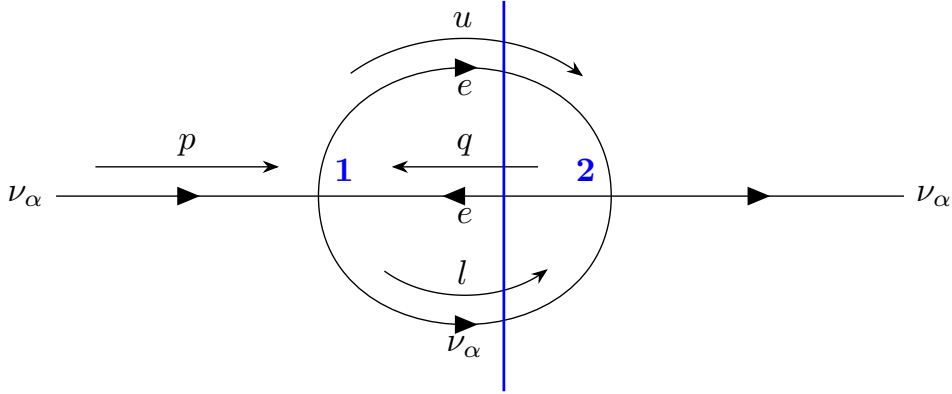


Figure 4.1: The leading order diagram for neutrino self interactions. The **blue** numbers denote the thermal indices.

The thermal indices in the diagram in figure 4.1 are put to 1 and 2, respectively, because we only want to calculate the production rate. Then we can write the following:

$$\begin{aligned} \text{Tr} [i\cancel{p}\Sigma^{12}] &= (-1)^{a+b} \left(\frac{i4G_F}{\sqrt{2}} \right)^2 \int_{l,q} \text{Tr} \left[\cancel{p}\gamma^\rho P_L iS_{\nu_\alpha}^{12}(l)\gamma^\sigma P_L \right] \\ &\quad \times \text{Tr} \left[iS_e^{12}(p+q-l)\gamma_\sigma (P_L g_L^\alpha + P_R g_R) iS_e^{21}(q)\gamma_\rho (P_L g_L^\alpha + P_R g_R) \right] , \end{aligned} \quad (4.6)$$

where $\int_q = \int \frac{d^4q}{(2\pi)^4}$. We use the thermal propagators that were derived in chapter 3. It is then possible to bring the equation (4.6) into the following form:

$$\text{Tr} [i\Sigma_{\text{LO}}^{12}] = \int_{l,q} (2\pi)^3 \delta(l^2) \delta(q^2 - m_e^2) \delta(u^2 - m_e^2) \mathcal{F}(l_0, q_0, u_0) \mathcal{T}_{\text{LO}} . \quad (4.7)$$

The thermal distribution functions are contained in:

$$\mathcal{F}(l_0, q_0, u_0) = [f_D(|l_0|) - \theta(-l_0)][f_D(|q_0|) - \theta(q_0)][f_D(|u_0|) - \theta(-u_0)] . \quad (4.8)$$

It is important to mention that the integral is symmetric under $u \leftrightarrow -q$, all the asymmetric

terms under this symmetry therefore drop out. For the traces over the γ -matrices we then get:

$$\mathcal{T}_{\text{LO}} = 2^7 G_F^2 \left[(g_L^\alpha)^2 (p \cdot q)^2 + g_R^2 (l \cdot q)^2 - g_L^\alpha g_R m_e^2 (p \cdot l) \right]. \quad (4.9)$$

This result is in complete agreement with the result of [11]. To evaluate the integrals over l and q we will work out a strategy in the next section 4.2.

4.2 The integral

We now want to calculate the integral for the general function $f(p, l, q)$:

$$I = \int d^4 l d^4 q \delta(l^2) \delta(q^2 - m_e^2) \delta(u^2 - m_e^2) f(p, l, q). \quad (4.10)$$

First, we can use the delta distributions $\delta(l^2)$, $\delta(q^2 - m_e^2)$ to fix $l_0 = \pm l$ and $q_0 = \pm \sqrt{q^2 + m_e^2}$. We therefore have to sum over these different solutions. Also $p_0 = p$ as p is an external particle.

$$I = \int \frac{d^3 l d^3 q}{4|l||q_0|} \delta(u^2 - m_e^2) f(p, l, q). \quad (4.11)$$

Now we choose a parameterization for p , l , q in the following way:

$$\mathbf{p} = |\mathbf{p}| \begin{pmatrix} 0 \\ 0 \\ 1 \end{pmatrix}, \quad \mathbf{l} = |\mathbf{l}| \begin{pmatrix} 0 \\ \sin \alpha \\ \cos \alpha \end{pmatrix} \quad \text{and} \quad |\mathbf{q}| = |\mathbf{q}| \begin{pmatrix} \sin \theta \sin \beta \\ \sin \theta \cos \beta \\ \cos \theta \end{pmatrix}. \quad (4.12)$$

We can use $\delta(u^2 - m_e^2)$ to fix $\cos \beta$. As we integrate β over $[0, 2\pi]$ we get two solutions for $\sin \beta$. Although $\sin \beta$ does not appear in the scalar products, we still have to form the sum. For $\cos \beta$ we get:

$$\cos \beta = \frac{-|\mathbf{l}||\mathbf{q}| \cos \alpha \cos \theta - |\mathbf{l}||\mathbf{p}| \cos \alpha + |\mathbf{p}||\mathbf{q}| \cos \theta + l_0 |\mathbf{p}| + l_0 q_0 - |\mathbf{p}| q_0}{|\mathbf{l}||\mathbf{q}| \sin \alpha \sin \theta}. \quad (4.13)$$

With that and $E_q = \sqrt{|\mathbf{q}|^2 + m_e^2}$ we get the following for the integral. We also have to add $\theta(1 - \cos^2 \beta)$ to ensure that $-1 < \cos \beta < 1$.

$$I = 2\pi \int_0^\infty d|\mathbf{l}| \int_0^\infty d|\mathbf{q}| \int_{-1}^1 d \cos \alpha \int_{-1}^1 d \cos \theta \frac{|\mathbf{l}|^2 |\mathbf{q}|^2 \sum_{\sin \beta} f(p, l, q) \theta(1 - \cos^2 \beta)}{4|\mathbf{l}| E_q 2|\mathbf{l}||\mathbf{q}| |\sin \alpha \sin \theta \sin \beta|} \quad (4.14)$$

Note that the integration over the azimuthal angle of \mathbf{l} was already done. From that we get the factor of 2π . We can write $\theta(1 - \cos^2 \beta)$ in the form $\theta(a \cos^2 \theta + b \cos \theta + c)$.

$$c = -|\mathbf{l}|^2 |\mathbf{p}|^2 \cos^2 \alpha + 2|\mathbf{l}||\mathbf{p}| \cos \alpha (l_0(|\mathbf{p}| + q_0) - |\mathbf{p}|q_0) + |\mathbf{l}|^2 |\mathbf{q}|^2 \sin^2 \alpha - l_0^2 (|\mathbf{p}| + q_0)^2 + 2l_0 |\mathbf{p}|q_0 (|\mathbf{p}| + q_0) - |\mathbf{p}|^2 q_0^2 \quad (4.15)$$

$$b = -2|\mathbf{q}|(|\mathbf{l}| \cos \alpha - |\mathbf{p}|)(|\mathbf{l}||\mathbf{p}| \cos \alpha - l_0(|\mathbf{p}| + q_0) + |\mathbf{p}|q_0) \quad (4.16)$$

$$a = -|\mathbf{q}|^2 (|\mathbf{p}|^2 + |\mathbf{l}|^2 - 2|\mathbf{p}\mathbf{l}| \cos \alpha) < 0 \quad (4.17)$$

Evaluating the θ -function one gets new endpoints for the integral over $\cos \theta = z$:

$$z_{\pm} = -\frac{b}{2a} \pm \sqrt{\left(\frac{b}{2a}\right)^2 - \frac{c}{a}}. \quad (4.18)$$

And we get a new θ -function: $\theta(b^2 - 4ac)$ that forces z_{\pm} to be real values. Also, the sum $\sum_{\sin \beta}$ just gives a factor of two. In addition, we note that $|\mathbf{l}||\mathbf{q}|\sin \alpha \sin \theta \sin \beta = \sqrt{(z_p - z)(z - z_m)}$.

$$I = \frac{\pi}{2} \int_0^{\infty} d|\mathbf{l}| \int_0^{\infty} d|\mathbf{q}| \frac{|\mathbf{l}||\mathbf{q}|^2}{E_q} \int_{-1}^1 d \cos \alpha \theta(b^2 - 4ac) \int_{z_m}^{z_p} dz \frac{f(p, l, q)}{\sqrt{(z_p - z)(z - z_m)}} \quad (4.19)$$

The function $f(p, l, q)$ has the form $\mathcal{Z}_0 + \mathcal{Z}_1 z + \mathcal{Z}_2 z^2$. We can use:

$$\int_{z_m}^{z_p} dz \frac{\mathcal{Z}_0 + \mathcal{Z}_1 z + \mathcal{Z}_2 z^2}{\sqrt{(z_p - z)(z - z_m)}} = \pi \left(\mathcal{Z}_0 - \frac{b}{2a} \mathcal{Z}_1 + \frac{3b^2 - 4ac}{a^2} \mathcal{Z}_2 \right). \quad (4.20)$$

Numerically it is also a huge improvement to do this integral analytically, this is because the integral has end point singularities, that are hard to calculate numerically. We get the following end result:

$$I = \frac{\pi^2}{2} \int_0^{\infty} d|\mathbf{l}| \int_0^{\infty} d|\mathbf{q}| \frac{|\mathbf{l}||\mathbf{q}|^2}{E_q} \int_{-1}^1 d \cos \alpha \theta(b^2 - 4ac) \left(\mathcal{Z}_0 - \frac{b}{2a} \mathcal{Z}_1 + \frac{3b^2 - 4ac}{8a^2} \mathcal{Z}_2 \right). \quad (4.21)$$

Chapter 5

Neutrino Interaction Rates – Next to leading order

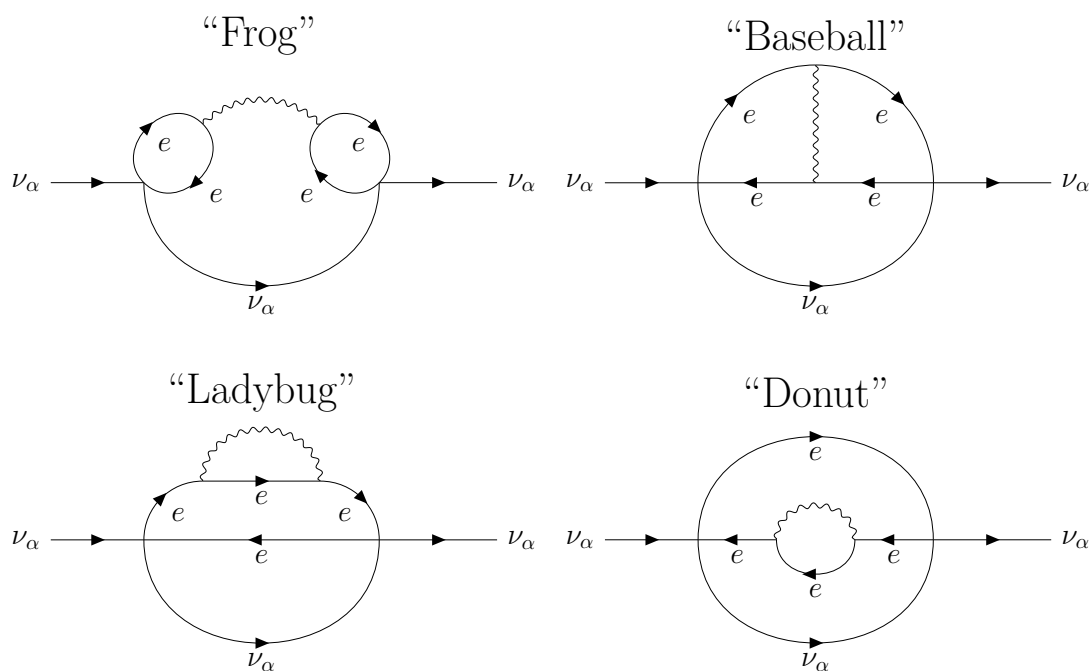


Figure 5.1: Schematic representation of the NLO diagrams. The main focus of this work is on the “Baseball” diagram. While also certain parts of the “Ladybug” and “Donut” diagrams are also calculated to cancel arising divergences.

On NLO there are four different diagrams (see figure 5.1). The three “Baseball”, “Frog” and “Donut” diagrams are connected because the Baseball diagram contains the virtual vertex correction while the real corrections that are needed to cancel the infrared divergence are contained

in the Baseball, Ladybug and Donut diagrams (see section 5.2). Only the “Frog” diagram gives a finite result by itself. It is also believed, that because of the t-channel enhancement the Frog diagram gives the biggest contribution of the NLO order diagrams. That is the reason why it was already calculated by [13].

5.1 Frog

Let us first calculate the rate of the Frog. In general $\text{Tr} [i\Sigma_{\text{Frog}}^{12}\not{p}]$ is a sum over all possible internal indices c and d . We first notice that the non-diagonal parts of $\text{Tr} [i\Sigma_{\text{Frog}}^{12,cd}\not{p}]$, the parts where $c \neq d$ are just zero because in both cases all particles of an $ee\gamma$ -Vertex are on shell. This process is kinematically forbidden. In addition, we have $\text{Tr} [i\Sigma_{\text{Frog}}^{12,11}\not{p}] = \text{Tr} [i\Sigma_{\text{Frog}}^{12,22}\not{p}]^*$. This yields:

$$\text{Tr} [i\Sigma_{\text{Frog}}^{12}\not{p}] = 2\text{Re} \left(\text{Tr} [i\Sigma_{\text{Frog}}^{12,11}\not{p}] \right) . \quad (5.1)$$

The corresponding diagram can be seen in figure 5.2.

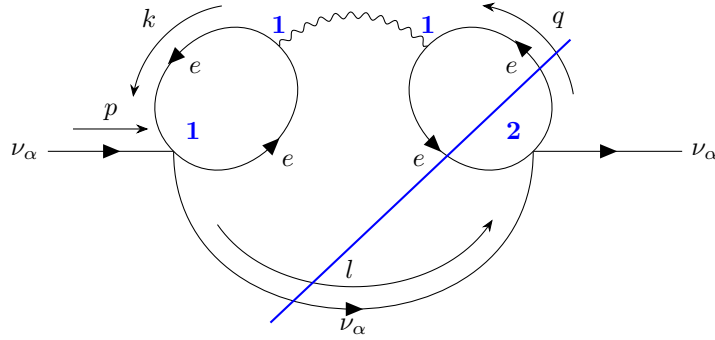


Figure 5.2: The **11** part of the Frog-diagram. The **blue** line denotes a cut through the diagram.

The interaction rate given by this diagram is written as:

$$\begin{aligned} \text{Tr} [i\Sigma_{\text{Frog}}^{12}\not{p}] &= (ie)^2 \left(\frac{i4G_F}{\sqrt{2}} \right)^2 \int_{l,q,k} \text{Tr} \left[\not{p}\gamma^\rho P_L iS_{\nu_\alpha}^{12}(l)\gamma^\sigma P_L \right] iD_{\mu\nu}^{11}(p-l) \\ &\quad \times \text{Tr} \left[iS_e^{11}(k)\gamma^\nu iS^{11}(p+k-l)\gamma_\sigma (P_L g_L^\alpha + P_R g_R) \right] \\ &\quad \times \text{Tr} \left[iS_e^{12}(p+q-l)\gamma^\mu iS^{21}(q)\gamma_\rho (P_L g_L^\alpha + P_R g_R) \right] . \end{aligned} \quad (5.2)$$

If we think about this diagram 5.2 in terms of cuts we just get the t -channel enhanced diagram (see figure 5.3) contracted with the tree diagram. We already see that we get a diagram that in itself contains an electron bubble which is the same for the photon self-energy. This will be the reason for using the photon self-energy to calculate the interaction rate.

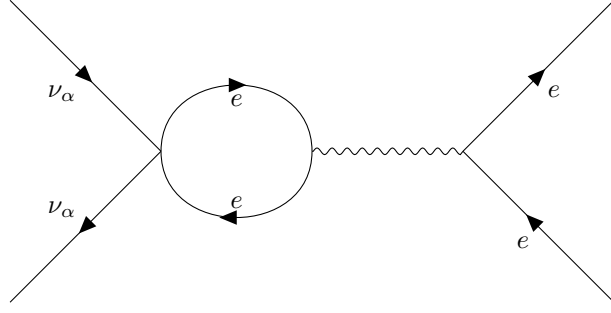


Figure 5.3: t-channel part of the Frog diagram, which contains the photon-self energy.

We can bring $\text{Tr} [i\Sigma_{\text{Frog}}^{12} \not{p}]$ in the same form as equation (4.7) but we have to change $\mathcal{T}_{\text{LO}} \rightarrow \mathcal{T}_{\text{Frog}}$. Now with the photon self-energy $\Pi_{11}^{\nu\sigma}(P)$ that contains the vacuum self-energy but also thermal correction to the photon self-energy, we can write:

$$\mathcal{T}_{\text{Frog}} = 16G_F^2 g_V^\alpha \text{Re} \left(\text{Tr} [(u + m_e)\gamma^\mu (q + m_e)\gamma_\rho (g_L^\alpha P_L + g_R P_R)] \right) \quad (5.3)$$

$$\times \text{Tr} [\not{p}\gamma^\rho P_L \not{l}\gamma^\sigma P_L] D_{\mu\nu}^{11}(P) \Pi_{11}^{\nu\sigma}(P) . \quad (5.4)$$

It is now useful to think of the rate as a vacuum and a thermal part $\mathcal{T}_{\text{Frog}} = \mathcal{T}_{\text{Vacuum}} + \mathcal{T}_{\text{Thermal}}$. The vacuum part contains only the vacuum part of the diagonal propagators, while the thermal part contains the rest. We call it the vacuum part because $\mathcal{T}_{\text{Vacuum}}$ is not temperature dependent while $\mathcal{T}_{\text{Thermal}}$ is temperature dependent. To write $\mathcal{T}_{\text{Vacuum}}$ we can use the well-known vacuum photon self-energy $\Pi_2(P^2)$:

$$\mathcal{T}_{\text{Vacuum}} = -2^{10} G_F^2 \alpha_{\text{em}} \frac{(g_V^\alpha)^2}{4\pi} [-m_e^2 (p \cdot l) + 2 (p \cdot q)^2] \text{Re} \Pi_2(P^2) . \quad (5.5)$$

At first one could think the rate is divergent, because the photon propagator is proportional to $\frac{1}{P^2}$ and could, in general, yield an infrared divergence. But the photon self-energy is proportional to P^2 . With that our rate is finite. This is not the case for thermal contributions to the self-energy because in these contributions $\Pi_{11} \propto T$ and therefore this rate divergence for $P \rightarrow 0$. To fix this one has to resum the photon propagator and give it a thermal mass. We write the resummed photon propagator as \bar{D} . For $\mathcal{T}_{\text{Thermal}}$ the thermal contributions for the photon self-energy have to be calculated (see section B.5). With them we get the following for the thermal rate:

$$\mathcal{T}_{\text{Thermal}}^{L/T} = 2^8 G_F^2 (g_V^\alpha)^2 \text{Re} \left(\bar{D}_R^{L/T}(P) \right) \text{Re} \left(\Pi_{R,T \neq 0}^{L/T}(P) \right) \quad (5.6)$$

$$\times \left[-2 (p \cdot q) P_{L/T}^{\mu\nu} p_\mu q_\nu + (p \cdot l) (-a_{L/T} (p \cdot l) + P_{L,T}^{\mu\nu} l_\mu l_\nu + P_{L/T}^{\mu\nu} q_\mu q_\nu) \right] .$$

Where $P_{L/T}$ are the longitudinal or transverse projector, $a_{L,T} = \frac{3\mp 1}{4}$, \bar{D}_R is the retarded and resummed photon propagator and $\Pi_{R,T \neq 0}^{L/T}(P)$ is the retarded thermal photon self-energy.

5.2 Cancellation of infrared divergences

When working with massless particles, one frequently encounters infrared divergences. As the name suggests, these divergences appear when the momentum of a massless particle approaches zero. In vacuum quantum field theory, it has been proven that all infrared divergences cancel out in the end, as stated by the Kinoshita-Lee-Nauenberg (KLN) theorem [40]. Consequently, the interaction rates are finite.

In thermal field theory, additional infrared divergences can arise. These divergences may be more severe due to the presence of Bose-Einstein distributions. Nevertheless it is widely believed that the KLN theorem also holds [41, 42], although a formal proof is still lacking. The aim of this section is to explain how one can generally deal with infrared divergences and to demonstrate explicitly how these divergences cancel out in the NLO calculation for the neutrino interaction rates.

5.2.1 Phase-space slicing & soft photon approximation

Phase-space slicing is a method to deal with infrared divergences in real emission diagrams. The divergence lies in the phase-space part, where we have a low-energy photon (soft photon). Therefore, we slice the phase space into two parts. The first is where the photon is soft, and so the photon momentum is smaller than all other momenta and masses that are arising. The other part where the photon is hard. So now there is an artificially introduced cut Energy ΔE for the rates, it follows:

$$\mathcal{T}_{\text{real}}(\lambda) = \mathcal{T}_{\text{soft}}(\Delta E, \lambda) + \mathcal{T}_{\text{hard}}(\Delta E) . \quad (5.7)$$

The end result should not depend on ΔE as this is not a physical parameter. Also, the divergence lies only in the soft part, so we can safely send $\lambda \rightarrow 0$ in the hard part. Now let us have a look at a real emission of a soft photon in a general process

$$M = A_0(p - k) \frac{i(\not{p} - \not{k} + m)}{(p - k)^2 - m^2} (-iQ_f)\not{\epsilon}(k)u(p) . \quad (5.8)$$

Here, Q_f is the charge of the fermion and $A_0(p - k)$ corresponds to the process that is indicated by the gray bubble in figure 5.4.

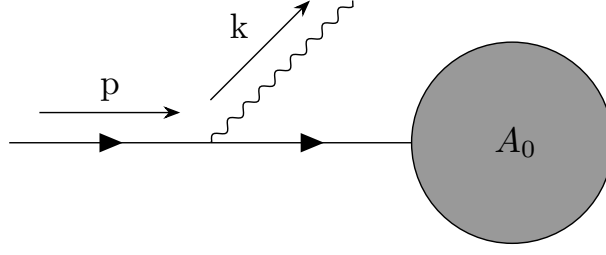


Figure 5.4: Schematic radiating of a photon from an external fermion line

As we are working in the soft part it holds that $k^\mu \ll p^\mu$. We therefore can neglect all k 's in the numerator, with which we get:

$$M = A_0(p) \frac{i(\not{p} + m)}{-2(p \cdot k)} (-iQ_f) \gamma^\mu u(p) \epsilon_\mu(k) \quad (5.9)$$

$$= A_0(p) \frac{i(-\gamma^\mu \not{p} + 2p^\mu + m)}{-2(p \cdot k)} (-iQ_f) u(p) \epsilon_\mu(k) \quad (5.10)$$

$$= A_0(p) \frac{(p \cdot \epsilon)}{(p \cdot k)} (-Q_f) u(p) , \quad (5.11)$$

where we used the Dirac equation in the end. With the Tree-level matrix element, which is given by $M_{\text{Tree}} = A_0(p)u(p)$ we get the end result, which also holds for anti fermions:

$$M = (-Q_f) \frac{(p \cdot \epsilon)}{(p \cdot k)} M_{\text{Tree}} . \quad (5.12)$$

5.2.2 Vacuum infrared divergences

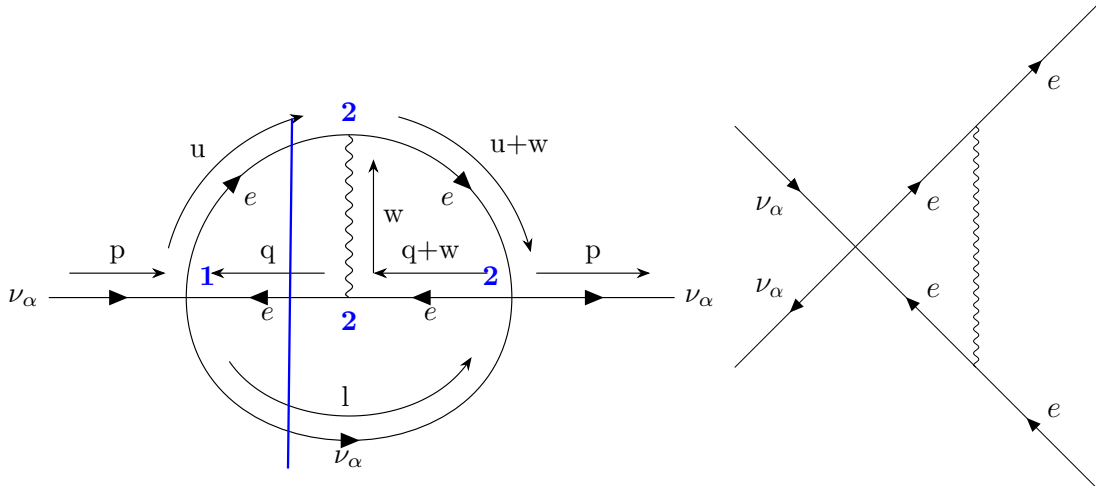


Figure 5.5: On the left side you can see the contribution of the Baseball diagram, that contains the virtual vertex correction, which you can see on the right side.

In the Baseball diagram, there is the vertex correction hidden in the 11 and 22 contributions (see Figure 5.5). We know that the vertex correction is infrared divergent. This can also be easily seen when one uses formfactors to calculate the rate. Similarly to equation (4.7) we can define $\mathcal{T}_{\text{Vertex}}$ to be the vacuum rate of the virtual vertex correction part of the Baseball diagram.

$$\begin{aligned} \mathcal{T}_{\text{Vertex}} = 2\text{Re} \left(\left(\frac{i4G_F}{\sqrt{2}} \right)^2 \int_{l,q} \text{Tr} \left[\not{p} \gamma^\rho P_L \not{l} \gamma^\sigma P_L \right] \text{Tr} \left[(\not{\psi} + m_e) \gamma_\sigma (g_V - g_A \gamma_5) (\not{q} + m_e) \right. \right. \\ \left. \left. \times \frac{\alpha}{\pi} \left[g_V \left(F_1 \gamma_\rho + F_2 \frac{i\sigma_{\rho\nu} P^\nu}{2m_e} \right) - g_A (F_1 - F_2) \gamma_\rho \gamma_5 \right] \right] \right) \end{aligned} \quad (5.13)$$

with $\sigma_{\rho\nu} = \frac{i}{2}[\gamma_\rho, \gamma_\nu]$ and $P = p - l$. When we talk about the infrared divergences only the part proportional to F_1 is important for us, as F_2 contains no infrared divergences. With that we get:

$$\begin{aligned} \mathcal{T}_{\text{Vertex}, \lambda} = 2\text{Re} \left(F_1 \frac{\alpha}{\pi} \left(\frac{i4G_F}{\sqrt{2}} \right)^2 \int_{l,q} \text{Tr} \left[\not{p} \gamma^\rho P_L \not{l} \gamma^\sigma P_L \right] \right. \\ \left. \text{Tr} \left[(\not{\psi} + m_e) \gamma_\sigma (\not{q} + m_e) \frac{\alpha}{\pi} \gamma_\rho (g_V - g_A \gamma_5) \right] \right) \end{aligned} \quad (5.14)$$

$$= 2\text{Re}(F_1) \frac{\alpha}{\pi} \mathcal{T}_{\text{Tree}} . \quad (5.15)$$

When we only keep the infrared divergent part of the formfactor, we are left with:

$$\mathcal{T}_{\text{Vertex}, \lambda} = -2 \frac{e^2}{(2\pi)^2} \ln \frac{\lambda}{m_e} \left[1 + \frac{1 + \theta^2}{1 - \theta^2} \ln \theta \right] \mathcal{T}_{\text{Tree}} \quad (5.16)$$

$$\theta = \left| \frac{1 - \sqrt{1 - \frac{4m_e^2}{P^2}}}{1 + \sqrt{1 - \frac{4m_e^2}{P^2}}} \right| . \quad (5.17)$$

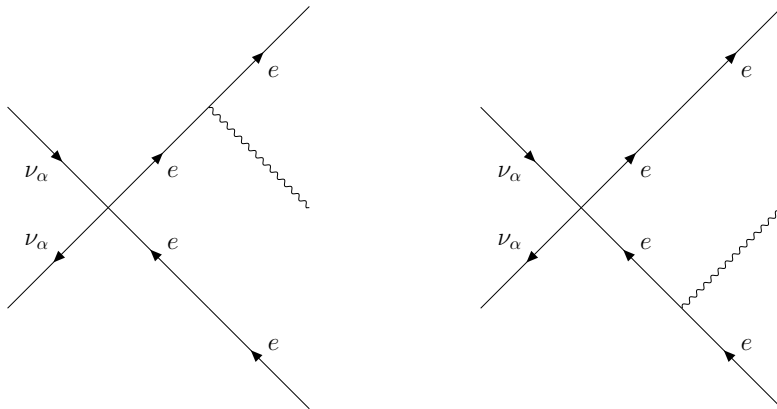


Figure 5.6: The real emission diagrams that cancel out the infrared divergence of the virtual diagram. Note that we have to take the square of the absolute value of the sum of these two diagrams.

This obviously now begs the question how to cancel this infrared divergence. As this is standard vacuum theory, there is also a standard answer: Also include real emission diagrams [37]. Real emission diagrams are diagrams in which a real photon gets emitted (see figure 5.6).

Now, one could argue that this is a different process because we have different particles in the final state. However, we can choose the photon energy so low that the detectors are not able to detect them. This holds not only practically, but also theoretically, because of the uncertainty principle. We can find the different contributions in the Ladybug, Donut and in the Baseball diagram. The squared terms lie in the Ladybug and Donut diagram, while the mixed term lies in the Baseball diagram (see figure 5.7). You can see this because in the Baseball diagram the photon connects to the upper and lower leg of the electron loop while in the Donut and Ladybug diagram it only connects to the upper or lower leg.

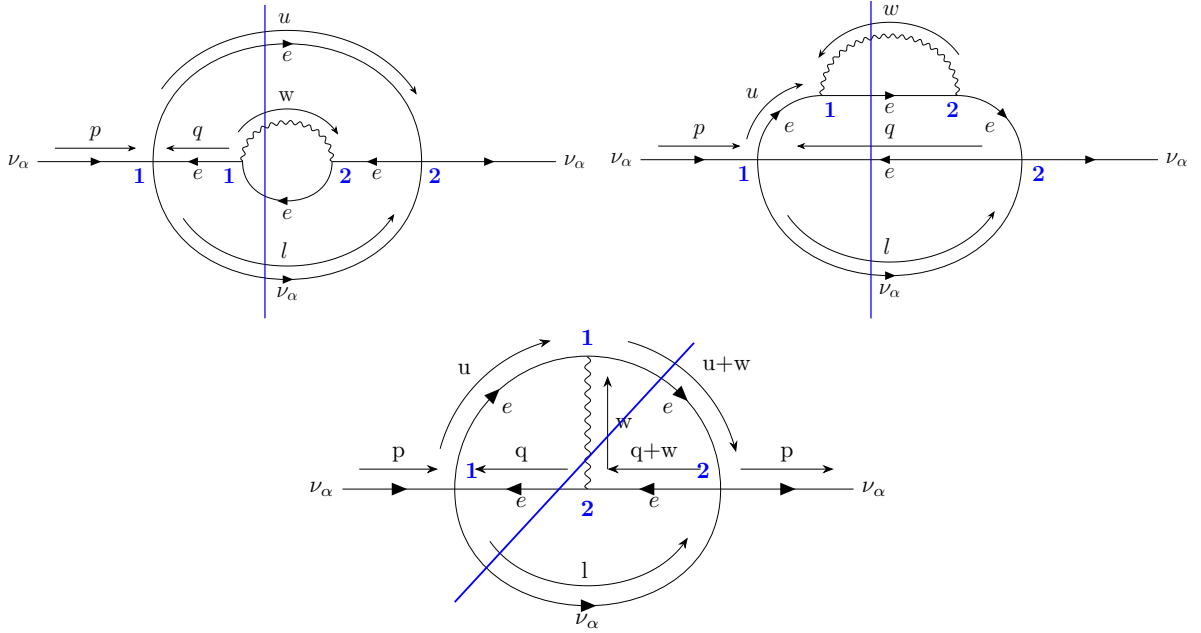


Figure 5.7: The parts of the NLO diagrams that contain the real emission diagrams.

For the soft part of the rate we can use the soft photon approximation (see section 5.2.1). With that we get the following for the soft interaction rate:

$$\mathcal{T}_{\text{soft}} = -e^2 \int_w \left[\underbrace{\frac{m_e^2}{(q \cdot w)^2}}_{\text{Donut}} + \underbrace{\frac{m_e^2}{(u \cdot w)^2}}_{\text{Ladybug}} - 2 \underbrace{\frac{(q \cdot u)}{(q \cdot w)(u \cdot w)}}_{\text{Baseball}} \right] 2\pi \delta(w^2) [f_B(|w_0|) + \theta(w_0)] \mathcal{T}_{\text{LO}} . \quad (5.18)$$

In the soft rate, there are now two parts. One part is proportional to $\theta(w_0)$. This is the vacuum-like part, which cancels the infrared divergence of the virtual correction. The theta function forces the photon to have a positive energy, as it should have as a real photon. The other part, which is proportional to $f_B(|w_0|)$ gives an additional thermal contribution. This thermal

contribution is also infrared divergent. Its even a stronger divergence as $f_B(|w_0|) \propto \frac{1}{|w_0|}$ for small w_0 . We will see how this cancels later in section 5.2.3. For now we just look at the vacuum term.

$$\mathcal{T}_{\text{soft}}^{\text{vac}} = -e^2 \int_w \left[\underbrace{\frac{m_e^2}{(-q \cdot w)^2}}_{\text{Donut}} + \underbrace{\frac{m_e^2}{(u \cdot w)^2}}_{\text{Ladybug}} - 2 \underbrace{\frac{(q \cdot u)}{(-q \cdot w)(u \cdot w)}}_{\text{Baseball}} \right] 2\pi \delta(w^2 - \lambda^2) \theta(w_0) \mathcal{T}_{\text{LO}}. \quad (5.19)$$

The minus in front of the q is induced because the momentum was defined in the opposite direction in the soft-photon approximation. This can be evaluated with the integral of section A.4. When we focus only on the infrared divergent part of the integrals, we get:

$$I_{ab} = \int_{0 \leq \mathbf{w} \leq \Delta} \frac{d^3 w}{w_0} \frac{(a \cdot b)}{(w \cdot a)(w \cdot b)} \Rightarrow I_{aa}^\lambda = 2\pi \ln \frac{4\Delta^2}{\lambda^2}, \quad I_{ab}^\lambda = \frac{2\pi \alpha (a \cdot b)}{(\alpha a)^2 - b^2} \ln \frac{4\Delta^2}{\lambda^2} \ln \frac{(\alpha a)^2}{b^2}, \quad (5.20)$$

where α is defined by $(\alpha a - b)^2 = 0$ and $\frac{\alpha a_0 - b_0}{b_0} > 0$. When calculating α it makes sense to write it in terms of P to see the connection to θ of the virtual correction (5.17). We therefore use $(q \cdot u) = m_e^2 - \frac{P^2}{2}$:

$$\begin{aligned} \alpha^2 m_e^2 + 2\alpha (q \cdot u) + m_e^2 &= \alpha^2 m_e^2 - \alpha(P^2 - 2m_e^2) + m_e^2 \\ \Rightarrow \alpha_\pm &= \frac{-2m_e^2 + P^2 \pm \sqrt{P^2(P^2 - 4m_e^2)}}{2m_e^2}. \end{aligned} \quad (5.21)$$

In fact, $\frac{\alpha(-q_0) - u_0}{u_0} > 0$ is only fully filled for α_- . Now we define $\beta = \sqrt{1 - \frac{4m_e^2}{P^2}}$ and multiply by $\frac{\frac{1}{2m_e}(1+\beta)}{\frac{1}{2m_e}(1+\beta)}$ we then get:

$$\begin{aligned} \alpha &= \frac{\frac{1}{2m_e^2} (-2m_e^2 + P^2 + \beta(-2m_e^2 + P^2 - P^2) - (P^2 - 4m_e^2))}{1 + \beta} \\ &= \frac{1 - \beta}{1 + \beta}. \end{aligned} \quad (5.22)$$

You can see that the absolute values of α and θ are the same. Inserting this into equation (5.19) we get:

$$\begin{aligned} \mathcal{T}_{\text{soft}}^{\text{vac}} &= -\frac{e^2}{(2\pi)^3} \left(\frac{I_{qq}}{2} + \frac{I_{uu}}{2} - 2 \frac{I_{-qu}}{2} \right) \\ &= -\frac{1}{2} \frac{e^2}{(2\pi)^3} \left(4\pi \ln \frac{4\Delta^2}{\lambda^2} - 4\pi \frac{\alpha(-q \cdot u)}{(\alpha q)^2 - u^2} \ln \frac{4\Delta^2}{\lambda^2} \ln \frac{(\alpha q)^2}{u^2} \right) \mathcal{T}_{\text{LO}} \end{aligned} \quad (5.23)$$

$$\begin{aligned}
 \mathcal{T}_{\text{soft}}^{\text{vac}} &= -\frac{e^2}{(2\pi)^2} \left(\ln \frac{4\Delta^2}{\lambda^2} - \left(\frac{-1}{2} \frac{1+\alpha^2}{1-\alpha^2} \right) \ln \frac{4\Delta^2}{\lambda^2} \ln \alpha^2 \right) \mathcal{T}_{\text{LO}} \\
 &= 2 \frac{e^2}{(2\pi)^2} \ln \frac{\lambda}{4\Delta} \left(1 + \frac{1+\theta^2}{1-\theta^2} \ln \theta \right) \mathcal{T}_{\text{LO}} .
 \end{aligned} \tag{5.24}$$

Now you can see that λ is exactly canceling out if we take the sum of the infrared divergent part of the virtual correction and the infrared divergent part of the real correction:

$$\mathcal{T}_{\text{soft}}^{\text{vac}} + \mathcal{T}_{\text{Vertex}, \lambda} = 2 \frac{e^2}{(2\pi)^2} \ln \frac{m_e}{4\Delta} \left(1 + \frac{1+\theta^2}{1-\theta^2} \ln \theta \right) \mathcal{T}_{\text{LO}} . \tag{5.25}$$

We therefore can see that our total rate is finite, as it should. This cancellation is also a good numerical check that everything was calculated correctly.

5.2.3 Thermal infrared divergences

Now it is still left to cancel the thermal infrared divergence that we left out during our considerations in the last chapter. For this cancellation, we need another part of the diagram with an infrared divergence, a Bose-Einstein distribution, and an on-shell photon. This divergence is found in the “thermal cut” through the photon propagator (see figure 5.8). By a “thermal cut”, we mean the part of the 11 or 22 propagator that contains a δ -distribution. Of course, this only cancels the Baseball part from equation (5.18). To cancel the other parts, we would need the corresponding pieces from the Ladybug and Donut diagram. As these parts are out of the scope of this work, we will only focus on the part canceling the remaining thermal divergence from the real emission diagram of the Baseball.

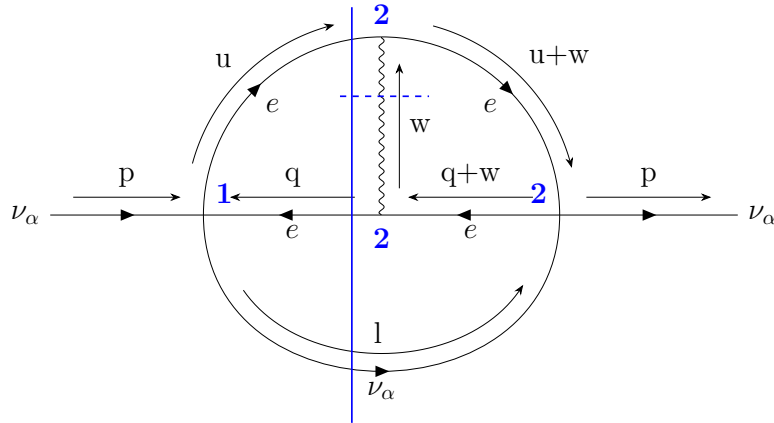


Figure 5.8: By the dashed blue line we mean the thermal part of the 22 propagator. In a sense this is a „thermal cut“ because it sets the photon on-shell.

For this we do not have to calculate the integrals because we can see that the two rates get the

same form for $w \rightarrow 0$ with a different sign. The rate for the thermal cut through the photon line is given by:

$$\mathcal{T}_{\text{Thermal}}^\gamma = 2\text{Re} \left(-e^2 \left(\frac{i4G_F}{\sqrt{2}} \right)^2 \int_{l,q,w} \text{Tr} [\not{p}\gamma^\rho P_L \not{l}\gamma^\sigma P_L] \right) \quad (5.26)$$

$$\begin{aligned} & \times \text{Tr} \left[(\not{\psi} + m_e)\gamma_\sigma (g_V - g_A\gamma_5)(\not{q} + m_e)\gamma_\mu (\not{q} + \not{\psi} + m_e)\gamma_\rho (g_V - g_A\gamma_5)(\not{\psi} + \not{\psi} + m_e)\gamma_\nu \right] \\ & \times \frac{i}{(q+w)^2 - m_e^2 - i\epsilon} \frac{i}{(u+w)^2 - m_e^2 - i\epsilon} (2\pi)^4 \delta(l^2) \delta(q^2 - m_e^2) \delta(u^2 - m_e^2) \delta(w^2) \end{aligned} \quad (5.27)$$

$$\times [f_D(|l_0|) - \theta(-l_0)][f_D(|q_0|) - \theta(q_0)][f_D(|u_0|) - \theta(-u_0)][f_B(|w_0|)] \Big) . \quad (5.28)$$

Due to the soft photon approximation we can drop all terms in the numerator. The Traces then get a direct connection to the Tree-level traces, and we get:

$$\mathcal{T}_{\text{Thermal}}^\gamma = -2\text{Re} \left(e^2 \int_w \frac{1}{(q+w)^2 - m_e^2 - i\epsilon} \frac{1}{(u+w)^2 - m_e^2 - i\epsilon} 2\pi\delta(w^2) f_B(|w_0|) 4(q \cdot u) \mathcal{T}_{\text{LO}} \right) \quad (5.29)$$

$$= -2\text{Re} \left(e^2 \int_w \frac{1}{2(q \cdot w) - i\epsilon} \frac{1}{2(u \cdot w) - i\epsilon} 2\pi\delta(w^2) f_B(|w_0|) 4(q \cdot u) \mathcal{T}_{\text{LO}} \right) . \quad (5.30)$$

It is important to note that the minus comes in because we also have one additional minus from the fermion loop in the Tree-level interaction rate. The scalar products $(q \cdot w)$ and $(u \cdot w)$ are only zero when w is zero. This is the only possibility because $|q_0| > \mathbf{q}$, $|u_0| > \mathbf{u}$. Therefore, we can disregard $i\epsilon$

$$\mathcal{T}_{\text{Thermal}}^\gamma = -2e^2 \int_w \frac{(q \cdot u)}{(q \cdot w)(u \cdot w)} 2\pi\delta(w^2) f_B(|w_0|) \mathcal{T}_{\text{LO}} . \quad (5.31)$$

We can compare this with the part that we have previously neglected:

$$\mathcal{T}_{\text{soft}}^{\text{therm}} = -e^2 \int_w \left[\underbrace{\frac{m_e^2}{(q \cdot w)^2}}_{\text{Donut}} + \underbrace{\frac{m_e^2}{(u \cdot w)^2}}_{\text{Ladybug}} - 2 \underbrace{\frac{(q \cdot u)}{(q \cdot w)(u \cdot w)}}_{\text{Baseball}} \right] 2\pi\delta(w^2) f_B(|w_0|) \mathcal{T}_{\text{LO}} \quad (5.32)$$

In the limit $w \rightarrow 0$, the term $\mathcal{T}_{\text{Thermal}}^\gamma$ exactly cancels the Baseball contribution from $\mathcal{T}_{\text{soft}}^{\text{therm}}$. The other parts are canceled with parts of the Donut or Ladybug diagram. In the vacuum calculation, we have to add a finite part for the integral between 0 and ΔE , this is not needed here, as both contributions get exactly the same for $w \rightarrow 0$.

5.3 Baseball

The Baseball diagram (see figure 5.1) has an interesting structure. First of all, it contains the virtual vertex correction in the 11 and 22 elements. This contribution is infrared and UV-divergent. To eliminate the UV-divergence, one must renormalize the electron wavefunction. This corresponds to including the counter term. To cancel the infrared divergence one has to find the real emission diagrams (see also section 5.2) in the remaining diagrams that cancel the infrared divergence. The mixed term of the real emission diagram lies in the 12 or 21 parts of the Baseball diagram, the squared terms lie in the Donut and Ladybug diagram. To get a finite result we therefore have to include the real emission parts of the Donut and Ladybug diagram.

Similarly to the Frog calculation we can find the following connections (see for more details section B.6):

$$\text{Tr} \left[i\Sigma_{\text{Baseball}}^{12,22} \not{p} \right] = \text{Tr} \left[i\Sigma_{\text{Baseball}}^{12,11} \not{p} \right]^* \quad (5.33)$$

$$\text{Tr} \left[i\Sigma_{\text{Baseball}}^{12,12} \not{p} \right] = \text{Tr} \left[i\Sigma_{\text{Baseball}}^{12,21} \not{p} \right]^* . \quad (5.34)$$

With that we can write the sum over all CTP indices as:

$$\text{Tr} \left[i\Sigma_{\text{Baseball}}^{12} \not{p} \right] = 2\text{Re} \left(\text{Tr} \left[i\Sigma_{\text{Baseball}}^{12, 22} \not{p} \right] + \text{Tr} \left[i\Sigma_{\text{Baseball}}^{12, 21} \not{p} \right] \right) . \quad (5.35)$$

This then corresponds to the diagrams in Figure 5.9

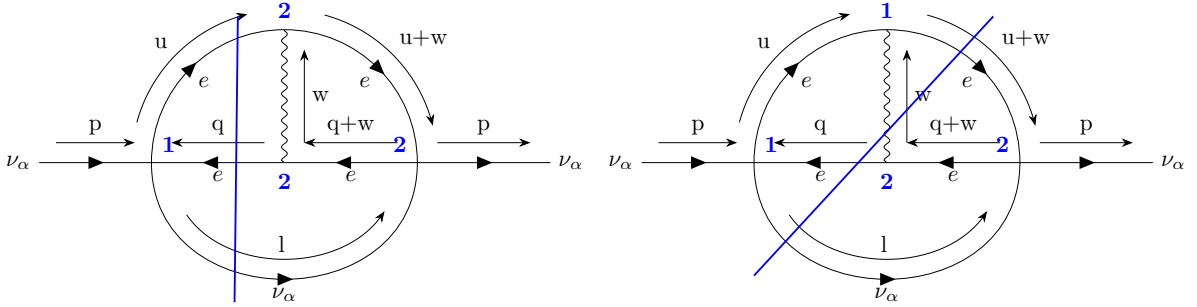


Figure 5.9: The two parts of the Baseball diagram that together form the sum over all CTP indices.

The rate of these diagrams is given by:

$$\begin{aligned} \text{Tr} \left[i\Sigma_{\text{Baseball}}^{12, cd} \not{p} \right] &= (-1)^{1+2+c+d+1} (ie)^2 \left(\frac{i4G_F}{\sqrt{2}} \right)^2 \int_{l,q,w} \text{Tr} \left[\not{p} \gamma^\rho P_L iS_{\nu_\alpha}^{12}(l) \gamma^\sigma P_L \right] iD_{\mu\nu}^{cd}(w) \\ &\quad \times \text{Tr} \left[iS_e^{d2}(u+w) \gamma_\mu iS_e^{1d}(u) \gamma_\sigma (P_L g_L + P_R g_R) iS_e^{c1}(q) \right. \\ &\quad \left. \times \gamma_\nu iS_e^{2c}(q+w) \gamma_\rho (P_L g_L + P_R g_R) \right] , \end{aligned} \quad (5.36)$$

where c and d denote the internal CTP indices. First we notice that in the $\text{Tr} \left[i\Sigma_{\text{Baseball}}^{12, 21} \not{p} \right]$ diagram if we set u or q on-shell, by using the thermal part of the 11 or 22 propagator we would get a QED vertex with all particles on shell, which is kinematically forbidden. We therefore deduce that this part does not have thermal contributions, as the thermal contribution of one of the u or q propagators would also force them to be on-shell. For $\text{Tr} \left[i\Sigma_{\text{Baseball}}^{12, 22} \not{p} \right]$ this is not the case. It is therefore again instructive to define a vacuum rate and a thermal rate. They are defined through the following

$$\text{Tr} \left[i\Sigma_{\text{Baseball}}^{12, 22} \not{p} \right] = \int_{l,q} (2\pi)^3 \delta(l^2) \delta(q^2 - m_e^2) \delta(u^2 - m_e^2) \mathcal{F}(l_0, q_0, u_0) (\mathcal{T}_{\text{Vacuum}} + \mathcal{T}_{\text{Thermal}}), \quad (5.37)$$

where we have pulled the integral over w into the rates \mathcal{T} . The thermal distribution functions are contained in the population factor:

$$\mathcal{F}(l_0, q_0, u_0) = [f_D(|l_0|) - \theta(-l_0)][f_D(|q_0|) - \theta(q_0)][f_D(|u_0|) - \theta(-u_0)]. \quad (5.38)$$

Now again $\mathcal{T}_{\text{Vacuum}}$ and $\mathcal{T}_{\text{Thermal}}$ are defined in such a way that $\mathcal{T}_{\text{Vacuum}}$ is not temperature dependent and directly connects to the terms we would also find in the Boltzmann formalism, while $\mathcal{T}_{\text{Thermal}}$ is a temperature-dependent correction. We could of course do the same for the 22 diagram. But there we would have distribution functions of four particles in the population factor, as we have an additional real photon.

To summarize, we get the following parts of the diagrams in figure 5.9 that we have to calculate now. Here we make a differentiation in the thermal corrections. The term “thermal cut” refers to the component of the 11 or 22 propagator that includes a δ -distribution. The other part of the 11 or 22 propagator would in a sense be the vacuum part of the propagator.

- $\text{Tr} \left[i\Sigma_{\text{Baseball}}^{12, 12} \not{p} \right] \left(\text{Tr} \left[i\Sigma_{\text{Ladybug}}^{12, 12} \not{p} \right], \text{Tr} \left[i\Sigma_{\text{Donut}}^{12, 12} \not{p} \right] \right)$
 - real emission diagrams, where we also include the Ladybug and Donut contributions (vacuum part)
 - no thermal corrections
- $\text{Tr} \left[i\Sigma_{\text{Baseball}}^{12, 12} \not{p} \right]$
 - virtual vertex correction (vacuum part)
 - additional thermal cut through photon propagator
 - additional thermal cut through electron or positron propagator
 - additional thermal cut through electron and positron propagator

In the $\text{Tr} \left[i\Sigma_{\text{Baseball}}^{12, 12} \not{p} \right]$ part there are now thermal cuts through the photon line and another line, as this is kinematically forbidden. This will also be the structure of this section.

5.3.1 Real emission diagrams

The real emission diagrams are contained in the diagrams in figure 5.6. We, of course, now have to define a different population factor \mathcal{F} as we now have five particles that are on-shell. We are also transforming $q \leftrightarrow -u$ and $w \rightarrow -w$ in the Donut diagram to bring the population factor and the delta distributions in the same form as it is in the other diagrams. Further we can safely neglect $i\epsilon$ in the propagator because the phase space region where $u^2 = m_e^2$ and $(q+w)^2 = m_e^2$ is kinematically forbidden. The rates are then given by:

$$\text{Tr} \left[i\Sigma_{\text{Ladybug}}^{12,12} \not{p} \right] = -(ie)^2 \left(\frac{i4G_F}{\sqrt{2}} \right)^2 \int_{l,q,w} \text{Tr} \left[\not{p} \gamma^\rho P_L \not{l} \gamma^\sigma P_L \right] \frac{(-g^{\mu\nu})\mathcal{P}}{[u^2 - m_e^2]^2} \quad (5.39)$$

$$\times \text{Tr} \left[(\not{\psi} + \not{\psi} + m_e) \gamma_\mu (\not{\psi} + m_e) \gamma_\sigma (P_L g_L + P_R g_R) (\not{q} + m_e) \gamma_\rho (P_L g_L + P_R g_R) (\not{\psi} + m_e) \gamma_\nu \right]$$

$$\text{Tr} \left[i\Sigma_{\text{Donut}}^{12,12} \not{p} \right] = -(ie)^2 \left(\frac{i4G_F}{\sqrt{2}} \right)^2 \int_{l,q,w} \text{Tr} \left[\not{p} \gamma^\rho P_L \not{l} \gamma^\sigma P_L \right] \frac{(-g^{\mu\nu})\mathcal{P}}{[u^2 - m_e^2]^2} \quad (5.40)$$

$$\times \text{Tr} \left[(\not{q} + \not{\psi} - m_e) \gamma_\mu (\not{q} - m_e) \gamma_\sigma (P_L g_L + P_R g_R) (\not{\psi} - m_e) \gamma_\rho (P_L g_L + P_R g_R) (\not{q} - m_e) \gamma_\nu \right]$$

$$\text{Tr} \left[i\Sigma_{\text{Baseball}}^{12,12} \not{p} \right] = -(ie)^2 \left(\frac{i4G_F}{\sqrt{2}} \right)^2 \int_{l,q,w} \text{Tr} \left[\not{p} \gamma^\rho P_L \not{l} \gamma^\sigma P_L \right] \frac{(-g^{\mu\nu})\mathcal{P}}{[u^2 - m_e^2][(q+w)^2 - m_e^2]} \quad (5.41)$$

$$\times \text{Tr} \left[(\not{\psi} + \not{\psi} + m_e) \gamma_\mu (\not{\psi} + m_e) \gamma_\sigma (P_L g_L + P_R g_R) (\not{q} + m_e) \gamma_\nu (\not{q} + \not{\psi} + m_e) \gamma_\rho (P_L g_L + P_R g_R) \right]$$

You can already see, that the Baseball diagram will be more involved to evaluate, due to the more complicated propagator structure. The phase space factor \mathcal{P} is defined as:

$$\begin{aligned} \mathcal{P} = & (2\pi)^4 \delta(l^2) \delta(w^2) \delta(q^2 - m_e^2) \delta((u+w)^2 - m_e^2) [f_D(|l_0|) - \theta(-l_0)] \\ & \times [f_D(|q_0|) - \theta(q_0)] [f_D(|u_0 + w_0|) - \theta(-u_0 - w_0)] [f_B(|w_0|) + \theta(w_0)] \end{aligned} \quad (5.42)$$

Also note that the opposing parts $\text{Tr} \left[i\Sigma_{\text{Ladybug}}^{12,21} \not{p} \right] = \text{Tr} \left[i\Sigma_{\text{Donut}}^{12,21} \not{p} \right] = 0$ for the Ladybug and Donut diagrams are just zero because all particles of a QED-vertex would be on-shell, which is kinematically forbidden. This does not hold for the Baseball diagram. We have $\text{Tr} \left[i\Sigma_{\text{Baseball}}^{12,21} \not{p} \right] = \text{Tr} \left[i\Sigma_{\text{Baseball}}^{12,12} \not{p} \right]^*$ this is where the mixed terms get their factor of two of.

Because of the structure of the δ -distributions and the propagator, it is now sensible to choose a different parameterization for the integral. We can see that only the momentum $P = p - l$ flows into the electron loop. That is why we choose the following:

$$\mathbf{p} = |\mathbf{p}| \begin{pmatrix} 0 \\ 0 \\ 1 \end{pmatrix}, \quad \mathbf{l} = |\mathbf{l}| \begin{pmatrix} 0 \\ \sin(\alpha) \\ \cos(\alpha) \end{pmatrix}, \quad \mathbf{P} = \mathbf{p} - \mathbf{l}, \quad (5.43a)$$

$$\mathbf{q} = |\mathbf{q}| \left(\cos(\theta_q) \hat{P} + \sin \theta_q \sin \beta_q \hat{e}_1 + \sin \theta_q \cos \beta_q \hat{e}_2 \right), \quad (5.43b)$$

$$\mathbf{w} = |\mathbf{w}| \left(\cos(\theta_w) \hat{P} + \sin \theta_w \sin \beta_w \hat{e}_1 + \sin \theta_w \cos \beta_w \hat{e}_2 \right), \quad (5.43c)$$

where \hat{P} , \hat{e}_1 and \hat{e}_2 are unit vectors. Further for the evaluation of $\delta((u+w)^2 - m_e^2)$ it is useful to define:

$$\beta = \beta_q - \beta_w. \quad (5.44)$$

The strategy for these integrals will then be similar to that of section 4.2. For abbreviation purposes, we write the population factor:

$$\mathcal{F} = [f_D(|l_0|) - \theta(-l_0)][f_D(|q_0|) - \theta(q_0)][f_D(|u_0 + w_0|) - \theta(-u_0 - w_0)][f_B(|w_0|) + \theta(w_0)]. \quad (5.45)$$

Also the traces and the propagators are combined in the rate \mathcal{T} . The integral can then be written as

$$\text{Tr} \left[i \Sigma_{\text{Real}}^{12, 12} \not{p} \right] = (2\pi)^4 \int_{l, q, w} \delta(l^2) \delta(q^2 - m_e^2) \delta(w^2) \delta((u+w)^2 - m_e^2) \mathcal{F} \cdot \mathcal{T} \quad (5.46)$$

$$= \frac{1}{(2\pi)^8} \sum_{l_0, q_0, w_0} \int \frac{d^3 l}{2|\mathbf{l}|} \frac{d^3 q}{2E_q} \frac{d^3 w}{2|\mathbf{w}|} \delta((u+w)^2 - m_e^2) \mathcal{F} \cdot \mathcal{T} \quad (5.47)$$

$$= \frac{1}{(2\pi)^7} \frac{1}{2} \sum_{l_0, q_0, w_0} \int_0^\infty d|\mathbf{l}| \int_{-1}^1 d \cos \alpha \int \frac{d^3 q}{2E_q} \frac{d^3 w}{2|w|} \delta((u+w)^2 - m_e^2) \mathcal{F} \cdot \mathcal{T}, \quad (5.48)$$

where the sum \sum_{l_0, q_0, w_0} over the positive and negative energy solution for the corresponding particle was introduced. At this point, we can use $\delta((u+w)^2 - m_e^2)$ for $\cos \beta$. In this parametrization, we get

$$\cos \beta_i = \frac{q_0 w_0 - \cos \theta_q \cos \theta_w |\mathbf{q}| |\mathbf{w}| - \cos \theta_q |\mathbf{P}| |\mathbf{q}| - \cos \theta_w |\mathbf{P}| |\mathbf{w}| + \frac{1}{2}(P_0^2 - |\mathbf{P}|^2) + P_0 q_0 + P_0 w_0}{|\mathbf{q}| |\mathbf{w}| \sin \theta_q \sin \theta_w}. \quad (5.49)$$

We then also have to sum over the solutions for $\sin \beta_i$ because β is integrated over $[0, 2\pi]$.

$$\text{Tr} \left[i \Sigma_{\text{Real}}^{12, 12} \not{p} \right] = \frac{1}{(2\pi)^7} \frac{1}{2} \sum_{l_0, q_0, w_0, \beta_i} \int_0^\infty d|\mathbf{l}| \int_{-1}^1 d \cos \alpha \int \frac{d^3 q}{2E_q} \frac{d^3 w}{2|\mathbf{w}|} \frac{\theta(1 - \cos^2(\beta_i)) \mathcal{F} \cdot \mathcal{T}}{|2|\mathbf{q}| |\mathbf{w}| \sin \theta_q \sin \theta_w \sin \beta_i|} \quad (5.50)$$

The $\theta(1 - \cos^2(\beta_i))$ can be evaluated to get the boundaries for the integral. For that, one has to notice that $\theta(1 - \cos^2(\beta_i)) = \theta(az^2 + bz + c)$, where $z = \cos \theta_w$ was introduced. This can be achieved by multiplying $1 - \cos^2(\beta_i)$ with $(2q \sin \beta_i \sin \theta_q \sin \theta_w)^2$

$$a = -4|\mathbf{w}|^2 \left(2 \cos \theta_q |\mathbf{P}| |\mathbf{q}| + |\mathbf{P}|^2 + |\mathbf{q}|^2 \right) < 0 \quad (5.51)$$

$$b = -4|\mathbf{w}| (\cos \theta_q |\mathbf{q}| + |\mathbf{P}|) \left(2 \cos \theta_q |\mathbf{P}| |\mathbf{q}| + |\mathbf{P}|^2 - 2w_0(P_0 + q_0) - P_0(P_0 + 2q_0) \right) \quad (5.52)$$

$$c = - \left(\left(2 \cos \theta_q |\mathbf{P}| |\mathbf{q}| + |\mathbf{P}|^2 - 2w_0(P_0 + q_0) - P_0(P_0 + 2q_0) - 2|\mathbf{q}| |\mathbf{w}| \sin \theta_q \right) \right. \\ \left. \times \left(2 \cos \theta_q |\mathbf{P}| |\mathbf{q}| + |\mathbf{P}|^2 - 2w_0(P_0 + q_0) - P_0(P_0 + 2q_0) + 2|\mathbf{q}| |\mathbf{w}| \sin \theta_q \right) \right). \quad (5.53)$$

We then get the new bounds for the integral over z by solving the quadratic equation. The

solutions are

$$z_{\pm} = -\frac{b}{2a} \pm \sqrt{\left(\frac{b}{2a} - \frac{c}{a}\right)^2}. \quad (5.54)$$

To ensure that the boundaries exist, we introduce $\theta(b^2 - 4ac)$. Putting this back into the integral, we find:

$$\begin{aligned} \text{Tr} \left[i \Sigma_{\text{Real}}^{12, 12} \not{p} \right] &= \frac{1}{(2\pi)^7} \frac{1}{2} \sum_{l_0, q_0, w_0, \beta_i} \int_0^\infty d|\mathbf{l}||\mathbf{l}| \int_{-1}^1 d \cos \alpha \int_0^\infty \frac{d|\mathbf{q}||\mathbf{q}|^2}{2E_q} \int d \cos \theta_q \int d\beta_q \int_0^\infty \frac{d|\mathbf{w}||\mathbf{w}|}{2} \\ &\quad \times \theta(b^2 - 4ac) \int_{z_-}^{z_+} dz \frac{\mathcal{F} \cdot \mathcal{T}}{\sqrt{a} \sqrt{(z_+ - z)(z - z_-)}}. \end{aligned} \quad (5.55)$$

For the Donut and Ladybug diagram we only get factors of z in the numerator, we therefore can use the known integrals we already used in for the LO-diagram (see equation (4.20)). The problem for the Baseball diagram is that the propagator $\frac{1}{(q+w)^2 - m_e^2} = \frac{1}{P^2 + P(q+w)}$ contains a z . The integrals are therefore more involved. For these integrals, we have to use:

$$\int_{z_-}^{z_+} dz \frac{1}{\sqrt{(z_+ - z)(z - z_-)}} \frac{1}{d + ez} = \frac{\pi}{\sqrt{d + ez_-} \sqrt{d + ez_+}} \quad (5.56)$$

$$\int_{z_-}^{z_+} dz \frac{z}{\sqrt{(z_+ - z)(z - z_-)}} \frac{1}{d + ez} = \frac{\pi \left(-d \left(\sqrt{\frac{d + ez_-}{d + ez_+}} + 1 \right) + ez_- \right)}{e(d + ez_-)} \quad (5.57)$$

$$\int_{z_-}^{z_+} dz \frac{z^2}{\sqrt{(z_+ - z)(z - z_-)}} \frac{1}{d + ez} = \frac{\pi \left(2d \left(\frac{d \sqrt{\frac{d + ez_-}{d + ez_+}}}{d + ez_-} - 1 \right) + e(z_- + z_+) \right)}{2e^2}. \quad (5.58)$$

These integrals hold only when $0 < d + ez_- < d + ez_+$ or when $d + ez_- < d + ez_+ < 0$, in the case that $d + ez_- < 0 < d + ez_+$ the integrals would diverge, but this phase space area is kinematically forbidden. We further can analytically integrate over β_q as $\cos \beta_q$ and $\sin \beta_q$ only appear in the numerator in \mathcal{T} . The last step we are going to take is now numerically important. As we know, the integral diverges in the area where $w \rightarrow 0$. But also $z_+ - z_- \rightarrow 0$. That means that the integrator does not find the phase space area where we get a contribution. The integral becomes then very expensive to evaluate in the regions where $w \ll m_e$. We therefore should evaluate $\theta(b^2 - 4ac)$ into boundaries to make sure that the integration routine also works for small w .

$$b^2 - 4ac =$$

$$\begin{aligned} &16 \left(\cos^2 \theta_q - 1 \right) |\mathbf{q}|^2 |\mathbf{w}|^2 \left[-2|\mathbf{P}|^2 \left(2 \left(-\cos^2 \theta_q |\mathbf{q}|^2 + q_0 w_0 + |\mathbf{w}|^2 \right) + P_0^2 + 2P_0(q_0 + w_0) \right) \right. \\ &\quad + 4 \cos \theta_q |\mathbf{P}|^3 |\mathbf{q}| - 4 \cos \theta_q |\mathbf{P}| |\mathbf{q}| \left(P_0^2 + 2P_0(q_0 + w_0) + 2 \left(q_0 w_0 + |\mathbf{w}|^2 \right) \right) + |\mathbf{P}|^4 \\ &\quad \left. + \left(P_0^2 + 2w_0(P_0 + q_0) + 2P_0 q_0 + 2|\mathbf{q}||\mathbf{w}| \right) \left(P_0^2 + 2P_0(q_0 + w_0) - 2|\mathbf{q}||\mathbf{w}| + 2q_0 w_0 \right) \right] \end{aligned} \quad (5.59)$$

In general, this is a polynomial of fourth degree. This would be very tedious to solve. But when we realize that these are just two polynomials of second degree multiplied, the evaluation simplifies drastically. As $\cos^2 \theta_q - 1 \leq 0$ we can divide by $-16 (\cos^2 \theta_q - 1) |\mathbf{q}|^2 |\mathbf{w}|^2$ and still do not change the θ -function. The remaining polynomial $\tilde{a} \cos^2 \theta_q + \tilde{b} \cos \theta_q + \tilde{c}$ with:

$$\tilde{a} = -4|\mathbf{P}|^2 |\mathbf{q}|^2 < 0 \quad (5.60)$$

$$\tilde{b} = -4|\mathbf{P}|^3 |\mathbf{q}| + 4|\mathbf{P}| P_0^2 |\mathbf{q}| + 8|\mathbf{P}| P_0 |\mathbf{q}| q_0 + 8|\mathbf{P}| P_0 |\mathbf{q}| w_0 + 8|\mathbf{P}| |\mathbf{q}| q_0 w_0 + 8|\mathbf{P}| |\mathbf{q}| |\mathbf{w}|^2 \quad (5.61)$$

$$\begin{aligned} \tilde{c} = & -|\mathbf{P}|^4 + 2|\mathbf{P}|^2 P_0^2 + 4|\mathbf{P}|^2 P_0 q_0 + 4|\mathbf{P}|^2 P_0 w_0 + 4|\mathbf{P}|^2 q_0 w_0 + 4|\mathbf{P}|^2 |\mathbf{w}|^2 - P_0^4 - 4P_0^3 q_0 \\ & - 4P_0^3 w_0 - 4P_0^2 q_0^2 - 12P_0^2 q_0 w_0 - 4P_0^2 w_0^2 - 8P_0 q_0^2 w_0 - 8w_0 P_0 w_0^2 + 4|\mathbf{q}|^2 |\mathbf{w}|^2 - 4q_0^2 w_0^2 . \end{aligned} \quad (5.62)$$

We then get for the integration over $\cos \theta_q$ the bounds

$$\tilde{z}_{\pm} = -\frac{\tilde{b}}{2\tilde{a}} \pm \sqrt{\left(\frac{\tilde{b}}{2\tilde{a}} - \frac{\tilde{c}}{\tilde{a}}\right)^2} . \quad (5.63)$$

And we have to introduce $\theta(\tilde{b}^2 - 4\tilde{a}\tilde{c})$ to ensure that \tilde{z}_{\pm} exists. It should be noted that we could again use $\theta(\tilde{b}^2 - 4\tilde{a}\tilde{c})$ to find boundaries for $\cos \alpha$ but this numerically is only a minor change; that is why we are not going to do it. Using the integrals of equation (4.20) or (5.56) we get an analytical term for $\int d\beta \int_{z_-}^{z_+} dz \frac{\sum \beta_i \mathcal{T}}{\sqrt{(z_+ - z)(z - z_-)}} = \mathcal{Z}$ and the end result

$$\begin{aligned} \text{Tr} \left[i\Sigma_{\text{Real, hard}}^{12, 12} \not{p} \right] = & \frac{1}{(2\pi)^7} \frac{1}{8} \int_0^\infty d|\mathbf{l}| |\mathbf{l}| \int_{-1}^1 d \cos \alpha \int_0^\infty \frac{d|\mathbf{q}| |\mathbf{q}|^2}{E_q} \int_{\tilde{z}_-}^{\tilde{z}_+} d \cos \theta_q \\ & \times \int_{\Delta E}^\infty d|\mathbf{w}| |\mathbf{w}| \frac{\theta(\tilde{b}^2 - 4\tilde{a}\tilde{c}) \mathcal{F} \cdot \mathcal{Z}}{\sqrt{\tilde{a}}} , \end{aligned} \quad (5.64)$$

where we have also introduced the cut off ΔE to regularize the infrared divergence, this is therefore only the hard part of the rate. As discussed already in chapter 5.2 there are different contributions in this rate. There is the vacuum part that we would also see in the Boltzmann-formalism, which comes from the $\theta(w_0)$ out of the population factor \mathcal{F} and then there also is the thermal part with the additional Bose-Einstein distribution $f_B(|w_0|)$. The divergence for $f_B(|w_0|)$ cancels with another part (see chapter 5.2) without leaving a finite part of $\int_0^{\Delta E} d\mathbf{w}$. This does not hold for the $\theta(w_0)$ part, that is why we calculated the soft part for that (also in section 5.2). The full result for the real emission diagrams is then given by the sum of the soft and hard part

$$\text{Tr} \left[i\Sigma_{\text{Real}}^{12, 12} \not{p} \right] = \text{Tr} \left[i\Sigma_{\text{Real, soft}}^{12, 12} \not{p} \right] + \text{Tr} \left[i\Sigma_{\text{Real, hard}}^{12, 12} \not{p} \right] . \quad (5.65)$$

For the real emission diagrams there are no more thermal corrections, as the thermal corrections would set all particles of a QED vertex on shell, which is kinematically forbidden.

5.3.2 Vacuum virtual correction

To write the vacuum virtual vertex correction $\mathcal{T}_{\text{Vertex}}$ of figure 5.5 (that we also looked at in section 5.2.2) it is convenient to use the well-known QED form factors [43, 44]. With them we can write:

$$\begin{aligned} \mathcal{T}_{\text{Vertex}} = 2\text{Re} & \left(\left(\frac{i4G_F}{\sqrt{2}} \right) \text{Tr} \left[\not{p} \gamma^\rho P_L \not{l} \gamma^\sigma P_L \right] \right. \\ & \left. \times \text{Tr} \left[(\not{\psi} + m_e) \gamma_\gamma (g_V - g_A \gamma_5) (\not{q} + m_e) \frac{\alpha}{\pi} \left[g_V \left(F_1 \gamma_\rho + F_2 \frac{i\sigma_{\rho\nu} P_\nu}{2m_e} \right) - g_A (F_1 - F_2) \gamma_\rho \gamma_5 \right] \right] \right). \end{aligned} \quad (5.66)$$

Defining $f_{1,2}$ to be the real part of $F_{1,2}$ and evaluating the traces, it yields the result:

$$\begin{aligned} \mathcal{T}_{\text{Vacuum}} = \frac{2^8 \alpha_{\text{em}}}{\pi} & \left(g_V^2 \left[f_1 \left(- (p \cdot l) ((l \cdot q) + m_e^2) + (p \cdot q) ((p \cdot l) + 2(l \cdot q)) \right) + f_2 (p \cdot l)^2 \right] \right. \\ & + g_A^2 \left[(f_1 - f_2) \left((p \cdot l) (- (l \cdot q) + (p \cdot q) + m_e^2) + 2(l \cdot q) (p \cdot q) \right) \right] \\ & \left. + 2g_V g_A \left[f_2 (p \cdot l) ((l \cdot q) + (p \cdot q)) \right] \right). \end{aligned} \quad (5.67)$$

From this point on, to calculate the integrals \int_{q_l} we can use the exact strategy of section 4.2.

It is also possible to use Passarino-Veltman reduction A.2 to evaluate the loop integrals. Then for the evaluation of the scalar integrals one could use `LoopTools` [45], which is a library for optimized evaluation of loop integrals. But this is still slower than the calculation with the formfactors and serves only to verify the results.

5.3.3 Thermal virtual correction - Photon cut

To calculate the photon cut part of the thermal virtual correction we are using the integrals L , L^μ and $L^{\mu\nu}$ (definition in equation (5.89)) that were worked out in section 5.5. The corresponding diagram can be seen in figure 5.8, the divergence of this diagram was already discussed in section 5.2.3. We can then write the rate as:

$$\begin{aligned} \mathcal{T}_{\text{Thermal}}^\gamma = 2\text{Re} & \left((ie)^2 \left(\frac{i4G_F}{\sqrt{2}} \right)^2 \int_w \frac{i}{(u+w)^2 - m_e^2 - i\epsilon} \frac{i}{(q+w)^2 - m_e^2 - i\epsilon} 2\pi\delta(w^2) f_B(|w_0|) \right. \\ & \times \text{Tr} \left[(\not{\psi} + m_e) \gamma_\sigma (g_R P_R + g_L P_L) (\not{q} + m_e) \gamma_\nu (\not{q} + \not{\psi} + m_e) \right. \\ & \quad \left. \times \gamma_\rho (g_R P_R + g_L P_L) (\not{\psi} + \not{\psi} + m_e) \gamma_\mu \right] \\ & \left. \times \text{Tr} \left[\not{p} \gamma^\rho P_L \not{l} \gamma^\sigma P_L \right] (-g^{\mu\nu}) \right). \end{aligned} \quad (5.68)$$

When evaluating the traces, it is possible to drop all terms that contain only one w^μ , because $L^\mu = 0$ these terms simply drop out. For the g_L^2 -terms it was also used that the integrand is invariant under $q \leftrightarrow -u$. In the end, we then get:

$$\begin{aligned} \mathcal{T}_{\text{Thermal}}^\gamma &= \frac{2^9 e^2 G_F^2}{(2\pi)^3} \left(L \left[2(g_R^2 + g_L^2) (l \cdot u) (p \cdot q) (q \cdot u) - 2g_L g_R (l \cdot p) (q \cdot u) m_e^2 \right] \right. \\ &\quad \left. + L_{\mu\nu} \left[(g_R^2 + g_L^2) \{ q^\mu u^\nu (l \cdot p) - p^\mu q^\nu (l \cdot u) + l^\mu p^\nu (q \cdot u) - l^\mu u^\nu (p \cdot q) \} - 2g_L g_R l^\mu p^\nu m_e^2 \right] \right). \end{aligned} \quad (5.69)$$

5.3.4 Thermal virtual correction - Electron cut

The calculation for the thermal correction due to a cut through the electron or positron propagators is similar to the calculation in section 5.3.1, but a bit more involved. We pull the traces and the population factor \mathcal{F} in the function $f(p, l, q, w)$, the corrections from the cut through the electron and through the positron then have the following form.

$$\begin{aligned} \text{Tr} \left[i\Sigma_{e^+ \text{-cut}}^{12,12} \not{p} \right] &= \int_{l,q,w} \frac{1}{w^2 - i\epsilon} \frac{1}{(u+w)^2 - m_e^2 - i\epsilon} f(p, l, q, w) \delta(l^2) \delta(q^2 - m_e^2) \delta(u^2 - m_e^2) \\ &\quad \times \left[-2\pi\delta((q+w)^2 - m_e^2) f_D(|q_0 + w_0|) \right] \end{aligned} \quad (5.70)$$

$$\begin{aligned} \text{Tr} \left[i\Sigma_{e^- \text{-cut}}^{12,12} \not{p} \right] &= \int_{l,q,w} \frac{1}{w^2 - i\epsilon} \frac{1}{(q+w)^2 - m_e^2 - i\epsilon} f(p, l, q, w) \delta(l^2) \delta(q^2 - m_e^2) \delta(u^2 - m_e^2) \\ &\quad \times \left[-2\pi\delta((u+w)^2 - m_e^2) f_D(|u_0 + w_0|) \right] \end{aligned} \quad (5.71)$$

Now we substitute $q \leftrightarrow -u$ and $w \rightarrow -w$ in $\text{Tr} \left[i\Sigma_{e^- \text{-cut}}^{12,12} \not{p} \right]$. We then get the same phase space for both cuts. The result therefore can be written as:

$$\begin{aligned} \text{Tr} \left[i\Sigma_{e^\pm \text{-cut}}^{12,12} \not{p} \right] &= \int_{l,q,w} \frac{1}{w^2 - i\epsilon} \frac{1}{(u+w)^2 - m_e^2 - i\epsilon} [f(p, l, q, w) + f_{q \leftrightarrow -u, w \rightarrow -w}(p, l, q, w)] \\ &\quad \times \left[-2\pi\delta((q+w)^2 - m_e^2) f_D(|q_0 + w_0|) \right] \delta(l^2) \delta(q^2 - m_e^2) \delta(u^2 - m_e^2). \end{aligned} \quad (5.72)$$

To evaluate this, we first look into the structure of the propagator poles. The first propagator has a pole at $w^2 = 0$, but this is forbidden because this would be the point where all particles on a QED vertex are on-shell. We can therefore safely neglect the $+i\epsilon$ in this propagator. Furthermore, we can use the identity

$$\frac{1}{k^2 - m^2 + i\epsilon} = \mathbf{PV} \frac{1}{k^2 - m^2} - i\pi\delta(k^2 - m^2), \quad (5.73)$$

where $\mathbf{P}\mathbf{V}$ denotes the principal value of the integral for the other propagator. Using $(u+w)^2 = 2(P \cdot w)$, we can write

$$\begin{aligned} \text{Tr} \left[i \Sigma_{e^\pm\text{-cut}}^{12,12} \not{p} \right] &= \mathbf{P}\mathbf{V} \int_{l,q,w} \frac{1}{w^2} \frac{1}{2(P \cdot w)} [f(p, l, q, w) + f_{q \leftrightarrow -u, w \rightarrow -w}(p, l, q, w)] \\ &\times [-2\pi \delta((q+w)^2 - m_e^2) f_D(|q_0 + w_0|)] \delta(l^2) \delta(q^2 - m_e^2) \delta(w^2 - m_e^2). \end{aligned} \quad (5.74)$$

We then use the parameterization that was defined for the real emission diagrams in equation (5.43) and (5.44). Evaluating the different δ -distributions, we get:

$$\cos \theta_q = \frac{-|\mathbf{P}|^2 + P_0^2 + 2P_0 q_0}{2|\mathbf{P}||\mathbf{q}|} \quad (5.75)$$

$$\cos \beta_i = \frac{-2 \cos \theta_q \cos \theta_w |\mathbf{q}||\mathbf{w}| + 2q_0 w_0 - |\mathbf{w}|^2 + w_0^2}{2|\mathbf{q}||\mathbf{w}| \sin \theta_q \sin \theta_w}. \quad (5.76)$$

Note that we get two solutions for β_i that we have to sum over. To make sure that $\cos \theta_q$ and $\cos \beta_q$ are both smaller than one we get two θ -functions, namely $\theta(1 - \cos^2 \theta_q)$ and $\theta(1 - \cos^2 \beta)$. The second is a polynomial in $\cos \theta_w$, which has the following form $a \cos^2 \theta_w + b \cos \theta_w + c$ with:

$$a = -4|\mathbf{q}||\mathbf{w}| < 0 \quad (5.77)$$

$$b = 4 \cos \theta_q |\mathbf{q}||\mathbf{w}| (w_0(2q_0 + w_0) - |\mathbf{w}|^2) \quad (5.78)$$

$$c = -4 (\cos^2 \theta_q - 1) |\mathbf{q}|^2 |\mathbf{w}|^2 - (|\mathbf{w}|^2 - w_0(2q_0 + w_0))^2 \quad (5.79)$$

$$z_{\pm} = -\frac{b}{2a} \pm \sqrt{\left(\frac{b}{2a}\right)^2 - \frac{c}{a}}. \quad (5.80)$$

With $z = \cos \theta_w$ the rate reads

$$\begin{aligned} \text{Tr} \left[i \Sigma_{e^\pm\text{-cut}}^{12,12} \not{p} \right] &= \mathbf{P}\mathbf{V} \frac{2\pi}{4} \sum_{l_0, q_0, w_0, \beta_i} \int d|\mathbf{l}| \int_{-1}^1 d \cos \alpha \int d|\mathbf{q}| \int_0^{2\pi} d\beta_q \frac{|\mathbf{l}||\mathbf{q}|^2}{E_q(2|\mathbf{P}||\mathbf{q}|)} \\ &\times \int dw_0 \int d|\mathbf{w}| \frac{|\mathbf{w}|^2}{w_0^2 - |\mathbf{w}|^2} \frac{1}{\sqrt{a}} \int_{z_-}^{z_+} dz \frac{1}{2(P_0 w_0 - |\mathbf{P}||\mathbf{w}|z)} \frac{1}{\sqrt{(z_+ - z)(z - z_-)}} \\ &\times [f(p, l, q, w) + f_{q \leftrightarrow -u, w \rightarrow -w}(p, l, q, w)] [-2\pi f_D(|q_0 + w_0|)]. \end{aligned} \quad (5.81)$$

The introduced sum $\sum_{l_0, q_0, w_0, \beta_i}$ just sums over the two solutions that we get for the variables. At this point now it is possible to do the integral over β_q as there are only $\cos \beta_q$ and $\sin \beta_q$ appearing in $[f(p, l, q, w) + f_{q \leftrightarrow -u, w \rightarrow -w}(p, l, q, w)]$. We can then also use the integrals of equation (5.56) to perform the integral over z . But this time it is possible that $P_0 w_0 - |\mathbf{P}||\mathbf{w}|z_+ < 0 < P_0 w_0 - |\mathbf{P}||\mathbf{w}|z_-$. The integral then includes a pole, which gets regulated by taking the principle value, in this phase space area we have to use the following integrals

for the integration over z

$$\int_{z_-}^{z_+} dz \frac{1}{\sqrt{(z_p - z)(z - z_m)}} \frac{1}{d + ez} = 0 \quad (5.82)$$

$$\int_{z_-}^{z_+} dz \frac{z}{\sqrt{(z_p - z)(z - z_m)}} \frac{1}{d + ez} = \frac{\pi}{e} \quad (5.83)$$

$$\int_{z_-}^{z_+} dz \frac{z^2}{\sqrt{(z_p - z)(z - z_m)}} \frac{1}{d + ez} = \frac{\pi(e(z_m + z_p) - 2d)}{2e^2} . \quad (5.84)$$

5.3.5 Thermal virtual correction - Two cuts

It is now also possible to have to thermal cuts at the same time. This can occur when we put the photon and either the electron or the positron on-shell. But this contribution is kinematically forbidden. The other option is to put the electron and the positron both on-shell. The corresponding rate is given by:

$$\begin{aligned} \text{Tr} \left[i\Sigma_{\text{two-cut}}^{12,12} \not{p} \right] &= \int_{l,q,w} \text{Tr} [\dots] \frac{i}{w^2 - i\epsilon} \delta((u+w)^2 - m_e^2) \delta(l^2) \delta(q^2 - m_e^2) \delta(u^2 - m_e^2) \\ &\quad \times \delta((q+w)^2 - m_e^2) \mathcal{F} . \end{aligned} \quad (5.85)$$

Here we can again use the identity of equation (5.73), to get

$$\begin{aligned} &= \mathbf{PV} \int_{l,q,w} \text{Tr} [\dots] \frac{i}{w^2} \delta((u+w)^2 - m_e^2) \delta(l^2) \delta(q^2 - m_e^2) \delta(u^2 - m_e^2) \delta((q+w)^2 - m_e^2) \mathcal{F} \quad (5.86) \\ &\quad + \int_{l,q,w} \text{Tr} [\dots] \delta(w^2) \delta((u+w)^2 - m_e^2) \delta(l^2) \delta(q^2 - m_e^2) \delta(u^2 - m_e^2) \delta((q+w)^2 - m_e^2) \mathcal{F} . \end{aligned}$$

The first term is just imaginary and therefore cancels out when we perform the sum over the CTP indices. The second term gives zero because it is kinematically forbidden; you can see this by investigating the δ -distributions.

5.4 Donut and Ladybug overview

There are still some parts left for the Donut and Ladybug diagrams. In general, for these diagrams the following holds:

- $\text{Tr} \left[i\Sigma_{\text{Donut \& Ladybug}}^{12,12} \not{p} \right] = \text{Real emissions, already calculated}$
- $\text{Tr} \left[i\Sigma_{\text{Donut \& Ladybug}}^{12,11} \not{p} \right] = \text{Tr} \left[i\Sigma_{\text{Donut \& Ladybug}}^{12,22} \not{p} \right]^*$

- $\text{Tr}\left[i\Sigma_{\text{Donut \& Ladybug}}^{12,21}\right] = 0$ QED-Vertex on-shell .

Therefore, it is only left to calculate

$$\text{Tr}\left[i\Sigma_{\text{Donut \& Ladybug}}^{12,11}\right] + \text{Tr}\left[i\Sigma_{\text{Donut \& Ladybug}}^{12,22}\right] = 2\text{Re}\left(\text{Tr}\left[i\Sigma_{\text{Donut \& Ladybug}}^{12,11}\right]\right) \quad (5.87)$$

The corresponding diagrams to these rates can be seen in figure 5.10. These parts contain the electron self-energy on an outer leg, which is normally absorbed into the mass.

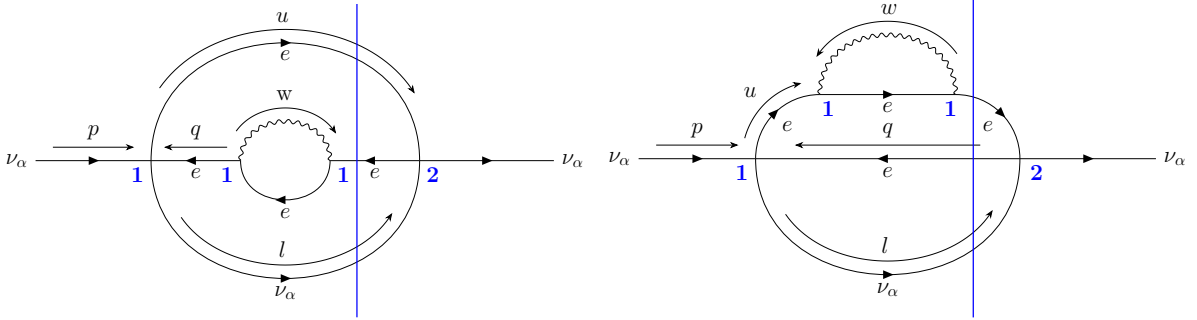


Figure 5.10: The parts of the Donut and Ladybug diagram, that are still left to calculate. Both diagrams contain the electron self-energy on a propagator with an on-shell particle. These diagrams would not arise in the Boltzmann formalism

The parts of these diagrams that contain the electron self-energy on an outer leg contain the following structure, which arises because we have a propagator with momentum q (Donut) or u (Ladybug) and also set that momentum on shell due to the cut trough the diagram:

$$\frac{1}{q^2 - m_e^2 + i\epsilon} \delta(q^2 - m_e^2) = -\frac{1}{2} \delta'(q^2 - m_e^2) - i\pi \delta^2(q^2 - m_e^2), \quad (5.88)$$

where the derivative of the δ -distribution acts as $\delta'(x)f(x) = -\delta(x)f'(x)$. But now we get terms with $\delta^2(q^2 - m_e^2)$, which are known as pinch singularities. These terms, of course, have to cancel, and they do, because they are purely imaginary. This holds for all pinch singularities arising in these diagrams, they are purely imaginary. If we then sum over the CTP-indices they just drop out.

Further, it is important to find the contributions that cancel the remaining infrared divergence of the squared real emission diagrams. This divergence also contains a Bose-Einstein-distribution. It is therefore believed that this divergence gets canceled with the thermal correction to the photon propagator, which sets the photon on-shell and also introduces a Bose-Einstein-distribution.

5.5 Thermal integrals for the photon cut

While calculating the cuts through the photon propagator, we encounter quite complicated integrals. The integrals are given in equation (5.89). It is useful to reduce them analytically as far as we can.

$$L = \int d^4w \frac{1}{(u+w)^2 - m_e^2 - i\epsilon} \frac{1}{(q+w)^2 - m_e^2 - i\epsilon} \delta(w^2) f_B(|w_0|) \quad (5.89a)$$

$$L^\mu = \int d^4w \frac{w^\mu}{(u+w)^2 - m_e^2 - i\epsilon} \frac{1}{(q+w)^2 - m_e^2 - i\epsilon} \delta(w^2) f_B(|w_0|) \quad (5.89b)$$

$$L^{\mu\nu} = \int d^4w \frac{w^\mu w^\nu}{(u+w)^2 - m_e^2 - i\epsilon} \frac{1}{(q+w)^2 - m_e^2 - i\epsilon} \delta(w^2) f_B(|w_0|) \quad (5.89c)$$

I define $P = p - l$, kinematically it holds that $P^2 < 0$ or $P^2 > 4m_e^2$. The other momenta are defined in figure 5.9. It should also be noted that for this diagram $(P \cdot q) = -\frac{P^2}{2}$ holds.

5.5.1 Scalar integral L

First we want to bring the integral into the form that we know from the soft photon limit A.4, but note that we are not using the soft photon approximation here.

$$\begin{aligned} L &= \int d^4w \frac{1}{(u+w)^2 - m_e^2 - i\epsilon} \frac{1}{(q+w)^2 - m_e^2 - i\epsilon} \delta(w^2) f_B(|w_0|) \\ &= \int d^4w \frac{1}{2(u \cdot w)} \frac{1}{2(q \cdot w)} \delta(w^2) f_B(|w_0|) \\ &= \frac{1}{8} \int d^3w \frac{1}{(u \cdot w)} \frac{1}{(q \cdot w)} \frac{f_B(|w^0|)}{\mathbf{w}} \end{aligned} \quad (5.90)$$

When introducing Feynman parameters, one has to be careful not to integrate over 0. Therefore, we have to make different choices depending on whether $P^2 > 0$ or $P^2 < 0$. But first for $P^2 < 0$ we can proceed as follows

$$\begin{aligned} L &= \frac{1}{8} \int d^3w \int_0^1 dx \frac{1}{[x(u \cdot w) + (1-x)(q \cdot w)]^2} \frac{f_B(|w^0|)}{\mathbf{w}} \\ &= \frac{1}{8} \int d^3w \int_0^1 dx \frac{1}{[x(P \cdot w) + (q \cdot w)]^2} \frac{f_B(|w^0|)}{\mathbf{w}} \\ &= \frac{1}{8} \int d^3w \int_0^1 dx \frac{1}{((xP + q) \cdot w)^2} \frac{f_B(|w^0|)}{\mathbf{w}}. \end{aligned} \quad (5.91)$$

Now we can define w in the direction of $Q = xP + q$. That means $(Q \cdot w) = Q_0 w_0 - Qw \cos(\theta)$. So the integral over φ gives a factor of 2π . Also, we have to sum over the two solutions for

$w_0 = \pm w$.

$$L = \frac{\pi}{4} \int d\mathbf{w} w^2 \int_{-1}^1 d\cos(\theta) \int_0^1 dx \sum_{\pm} \frac{1}{(\pm Q_0 - \mathbf{Q} \cos(\theta))^2} \frac{f_B(|\mathbf{w}|)}{w^3} \quad (5.92)$$

This integral converges if $Q_0 > Q$ or $-Q_0 > Q \rightarrow Q^2 > 0 \rightarrow x^2 P^2 + q^2 + 2x(P \cdot q) > 0$ Now we can use that $2(P \cdot q) = -P^2$ to get $\rightarrow x^2 P^2 - xP^2 + q^2 > 0 \rightarrow P^2 < 0$. This was the reason to be careful with the Feynman parameters. Now we can use this integral:

$$\int_{-1}^1 d\cos(\theta) \frac{1}{(\pm Q_0 - \mathbf{Q} \cos(\theta))^2} = \frac{2}{Q^2}. \quad (5.93)$$

As we sum over the sign of Q_0 we get an additional 2.

$$\begin{aligned} L &= \pi \int d\mathbf{w} \int_0^1 dx \frac{1}{Q^2} \frac{f_B(|\mathbf{w}|)}{w} \\ &= \pi \int d\mathbf{w} \frac{f_B(|\mathbf{w}|)}{w} \int_0^1 dx \frac{1}{(x^2 P^2 + 2(P \cdot q)x + q^2)} \\ &= \pi \int d\mathbf{w} \frac{f_B(|\mathbf{w}|)}{w} \int_0^1 dx \frac{1}{(x^2 P^2 - xP^2 + m_e^2)} \end{aligned} \quad (5.94)$$

For the integral over x we use the following:

$$\begin{aligned} \int_0^1 dx \frac{1}{x^2 P^2 - xP^2 + m_e^2} &= 4 \frac{\arctan\left(\frac{\sqrt{P^2}}{\sqrt{4m_e^2 - P^2}}\right)}{\sqrt{P^2} \sqrt{4m_e^2 - P^2}} \\ &= 4 \frac{\arctan\left(i\sqrt{\frac{P^2}{P^2 - 4m_e^2}}\right)}{i\sqrt{P^2(P^2 - 4m_e^2)}} \end{aligned} \quad (5.95)$$

It follows with $\sqrt{\frac{P^2}{P^2 - 4m_e^2}} = \beta$ and $\arctan(ib) = i\frac{1}{2}\operatorname{arctanh}\left(\frac{2b}{b^2 + 1}\right)$ for $b < 0$:

$$\int_0^1 dx \frac{1}{x^2 P^2 - xP^2 + m_e^2} = 2 \frac{\beta}{|P^2|} \operatorname{arctanh}\left(\frac{2\beta}{\beta^2 + 1}\right). \quad (5.96)$$

In the end, we therefore get in the area where $P^2 < 0$:

$$L = 2\pi \frac{\beta}{|P^2|} \operatorname{arctanh}\left(\frac{2\beta}{\beta^2 + 1}\right) \int_0^\infty d\mathbf{w} \frac{f_B(|\mathbf{w}|)}{w}. \quad (5.97)$$

Now for the area where $P^2 > 4m_e^2$ we have to insert a minus to not integrate over 0. But the rest of the calculation is the same.

$$\begin{aligned}
 L &= \int d^4w \frac{1}{(u+w)^2 - m_e^2 - i\epsilon} \frac{1}{(q+w)^2 - m_e^2 - i\epsilon} \delta(w^2) f_B(|w_0|) \\
 &= \frac{1}{8} \int d^3w \frac{-1}{-(u \cdot w)} \frac{1}{(q \cdot w)} \frac{f_B(|w^0|)}{\mathbf{w}} \\
 &= \frac{1}{8} \int d^3w \int_0^1 dx \frac{-1}{[-x(u \cdot w) + (1-x)(q \cdot w)]^2} \frac{f_B(|w^0|)}{\mathbf{w}} \\
 &= \frac{1}{8} \int d^3w \int_0^1 dx \frac{-1}{((-x(u+q) + q) \cdot w)^2} \frac{f_B(|w^0|)}{\mathbf{w}} \tag{5.98}
 \end{aligned}$$

In this case, we choose $Q = (-x(u+q) + q)$. We get the same $\cos\theta$ integral as before. With $Q^2 = x^2(-P^2 + 4m_e^2) - x(-P^2 + 4m_e^2) + m_e^2$:

$$\begin{aligned}
 L &= \pi \int d\mathbf{w} \int_0^1 dx \frac{-1}{Q^2} \frac{f_B(|\mathbf{w}|)}{\mathbf{w}} \\
 &= \pi \int d\mathbf{w} \frac{f_B(|\mathbf{w}|)}{\mathbf{w}} \int_0^1 dx \frac{-1}{(x^2(4m_e^2 - P^2) - x(4m_e^2 - P^2) + q^2)} \tag{5.99}
 \end{aligned}$$

Now we are using:

$$\int_0^1 dx \frac{-1}{(x^2(4m_e^2 - P^2) + x(4m_e^2 - P^2) + m_e^2)} = -4 \frac{\operatorname{arctanh}\left(\sqrt{1 - \frac{4m_e^2}{P^2}}\right)}{\sqrt{P^2(P^2 - 4m_e^2)}} \tag{5.100}$$

We then get in the area where $P^2 > 0$:

$$\begin{aligned}
 L &= \pi \int d\mathbf{w} \frac{f_B(|\mathbf{w}|)}{\mathbf{w}} \int_0^1 dx \frac{-1}{(x^2 P^2 + 2(P \cdot q)x + q^2)} \\
 &= -4\pi \frac{\operatorname{arctanh}\left(\sqrt{1 - \frac{4m_e^2}{P^2}}\right)}{\sqrt{P^2(P^2 - 4m_e^2)}} \int d\mathbf{w} \frac{f_B(|\mathbf{w}|)}{\mathbf{w}} \\
 &= -4\pi \frac{\beta}{|P^2|} \operatorname{arctanh}\left(\frac{1}{\beta}\right) \int d\mathbf{w} \frac{f_B(|\mathbf{w}|)}{\mathbf{w}} . \tag{5.101}
 \end{aligned}$$

The full scalar integral is therefore:

$$L = \begin{cases} 2\pi \frac{\beta}{|P^2|} \operatorname{arctanh}\left(\frac{2\beta}{\beta^2 + 1}\right) \int_0^\infty d\mathbf{w} \frac{f_B(|\mathbf{w}|)}{\mathbf{w}} & \text{if } l_0 > 0 \Leftrightarrow P^2 < 0 \\ -4\pi \frac{\beta}{|P^2|} \operatorname{arctanh}\left(\frac{1}{\beta}\right) \int_0^\infty d\mathbf{w} \frac{f_B(|\mathbf{w}|)}{\mathbf{w}} & \text{if } l_0 < 0 \Leftrightarrow P^2 > 0 \end{cases} \tag{5.102}$$

5.5.2 Vector integral L^μ

$$\begin{aligned} L^\mu &= \int d^4w w^\mu \frac{1}{(u+w)^2 - m_e^2 - i\epsilon} \frac{1}{(q+w)^2 - m_e^2 - i\epsilon} \delta(w^2) f_B(|w_0|) \\ &= \int d^4w \frac{w^\mu}{2(u \cdot w)} \frac{1}{2(q \cdot w)} \delta(w^2) f_B(|w_0|) \end{aligned} \quad (5.103)$$

Now, this integral is an odd function in w . Therefore, it is just zero.

$$L^\mu = 0 \quad (5.104)$$

5.5.3 Tensor integral $L^{\mu\nu}$

In this part, to shorten the expressions, i will use the integrals defined in Appendix B.2. The Tensor Integral contains two scalar products, each including a photon momentum. Now we decompose these scalar products:

$$\begin{aligned} (x \cdot w)(y \cdot w) &= (x_0 w_0 - \vec{x} \vec{w})(y_0 w_0 - \vec{y} \vec{w}) \\ &= x_0 y_0 w_0^2 - (y_0 x_i + x_0 y_i) w_0 w^i + x_i y_j w^i w^j. \end{aligned} \quad (5.105)$$

For the first part that contains w_0^2 we can make the analog calculation as for the scalar integral L but we would get a B_1 integral (see Appendix B.2) form the integral over \mathbf{w} therefore:

$$L_{00} = \begin{cases} 2\pi \frac{\beta}{|P^2|} \operatorname{arctanh}\left(\frac{2\beta}{\beta^2 + 1}\right) T_1 & \text{if } l_0 > 0 \Leftrightarrow P^2 < 0 \\ -4\pi \frac{\beta}{|P^2|} \operatorname{arctanh}\left(\frac{1}{\beta}\right) T_1 & \text{if } l_0 < 0 \Leftrightarrow P^2 > 0. \end{cases} \quad (5.106)$$

For the second part, after defining $w_i = \hat{Q}_i \cos(\theta) + \vec{e}_{1i} \sin(\theta) \sin(\varphi) + \vec{e}_{2i} \sin(\theta) \cos(\varphi)$ we get the integral:

$$L^{0i} = \frac{1}{8} \int d^3w \int_0^1 dx \frac{w_0 \mathbf{w} (\hat{Q}_i \cos(\theta) + \vec{e}_{1i} \sin(\theta) \sin(\varphi) + \vec{e}_{2i} \sin(\theta) \cos(\varphi)) f_B(|\mathbf{w}|)}{(\pm Q_0 - \mathbf{Q} \cos(\theta))^2} \frac{1}{\mathbf{w}^3}. \quad (5.107)$$

The parts that depend on $\sin \varphi$ or $\cos \varphi$ drop out. Therefore, we get

$$\begin{aligned} L^{0i} &= \frac{\pi}{4} \int d\mathbf{w} \mathbf{w} f_B(\mathbf{w}) \int_{-1}^1 d \cos \theta \int_0^1 dx \sum_{\pm} \frac{\pm \cos(\theta)}{(\pm Q_0 - \mathbf{Q} \cos(\theta))^2} \hat{Q}_i \\ &= \frac{\pi}{2} T_1 \int_0^1 dx G_1 \hat{Q}_i \\ &= \frac{\pi}{2} T_1 \int_0^1 dx \frac{G_1}{\mathbf{Q}} \vec{Q}. \end{aligned} \quad (5.108)$$

Now we can put our definition for \vec{Q} back in. Recall that \vec{Q} was defined differently depending on P^2 to make sure that we are not integrating over 0. We then get:

$$L^{0i} = \frac{\pi}{2} T_1 \int_0^1 dx \frac{G_1}{\mathbf{Q}} \begin{cases} x\vec{P} + \vec{q} & \text{if } l_0 > 0 \Leftrightarrow P^2 < 0 \\ x(\vec{u} + \vec{q}) + \vec{q} & \text{if } l_0 < 0 \Leftrightarrow P^2 > 0 . \end{cases} \quad (5.109)$$

For the last remaining part, we can write:

$$w_i w_j = \mathbf{w}(\hat{Q}_i \cos(\theta) + \vec{e}_{1i} \sin(\theta) \sin(\varphi) + \vec{e}_{2i} \sin(\theta) \cos(\varphi)) \\ \times \mathbf{w}(\hat{Q}_j \cos(\theta) + \vec{e}_{1j} \sin(\theta) \sin(\varphi) + \vec{e}_{2j} \sin(\theta) \cos(\varphi)) . \quad (5.110)$$

All of the mixed terms now drop out because of the Integral over φ . The squared terms ($\cos^2 \varphi$ and $\sin^2 \varphi$) give a factor of π and the rest a factor of 2π Therefore it remains after integration over φ :

$$w_i w_j = 2\pi \mathbf{w}^2 (\cos^2 \theta \hat{Q}_i \hat{Q}_j + \frac{1}{2} \sin^2 \theta (\hat{e}_{1,i} \hat{e}_{1,j} + \hat{e}_{2,i} \hat{e}_{2,j})) . \quad (5.111)$$

With the completeness relation, this gives:

$$w_i w_j = 2\pi \mathbf{w}^2 (\cos^2 \theta \hat{Q}_i \hat{Q}_j + \frac{1}{2} \sin^2 \theta (\delta_{ij} - \hat{Q}_i \hat{Q}_j)) \\ = 2\pi \mathbf{w}^2 (\cos^2 \theta \hat{Q}_i \hat{Q}_j + \frac{1}{2} (1 - \cos^2 \theta) (\delta_{ij} - \hat{Q}_i \hat{Q}_j)) \\ = 2\pi \mathbf{w}^2 ((\frac{3}{2} \cos^2 \theta - \frac{1}{2}) \hat{Q}_i \hat{Q}_j + \frac{1}{2} (1 - \cos^2 \theta) \delta_{ij}) . \quad (5.112)$$

With all of this, we get the following:

$$L_{ij} = \frac{\pi}{2} T_1 \int_0^1 dx \begin{cases} \frac{1}{\mathbf{Q}^2} \left(\frac{3}{2} G_2 - \frac{1}{2} G_0 \right) [x^2 P_i P_j + x(P_i q_j + P_j q_i) + q_i q_j] \\ \quad + \frac{1}{2} (G_0 - G_2) \delta_{ij} & \text{if } l_0 > 0 \Leftrightarrow P^2 < 0 \\ \frac{1}{\mathbf{Q}^2} \left(\frac{3}{2} G_2 - \frac{1}{2} G_0 \right) [x^2 (u+q)_i (u+q)_j + x((u+q)_i q_j + (u+q)_j q_i) + q_i q_j] \\ \quad + \frac{1}{2} (G_0 - G_2) \delta_{ij} & \text{if } l_0 < 0 \Leftrightarrow P^2 > 0 \end{cases} \quad (5.113)$$

5.6 Connection to the Boltzmann formalism

In this section we build the connection between the well-known Boltzmann-formalism and the Keldysh-Schwinger formalism. As an example, we look at the LO process. In the Boltzmann picture the change of our distribution function is then given by the collisional integral \mathbf{C} in the

following way:

$$\frac{df_\alpha(p)}{dt} = \mathbf{C} . \quad (5.114)$$

In the Keldysh-Schwinger formalism we get the kinetic equation from the Kadanoff-Baym equations (3.56). Our distribution function can then be evolved by:

$$\frac{df_\alpha(p)}{dt} = [1 - f_\alpha(p)]\Gamma_\alpha^<(p) - f_\alpha(p)\Gamma_\alpha^>(p) , \quad (5.115)$$

where the production and destruction rates are given as:

$$\Gamma_\alpha^\gtrless(p) = \mp \frac{1}{2p_0} \text{Tr} \left[-i\hat{p}\Sigma_\alpha^\gtrless \right] \Big|_{p_0=\mathbf{p}} . \quad (5.116)$$

In the end we will find that on LO it holds that $\mathbf{C} = [1 - f_\alpha(p)]\Gamma_\alpha^<(p) - f_\alpha(p)\Gamma_\alpha^>(p)$. We can write the collisional integral \mathbf{C} for a ν as follows (see [22]):

$$\begin{aligned} \mathbf{C} = & \frac{1}{E_p} \int_0^\infty dl_0 dq_0 du_0 \int d^3\mathbf{l} d^3\mathbf{q} d^3\mathbf{u} (2\pi)^3 \delta(l^2) \delta(q^2 - m_e^2) \delta(u^2 - m_e^2) (2\pi)^4 \delta^{(4)}(p + q - l - u) \\ & \times \left[|\mathcal{M}_{\nu\bar{\nu} \rightarrow e^- e^+}|^2 f_p f_l (1 - f_q)(1 - f_u) - |\mathcal{M}_{e^- e^+ \rightarrow \nu\bar{\nu}}|^2 f_q f_u (1 - f_p)(1 - f_l) \right. \\ & \left. \times \left(|\mathcal{M}_{e^- \nu \rightarrow e^- \nu}|^2 + |\mathcal{M}_{e^+ \nu \rightarrow e^+ \nu}|^2 \right) [f_p f_l (1 - f_q)(1 - f_u) - f_q f_u (1 - f_p)(1 - f_l)] \right] \end{aligned} \quad (5.117)$$

Here, f_i are the respective distribution functions of the particles. Now, since our matrix element is CP invariant it holds that $|\mathcal{M}_{\nu\bar{\nu} \rightarrow e^- e^+}|^2 = |\mathcal{M}_{e^- e^+ \rightarrow \nu\bar{\nu}}|^2$. Then we can also use $\delta^{(4)}(p+q-l-u)$ for u and get:

$$\begin{aligned} \mathbf{C} = & \frac{1}{E_p} \int_0^\infty dl_0 dq_0 du_0 \int d^3\mathbf{l} d^3\mathbf{q} d^3\mathbf{u} (2\pi)^3 \delta(l^2) \delta(q^2 - m_e^2) \delta(u^2 - m_e^2) F \\ & \times \left(|\mathcal{M}_{\nu\bar{\nu} \rightarrow e^- e^+}|^2 + |\mathcal{M}_{e^- \nu \rightarrow e^- \nu}|^2 + |\mathcal{M}_{e^+ \nu \rightarrow e^+ \nu}|^2 \right) \end{aligned} \quad (5.118)$$

where we have defined the population factor:

$$F = [f_p f_l (1 - f_q)(1 - f_u) - f_q f_u (1 - f_p)(1 - f_l)] . \quad (5.119)$$

The crucial difference to our calculation before was that these integrals now only integrate over positive energy while the integrals we looked at before always integrated over positive and negative energies. Integrating over positive and negative energies of a particle can be thought of as flipping the leg from an incoming to an outgoing particle. The neutrino self-energy can be generally thought of as two tree level diagrams that are contracted. The integration over positive and negative energy then yield a lot of different types of the tree level diagram (see

figure 5.11).

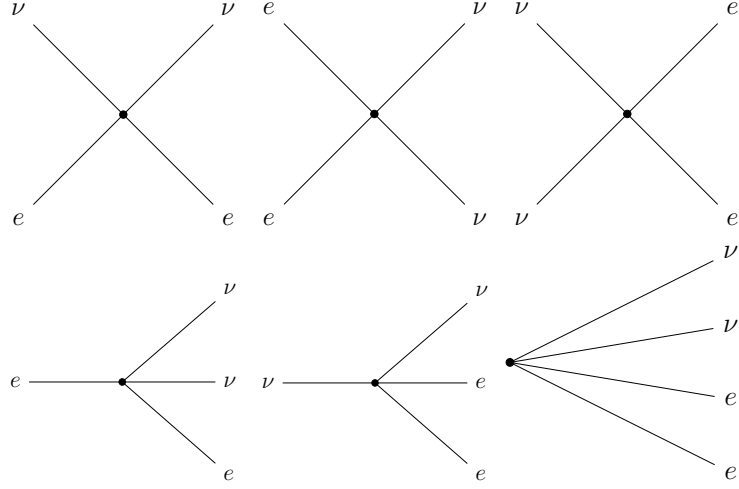


Figure 5.11: The three diagrams on the top are the only ones that are kinematically viable. There are also three more diagrams that are not included in this figure. These diagrams are just the complex conjugate of the diagrams in the bottom row.

A lot of those diagrams are kinematically forbidden, there are actually only three that survive namely $\nu\bar{\nu} \rightarrow e^-e^+$, $e^-\nu \rightarrow e^-\nu$ and $e^+\nu \rightarrow e^+\nu$ so exactly the ones we also get in our collisional integral \mathbf{C} . Let us see how these terms actually drop out of the LO self-energy.

$$\begin{aligned} \text{Tr} [i\psi\Sigma^{12}] &= \left(\frac{i4G_F}{\sqrt{2}}\right)^2 \int_{l,q} \text{Tr} [\not{p}\gamma^\rho P_L \not{l}\gamma^\sigma P_L] (2\pi)^3 \delta(l^2) \delta(q^2 - m_e^2) \delta(u^2 - m_e^2) \\ &\quad \times \text{Tr} [(\not{\psi} + m_e)\gamma_\sigma (P_L g_L^\alpha + P_R g_R) (\not{q} + m_e)\gamma_\rho (P_L g_L^\alpha + P_R g_R)] \\ &\quad \times [f_D(|l_0|) - \theta(-l_0)][f_D(|q_0|) - \theta(q_0)][f_D(|u_0|) - \theta(-u_0)] \end{aligned} \quad (5.120)$$

Now first lets only look at the traces and investigate how we get our two into two particle matrix elements.

$$\begin{aligned} &\left(\frac{i4G_F}{\sqrt{2}}\right)^2 \text{Tr} [\not{p}\gamma^\rho P_L \not{l}\gamma^\sigma P_L] \text{Tr} [(\not{\psi} + m_e)\gamma_\sigma (P_L g_L^\alpha + P_R g_R) (\not{q} + m_e)\gamma_\rho (P_L g_L^\alpha + P_R g_R)] \\ &= \left(\frac{i4G_F}{\sqrt{2}}\right)^2 [\not{p}_{ab}\gamma_{bc}^\rho P_L^{cd}\not{l}_{de}\gamma_{ef}^\sigma P_L^{fa}] \\ &\quad \times [(\not{\psi} + m_e)_{gh}\gamma_{\sigma}^{hi}(P_L g_L^\alpha + P_R g_R)_{jk}(\not{q} + m_e)_{kl}\gamma_{\rho}^{lm}(P_L g_L^\alpha + P_R g_R)_{mg}] \end{aligned} \quad (5.121)$$

Now it is we use the completeness relation for spinors $(\not{k} + m_k)_{ab} = \sum_s (u_s(k))_a (\bar{u}_s(k))_b$ and $(\not{k} - m_k)_{ab} = \sum_s (v_s(k))_a (\bar{v}_s(k))_b$. It has to be noted that these completeness relations are meant for positive energy's. Now let us look at the phase space area where $l_0, q_0 < 0$ and $u_0 > 0$. Recall that p is not integrated over and therefore $p_0 > 0$. To bring the terms in the form of the completeness relation namely that they have a positive energy, we have to make the substitutions $\vec{l} \rightarrow -\vec{l}$ and $\vec{q} \rightarrow -\vec{q}$. This gives $(\not{q} + m_e) \rightarrow (\not{q} - m_e)$, it is therefore clear that

we have to use v-spinors for q and u -spinors for u . It is not so clear, actually mathematically it does not matter. It only matters for the physical picture that underlies this calculation. If we look into our population factor we can see that for $l_0, q_0 < 0$ and $u_0 > 0$ it can be written as: $[f_D(|l_0|) - 1][f_D(|q_0|)][f_D(|u_0|)]$ out of this we know that q and u are out going particles and l is an incoming particle. To make this kinematically possible, p has to be also an incoming particle, therefore, we choose p to have u -spinors and l to have v -spinors. We therefore get:

$$\begin{aligned}
 &= \left(\frac{i4G_F}{\sqrt{2}}\right)^2 \sum_{\text{spins}} [u(p)_a \bar{u}(p)_b \gamma_{bc}^\rho P_L^{cd} v(l)_d \bar{v}(l)_e \gamma_{ef}^\sigma P_L^{fa}] \\
 &\quad \times [u(u)_g \bar{u}(u)_h \gamma_\sigma^{hi} (P_L g_L^\alpha + P_R g_R)_{jk} v(q)_k \bar{q}(l)_l \gamma_\rho^{lm} (P_L g_L^\alpha + P_R g_R)_{mg}] \\
 &= \left(\frac{i4G_F}{\sqrt{2}}\right)^2 \sum_{\text{spins}} [\bar{v}(l)_e \gamma_{ef}^\sigma P_L^{fa} u(p)_a] [\bar{u}(p)_b \gamma_{bc}^\rho P_L^{cd} v(l)_d] \\
 &\quad \times [\bar{q}(l)_l \gamma_\rho^{lm} (P_L g_L^\alpha + P_R g_R)_{mg} u(u)_g] [\bar{u}(u)_h \gamma_\sigma^{hi} (P_L g_L^\alpha + P_R g_R)_{jk} v(q)_k] \\
 &= - \sum_{\text{spins}} \left(\frac{i4G_F}{\sqrt{2}}\right) [\bar{v}(l) \gamma^\sigma P_L u(p)] [\bar{q}(l) \gamma_\rho (P_L g_L^\alpha + P_R g_R) u(u)] \\
 &\quad \times \left(\frac{i4G_F}{\sqrt{2}}\right)^* [\bar{v}(l) \gamma^\sigma P_L u(p)]^* [\bar{q}(l) \gamma_\rho (P_L g_L^\alpha + P_R g_R) u(u)]^* \\
 &= - |\mathcal{M}_{\nu\bar{\nu} \rightarrow e^- e^+}|^2 \tag{5.122}
 \end{aligned}$$

As you can see, we can connect the neutrino self-energy to the matrix element. In general one can say, that the interaction rate between neutrinos and electrons is included in the self energy $\text{Tr} [i\cancel{p}\Sigma^{12}]$. In addition, all other matrix elements are recovered for the different signs of l_0 , q_0 and u_0 . The only parts that we are still missing to fully connect to the collisional integral \mathbf{C} is the energy $\frac{1}{E_p} = \frac{1}{p_0}$ and also the phase space distribution function for p . But it is straightforward to see where these parts come from. The factor of $\frac{1}{p_0}$ comes out of the equation for the full production or destruction rate (5.116). The population factor is given by

$$[f_D(|l_0|) - \theta(-l_0)][f_D(|q_0|) - \theta(q_0)][f_D(|u_0|) - \theta(-u_0)] \tag{5.123}$$

of equation (5.120). Here, the θ -functions dynamically change if the particle swaps from an incoming to an out going particle. The remaining distribution function for p comes from the connection of the production and destruction rate to the change in f_α (5.115).

Chapter 6

Numerical evaluation

In this chapter, the numerical results of the rates that were discussed in chapter 5 are evaluated. The numerical evaluation was mainly done in \mathbb{C} , the integrals were solved by using the Cuba Library for multidimensional numerical integration [46]. For the experimentally determined parameters, the following from the Particle Data Group [47] given values were taken:

- Electron mass: $m_e = 0.51099895000(15)$ MeV
- Electromagnetic fine-structure constant: $\frac{1}{\alpha_{\text{EM}}} = 137.035999180(10)$
- Fermi constant: $G_F = 1.1663788(6) \frac{1}{\text{MeV}^2}$
- Weinberg angle: $\sin^2 \theta_W = 0.23863(5)$.

In the calculation of the virtual correction, one has to choose the renormalization scale μ_R and the photon mass λ . The numerical evaluation is not dependent on λ , as it should when the infrared divergence was canceled correctly, we therefore give no value for this here. The renormalization scale was set to the electron mass

- Renormalization scale $\mu_R = m_e$.

The calculation of the rates depends on the momentum of the incoming particle p and also on the temperature T . In general the momentum can be chosen freely but based on the mean momentum approach, discussed in section 2.2, we are going to set the incoming neutrino momentum to

- Incoming neutrino momentum: $p = 3.15T$.

6.1 Energy cut off independence

To cancel out the infrared divergences we introduced the parameter ΔE in chapter 5.2. As this parameter is not physical, our results can not depend on the energy cut off. Numerically, we

have to find the area where the result is not dependent on the energy cut off ΔE . As we made the approximation $w \ll p, q, l, m_e$ the area should lie below the electron mass. We are not able to expand this area to arbitrarily small energy cut offs, because the numerical evaluation will become unstable.

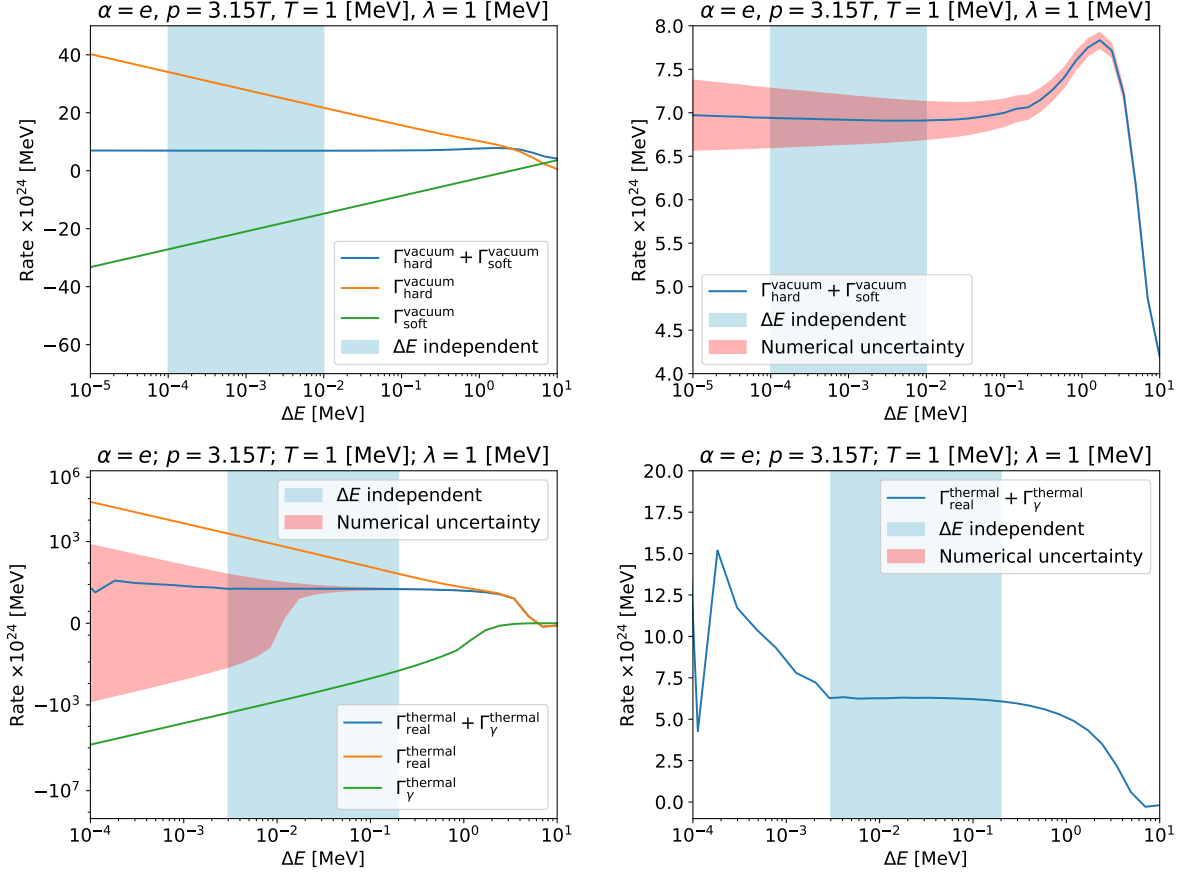


Figure 6.1: These are the results for the cut off dependence for ν_e . The top figures present the dependence for the vacuum rates, while the bottom figures display the dependence for the thermal rates. On the left side, the individual rates are shown alongside the sum of the canceling rates for comparison. On the right side, only the sum is plotted to highlight the ΔE -independent part in greater detail. The red shaded region represents the uncertainty in the results, which arises from a 1% uncertainty in Γ_{real} . The uncertainties in the other rates are smaller and therefore negligible. The blue shaded region indicates the range where the result is independent of ΔE .

You can see in the figures 6.1 and 6.2 that the results are independent of ΔE in the area $\Delta E \in [0.0001, 0.01]$ MeV for the vacuum part and $\Delta E \in [0.002, 0.2]$ MeV for the temperature-dependent part. The stable area for the temperature-dependent part is smaller because the divergence is harder. In the vacuum part, the divergence is proportional to $\log \Delta E$ but because of the additional Bose enhancement, the thermal divergence is proportional to $\frac{1}{\Delta E}$. The small tilt that you can see in figures 6.1 and 6.2 lies fully in the uncertainty. The uncertainty for this

calculation is rather big, as we are subtracting to divergent terms to get the remaining finite part. For the rest of the numerical evaluation we choose

- Energy cut off: $\Delta E = 0.05$ MeV .

The area where the result does not depend on the energy cut off is only very slightly dependent on the temperature, we can therefore choose this cut off also for different temperatures.

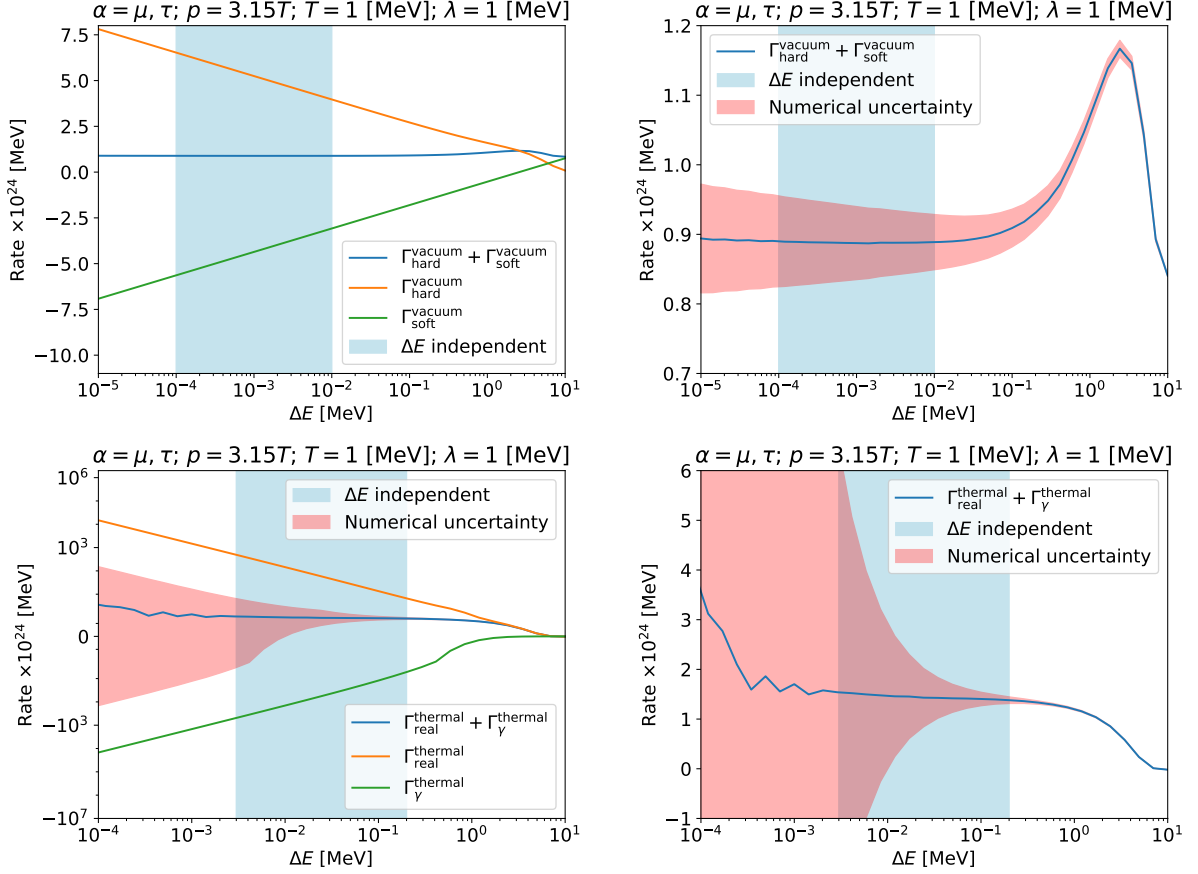


Figure 6.2: These are the results for the cut off dependence for $\nu_{\mu,\tau}$. The figures on the top show the cut of dependence for the vacuum rates while the lower two figures show the cut of dependence for the thermal rates. The sum of the canceling rates is given in comparison to the individual rates on the left side. On the right side only the sum was plotted to the the ΔE independent part in better detail. The red area is the uncertainty of the results, this results from the uncertainty of 1% of Γ_{real} respectively. The uncertainty of the other rates is smaller and can be neglected. The blue area marks the part where the result does not depend on ΔE .

6.2 Numerical results

The interaction rates Γ_e and $\Gamma_{\mu,\tau}$ at mean momentum $p = 3.15T$ can be seen in figures 6.3 and 6.4, where they are plotted against the LO correction. We find a correction up to 50% of the LO

correction. This result is orders of magnitude larger than the correction of the Frog, which was in the range of $0.2 + 0.1\%$ for ν_e and $0.0005 + 0.0002\%$ for $\nu_{\mu,\tau}$. In general, the results of the NLO corrections are believed to be orders of magnitude smaller than the LO correction, especially because it is believed that the Frog gives the largest contribution of the NLO diagrams [19].

The part of the results in the figures 6.3 and 6.4 that gets so big is the non divergent part of the interference term of the real emission diagrams. All other parts give results that are at the same order as the Frog results. Now there could be two reasons for that: (i) this is not the full NLO calculations; missing parts of the Donut and Ladybug diagram could in principle cancel these terms out, (ii) the interference term is due to the more complicated propagator structure the most complicated calculation. So there could be a mistake, which can not lie in the divergent term, as this cancels out perfectly (see figures 6.1 and 6.2). To verify this, one could generalize the thermal integrals of section 5.89 to also hold for the vacuum part. This would give another cross-check for the results and would also speed up the numerical evaluation.

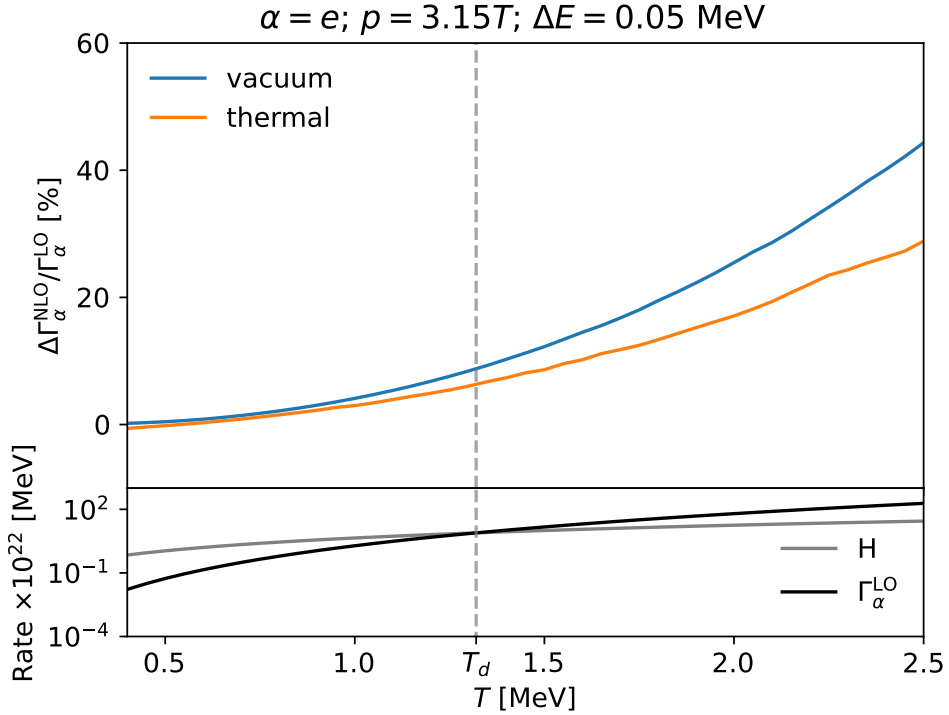


Figure 6.3: The results for ν_e , plotted in comparison to the LO rate. The important region for neutrino decoupling is marked by the decoupling temperature $T_d \simeq 1.321 \text{ MeV}$.

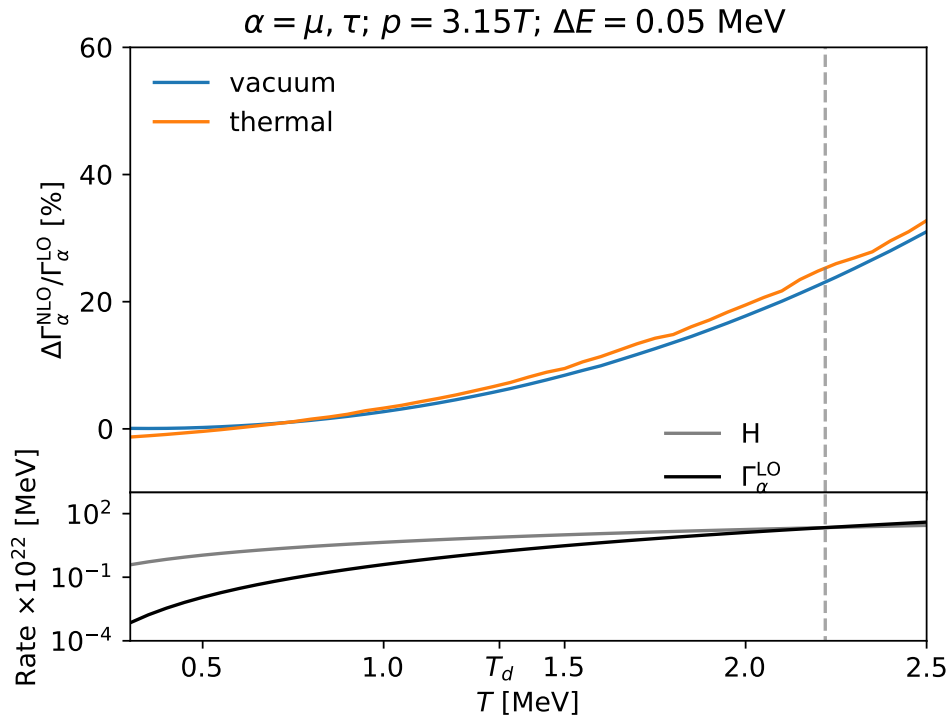


Figure 6.4: The results for $\nu_{\mu,\tau}$, plotted in comparison to the LO rate. The important region for neutrino decoupling is marked by the decoupling temperature $T_d \simeq 2.222$ MeV.

Chapter 7

Conclusion and outlook

In this thesis, parts of the NLO correction for the thermal interaction rates of neutrinos were calculated. The work focused on the Baseball diagram, which exhibits both vacuum and thermal infrared divergences. The cancellation of these divergences was demonstrated analytically in Chapter 5.2. For this cancellation, the squared contributions of real emission rates included in the Donut and Ladybug diagrams were also calculated.

The finite rates were evaluated numerically using thermal integrals. It was observed that the results were dominated by the mixed term of the real emission diagram. At high temperatures, this contribution increases to the same order of magnitude as the leading-order (LO) contribution, which is concerning. So far, the vacuum parts of the Donut and Ladybug diagrams that do not contribute to the infrared divergence have been neglected. In general, it is possible that cancellations occur between these parts and the mixed real emission diagram, which would constrain the result to remain at the level of $\mathcal{O}(1\%)$ corrections to the LO rate.

The next step, in order to complete a full NLO calculation, is to evaluate the missing parts of the Donut and Ladybug diagrams. Furthermore, it is possible to generalize the thermal integrals to also hold for the vacuum contributions, which would improve the numerical evaluation. Once all NLO contributions have been computed, the final step toward obtaining a complete result—accounting for neutrino oscillations and other relevant phenomena—is to implement the rates into a neutrino decoupling code such as `FortEPiano`.

Appendix A

Loop calculations

In loop calculations, there are usually one or more momenta that are not fixed by the in or out going momenta. We therefore have to integrate over these momenta. The arising integrals regularly diverge. There can be two types of different divergences. One appears when the integrand is not suppressed sufficiently hard for $p \rightarrow \infty$; this is a UV divergence. It is then obvious that the integral diverges if we integrate until ∞ . This is also the type of divergence that is being dealt with in this chapter. The other type of divergence is an infrared divergence, for more detail on that see section 5.2.

The idea for UV-divergent integrals is to introduce a new artificial parameter. The divergence will then be parametrized by this artificial parameter. That means that under the new introduced parameter the integrals converge. But in the limit where the parameter goes to zero (or ∞ for the cutoff) the divergence appears again in the new artificial parameter. This is called regularization. In the end, we can absorb these divergent parameters into the different free parameters of the Lagrangian. This is then called renormalization. There are two main regularization schemes. (1) Introducing an UV- Cutoff [48] Λ and (2) doing the calculations in $D = 4 - 2\epsilon$ dimensions [49] (Dimensional regularization). In this work we will use Dimensional regularization for the UV-divergences, therefore this chapter focuses on this regularization scheme.

A.1 Dimensional regularization

The idea in Dimensional regularization is that the integrals diverge in $D = 4$ dimensions but not in $D = 4 - 2\epsilon$ dimensions. We therefore go over to $D = 4 - 2\epsilon$ dimensions, but in the end we take the limit $\epsilon \rightarrow 0$.

$$\int \frac{d^4 p}{(2\pi)^4} \rightarrow \mu^{2\epsilon} \int \frac{d^D p}{(2\pi)^D} \quad (\text{A.1})$$

Where μ has mass dimension 1 and ensures, that the dimension of the integral stays the same. We therefore have two artificially introduced parameters μ and ϵ and our physical result should not depend on those in the end. When we do the calculation in D dimensions, we have to change the properties of our momentum vectors, metric and Dirac matrices:

$$p^\mu = (p^0, p^1, p^2, p^3) \rightarrow p^\mu = (p^0, p^1, \dots, p^{D-1}) \quad (\text{A.2})$$

$$g_\mu^\mu = 4 \rightarrow g_\mu^\mu = D \quad (\text{A.3})$$

It becomes very complicated, when one tries to generalize this also for γ_5 and $\epsilon^{\mu\nu\sigma\rho}$, as these are intrinsically four-dimensional properties for which one would have to use the BMHV-scheme [50]. Now we will take a look at a generic integral:

$$A_0(m^2) = \frac{(2\pi\mu)^{4-D}}{i\pi^2} \int \frac{d^D p}{(2\pi)^D} \frac{1}{p^2 - m^2 + i\epsilon}. \quad (\text{A.4})$$

Do not get confused with the two epsilon's that appear now. There is one ϵ that regulates our UV-divergence and the other one ϵ that comes from the structure of the Feynman propagator. After a wick rotation it is safe to neglect the $i\epsilon$ and we get:

$$A_0(m^2) = \frac{(2\pi\mu)^{4-D}}{\pi^2} (-i) \int \frac{d^D p}{(2\pi)^D} \frac{1}{p_E^2 + m^2}, \quad (\text{A.5})$$

where p_E means the vector with an euclidean metric. Now we introduce spherical coordinates:

$$A_0(m^2) = -\frac{(2\pi\mu)^{4-D}}{\pi^2} \frac{1}{(2\pi)^D} \int d\Omega \int dp_E \frac{p_E^{D-1}}{p_E^2 + m^2}, \quad (\text{A.6})$$

where the integral over all angles is denoted by $\int d\Omega = \frac{(2\pi)^{\frac{D+1}{2}}}{\Gamma(\frac{D+1}{2})}$ and the integral over the radius is given by $\int dp_E$. We then can calculate the integral over p_E . First we substitute $x = p_E^2$:

$$\int dp_E \frac{p_E^{D-1}}{p_E^2 + m^2} = \int dx \frac{x^{\frac{D}{2}-1}}{x + m} \quad (\text{A.7})$$

Then by substituting $y = \frac{m}{x+m}$ we can bring the integral into a form of a beta function

$$\int_0^\infty dx \frac{x^{\frac{D}{2}-1}}{x + m} = \frac{1}{m^{\frac{D}{2}-1}} \int_0^1 dy (1-y)^{\frac{D}{2}-1} y^{-\frac{D}{2}} \quad (\text{A.8})$$

$$= \frac{1}{m^{\frac{D}{2}-1}} \frac{\Gamma(\frac{D}{2})\Gamma(1-\frac{D}{2})}{\Gamma(1)} \quad (\text{A.9})$$

Putting this back in A.6, we get the following end result:

$$A_0(m^2) = -\frac{(2\pi\mu)^{4-D}}{\pi^2} \pi^{\frac{D}{2}} \Gamma\left(1 - \frac{D}{2}\right) m^{\frac{D}{2}-1}. \quad (\text{A.10})$$

You can see that we have a pole in the Γ function if we let $D \rightarrow 4$. It is therefore insightful to expand A_0 in ϵ . But first we are using $\Gamma\left(1 - \frac{D}{2}\right) = \Gamma(-1 + \epsilon) = \frac{1}{\epsilon(\epsilon-1)}\Gamma(1 + \epsilon)$.

$$A_0(m^2) = -\left(\frac{4\pi\mu^2}{m^2}\right)^\epsilon \frac{1}{\epsilon(\epsilon-1)}\Gamma(1 + \epsilon) \quad (\text{A.11})$$

Expanding up to order ϵ yields:

$$A_0(m^2) = m^2 \left(\frac{1}{\epsilon} - \gamma_E + \ln(4\pi) - \ln\left(\frac{m^2}{\mu^2}\right) + 1 + \mathcal{O}(\epsilon) \right), \quad (\text{A.12})$$

where γ_E Δ is the Euler-Mascharoni constant. You can see how this diverges for $\epsilon \rightarrow 0$ but we can directly identify our divergent parts and cancel them with the divergences of the counter term (see A.3) or with other loops. It is also common to define $\Delta = \frac{1}{\epsilon} - \gamma_E + \ln(4\pi)$.

A.2 Passarino-Veltman reduction

Now a general loop integral is given by

$$T_{\mu_1, \dots, \mu_m}^{N}(p_1, \dots, p_N, m_0, \dots, m_N) = \frac{(2\pi\mu)^{2\epsilon}}{i\pi^2} \int d^D q \frac{q_{\mu_1} \dots q_{\mu_m}}{\mathcal{D}_0 \dots \mathcal{D}_{n-1}}, \quad (\text{A.13})$$

where the propagators \mathcal{D}_i are defined like:

$$\mathcal{D}_0 = q^2 - m_0^2 + i\epsilon \quad (\text{A.14})$$

$$\mathcal{D}_1 = (q + p_1)^2 - m_1^2 + i\epsilon \quad (\text{A.15})$$

...

$$\mathcal{D}_N = (q + p_N)^2 - m_N^2 + i\epsilon \quad (\text{A.16})$$

The integral defined in equation (A.13) is a tensor integral. However, it can be reduced to the following scalar integrals [51]

$$A_0(m_0^2) = \frac{(2\pi\mu)^{2\epsilon}}{i\pi^2} \int d^D q \frac{1}{\mathcal{D}_0} \quad (\text{A.17})$$

$$B_0(p_1^2, m_0^2, m_1^2) = \frac{(2\pi\mu)^{2\epsilon}}{i\pi^2} \int d^D q \frac{1}{\mathcal{D}_0 \mathcal{D}_1} \quad (\text{A.18})$$

$$C_0(p_1^2, (p_2 - p_1)^2, p_2^2, m_0^2, m_1^2, m_2^2) = \frac{(2\pi\mu)^{2\epsilon}}{i\pi^2} \int d^D q \frac{1}{\mathcal{D}_0 \mathcal{D}_1 \mathcal{D}_2} \quad (\text{A.19})$$

...

by using

$$B^\mu = p_1^\mu B_1 \quad (\text{A.20})$$

$$B^{\mu\nu} = g^{\mu\nu} B_{00} + p_1^\mu p_1^\nu B_{11} \quad (\text{A.21})$$

$$C^\mu = p_1^\mu C_1 + p_2^\mu C_2 \quad (\text{A.22})$$

$$C^{\mu\nu} = g^{\mu\nu} C_{00} + p_1^\mu p_1^\nu C_{11} + p_1^\mu p_2^\nu C_{12} + p_2^\mu p_1^\nu C_{21} + p_2^\mu p_2^\nu C_{22} \quad (\text{A.23})$$

...

The introduced coefficient functions B_1 , B_{00} , B_{11} , ... can be calculated by contracting with the external momenta, and then solve the equations. For B^μ one would contract with $(p_1)_\mu$

$$B_1^\mu (p_1)_\mu = \frac{(2\pi\mu)^{2\epsilon}}{i\pi^2} \int d^D q \frac{(p_1 \cdot q)}{\mathcal{D}_0 \mathcal{D}_1} = p_1^2 B_1 . \quad (\text{A.24})$$

We can then use

$$(p_1 \cdot q) = \frac{1}{2} \left([(p_1 + q)^2 - m_1^2 + i\epsilon] - [q^2 - m_0^2 + i\epsilon] - [p_1^2 - m_1^2 + m_0^2] \right) \quad (\text{A.25})$$

to find a form of B_1 in terms of the scalar integrals that were defined in equation (A.17)

$$B_1(p_1^2, m_0^2, m_1^2) = \frac{1}{2p_1^2} \left(A_0(m_0^2) - A_0(m_1^2) - (p_1^2 - m_1^2 + m_0^2) B_0(p_1^2, m_0^2, m_1^2) \right) . \quad (\text{A.26})$$

The same procedure can be performed for all other coefficient functions to reduce them to the scalar integrals of equation (A.17).

A.3 Counter term

After renormalizing QED we get the following vertex counterterm, which stems from corresponding field renormalization factor:



$$= -ie_R \delta_1 \gamma^\mu , \quad (\text{A.27})$$

with

$$\delta_1 = \frac{\alpha}{4\pi} \frac{1}{\epsilon} - \frac{\alpha}{4\pi} \left(\ln \frac{\mu^2}{m^2} + 2 \ln \frac{\lambda^2}{m^2} + 4 \right) , \quad (\text{A.28})$$

where the photon gauge was set to one.

A.4 The integral I_{ab}

In the soft photon approximation we get integrals of the following form

$$I = \int_{0 \leq \mathbf{k} \leq \Delta} \frac{d^3 k}{k^0} \frac{1}{(k \cdot a)(k \cdot b)}, \quad (\text{A.29})$$

where k is the momentum of the photon. The calculation of this integral is quite involved; therefore, we mainly follow the discussion in [52]. As a first step, we want to use Feynman parameters, we therefore have to make sure not to integrate over 0. To do so, we introduce $p = \alpha a$ with $(p - b)^2 = 0$. This yields two solutions for α , from which we choose the one that fulfills:

$$\frac{\alpha a_0 - b_0}{b_0} > 0. \quad (\text{A.30})$$

We can then safely introduce the Feynman parameter x and define $P = (b + (p - b)x)$ to get

$$I = \alpha \int_0^1 dx \int \frac{d^3 k}{k_0} \frac{1}{(k \cdot P)^2} \quad (\text{A.31})$$

We introduce a photon mass λ to regulate the integral. With this we can write $k_0 = \sqrt{\mathbf{k}^2 + \lambda^2}$. We can then use spherical coordinates and substitute $t = \frac{k}{\lambda}$ to get

$$I = 4\pi\alpha \int_0^1 dx \int_0^{\frac{\Delta}{\lambda}} \frac{dt t^2}{\sqrt{t^2 + 1}} \frac{1}{t^2 (P_0^2 - \mathbf{P}^2) + P_0^2} \quad (\text{A.32})$$

We can now substitute $u = \frac{t}{1+t^2}$ to evaluate the integral. We then get

$$I = 2\pi\alpha \int_0^1 dx \frac{1}{\mathbf{P}^2} \left(\ln \left(\frac{2\Delta}{\lambda} \right)^2 + \frac{P_0}{\mathbf{P}} \ln \left(\frac{P_0 - \mathbf{P}}{P_0 + \mathbf{P}} \right) \right), \quad (\text{A.33})$$

where the only dependence on x lies in P_0 and \mathbf{P} . We introduce the short-hand notation $l = p_0 - b_0$ and $vl = (b \cdot (p - b))$. The first part of the integral is trivial to integrate and just gives

$$\int_0^1 \frac{dx}{\mathbf{P}^2} \ln \left(\frac{2\Delta}{\lambda} \right)^2 = \frac{1}{2vl} \ln \left(\frac{2\Delta}{\lambda} \right)^2 \ln \left(\frac{b^2 + 2vl}{b^2} \right). \quad (\text{A.34})$$

The second part is harder, but after some tedious calculations it is possible to find

$$\int_0^1 \frac{dx}{P^2} \frac{P_0}{\mathbf{P}} \ln \left(\frac{P_0 - \mathbf{P}}{P_0 + \mathbf{P}} \right) = \frac{1}{vl} \left[\frac{1}{4} \ln^2 \left(\frac{P_0 - \mathbf{P}}{P_0 + \mathbf{P}} \right) + \text{Li}_2 \left(1 - \frac{P_0 - \mathbf{P}}{v} \right) + \text{Li}_2 \left(1 - \frac{P_0 + \mathbf{P}}{v} \right) \right]_{P=b}^{P=p}, \quad (\text{A.35})$$

where Li_2 denotes the dilogarithm. Putting all together yields the final result $I_{ab} = (a \cdot b) \cdot I$

$$I_{ab} = \frac{4\pi\alpha (a \cdot b)}{(\alpha a)^2 - b^2} \left\{ \frac{1}{2} \ln \frac{4\Delta^2}{\lambda^2} \ln \frac{(\alpha a)^2}{b^2} + \left[\frac{1}{4} \ln^2 \frac{P_0 - \mathbf{P}}{P_0 + \mathbf{P}} + \text{Li}_2 \left(1 - \frac{P_0 - \mathbf{P}}{v} \right) + \text{Li}_2 \left(1 - \frac{P_0 + \mathbf{P}}{v} \right) \right]_{P=b}^{P=\alpha a} \right\}. \quad (\text{A.36})$$

If the momenta a and b are equal, we do not have to introduce Feynman parameters and can re-derive an easier version for the integral that can be written as:

$$I_{a^2} = 2\pi \left(\ln \frac{4\Delta^2}{\lambda^2} + \frac{a^0}{\mathbf{a}} \ln \left(\frac{a_0 - \mathbf{a}}{a_0 + \mathbf{a}} \right) \right). \quad (\text{A.37})$$

A.5 Formfactors

Form factors are really useful in the context of loop calculations. In QED these are well known in the sense of the anomalous magnetic moment. There we have a interaction that has a γ^μ structure. Now in fermi theory (see section B.4) one part of the interaction has a γ^μ structure while the other part has a $\gamma^\mu \gamma^5$ structure.

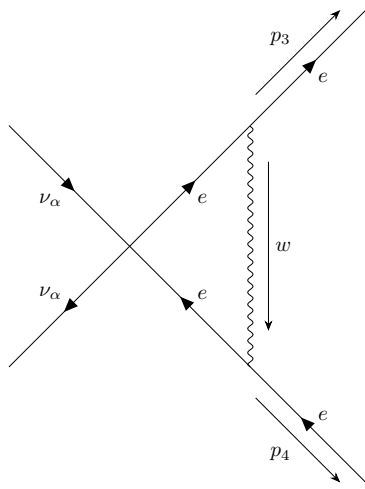


Figure A.1: Virtual vertex correction in fermi theory.

For calculating the form factors only the electron line of the diagram in figure A.1 is important. Therefore we get:

$$M_\mu = -e^2 \frac{4G_F}{\sqrt{2}} \bar{u}(p_3) \int_w \frac{\gamma^\rho (\psi + \not{p}_3 + m_e) \gamma_\mu (g_V - g_A \gamma_5) (\psi - \not{p}_4 + m_e) \gamma_\rho}{[w^2 - \lambda^2 + i\epsilon][(w + p_3)^2 - m_e^2 + i\epsilon][(w - p_4)^2 - m_e^2 + i\epsilon]} v(p_4) \quad (\text{A.38})$$

These integrals are UV- and infrared-divergent. To extract these divergences, we calculate this matrix element in $D = 4 - 2\epsilon$ dimensions. That is done because then in the end one gets $\frac{1}{\epsilon}$ -Terms that contain the divergence (for more information, see section A.1). To get rid of the UV-divergence we have to include the counter term. The electron wave function renormalization constant is given by [37]

$$e^2 \delta_2 = \frac{e^2}{8\pi^2} \left(-\frac{1}{\epsilon} - \frac{1}{2} \frac{\mu^2}{m_e^2} - 2 - \ln \frac{\lambda^2}{m_e^2} \right) \quad (\text{A.39})$$

From this we get:

$$M_{\text{Counter}}^\mu = \frac{4G_F}{\sqrt{2}} \bar{u}(p_3) \delta_2 \gamma^\mu (g_V - g_A \gamma_5) v(p_4) \quad (\text{A.40})$$

And we are also giving the photon a mass λ . This gives $\log(\frac{m_e}{\lambda})$ -Terms, that also diverge for $\lambda \rightarrow 0$. But in the end, we will see that all of these divergent terms cancel out between different diagrams (see section 5.2).

Normally, the formfactor is calculated only for the vector part (g_V). To get a modification for γ_μ but now we also have the axial part, therefore we also have to calculate a replacement for $\gamma_\mu \gamma_5$. We will see that the modifications are given by [44]:

$$\bar{e}(p_3) \gamma_\mu e(p_4) \rightarrow \bar{e}(p_3) \gamma_\mu e(p_4) + \frac{\alpha}{\pi} \bar{e}(p_3) \left(F_1 \gamma_\mu + F_2 \frac{i\sigma_{\mu\nu} q^\nu}{2m} \right) e(p_4), \quad (\text{A.41})$$

$$\bar{e}(p_3) \gamma_\mu \gamma_5 e(p_4) \rightarrow \bar{e}(p_3) \gamma_\mu \gamma_5 e(p_4) + \frac{\alpha}{\pi} (F_1 - F_2) \bar{e}(p_3) \gamma_\mu \gamma_5 e(p_4). \quad (\text{A.42})$$

F_1 and F_2 are the QED Formfactors.

A.5.1 Vector current

First, let us look at the vector part. The part that is proportional to g_V . For simplicity, we drop the factor of $-g_V e^2 \frac{4G_F}{\sqrt{2}}$:

$$M_\mu^{\text{Vector}} = \bar{u}(p_3) \gamma^\rho \underbrace{\int_w \frac{(\psi + \not{p}_3 + m_e) \gamma_\mu (\psi - \not{p}_4 + m_e)}{[w^2 - \lambda^2 + i\epsilon][(w + p_3)^2 - m_e^2 + i\epsilon][(w - p_4)^2 - m_e^2 + i\epsilon]}}_I \gamma_\rho v(p_4) \quad (\text{A.43})$$

For the integral I we want to use the Passarino-Veltman reduction (see A.2). But before we insert the different tensor integrals we bring the numerator into a form where it is easy to insert the tensor integrals

$$\begin{aligned}
 & (\psi + \not{p}_3 + m_e)\gamma_\mu(\psi - \not{p}_4 + m_e) \\
 & = 2w_\mu\psi + \gamma_\mu(m_e^2 - w^2) + m_e\gamma_\mu\psi + m_e\psi\gamma_\mu + \not{p}_3\gamma_\mu\psi \\
 & \quad - \not{k}\gamma_\mu\not{p}_4 + m_e\not{p}_3\gamma_\mu - m_e\gamma_\mu\not{p}_4 - \not{p}_3\gamma_\mu\not{p}_4
 \end{aligned} \tag{A.44}$$

For the w^2 it is now useful to insert a $\lambda^2 - \lambda^2$ to cancel the one propagator factor. In the end, this will yield a B_0 function.

$$\begin{aligned}
 & = 2w_\mu\psi + \gamma_\mu(m_e^2 - \lambda^2) - \gamma_\mu(w^2 - \lambda^2) + m_e\gamma_\mu\psi + m_e\psi\gamma_\mu \\
 & \quad + \not{p}_3\gamma_\mu\psi - \not{k}\gamma_\mu\not{p}_4 + m_e\not{p}_3\gamma_\mu - m_e\gamma_\mu\not{p}_4 - \not{p}_3\gamma_\mu\not{p}_4
 \end{aligned} \tag{A.45}$$

The other λ -Term just drops out in the end when $\lambda \rightarrow 0$. With that we can use Passarino-Veltman reduction. In the following, all C-functions have the argument set:

$$(p_3^2, (p_4 - p_3)^2, p_4^2, \lambda^2, m_e^2, m_e^2) = (m_e^2, 2(m_e^2 - (p_3 \cdot p_4)), m_e^2, \lambda^2, m_e^2, m_e^2) . \tag{A.46}$$

The B-function has the argument set:

$$((p_3 + p_4)^2, m_e^2, m_e^2) = (2(m_e^2 + (p_3 \cdot p_4)), m_e^2, m_e^2) . \tag{A.47}$$

For simplicity, we also dropped the factor $\frac{(2\pi\mu)^{2\epsilon}}{i\pi^2}$. In the end, when we put everything back in again, we have to expand this factor in ϵ . We can also use that in this case, because of permutation symmetries of the scalar functions $C_1 = C_2$ and $C_{11} = C_{22}$ [52] For I we then get:

$$\begin{aligned}
 I^\mu & = -B_0\gamma^\mu + C_0(m_e^2\gamma^\mu + m_e\not{p}_3\gamma^\mu - m_e\gamma^\mu\not{p}_4 - \not{p}_3\gamma^\mu\not{p}_4) \\
 & \quad + C_1(2m_e(p_3^\mu - p_4^\mu) + \not{p}_3\gamma^\mu\not{p}_3 - 2\not{p}_3\gamma^\mu\not{p}_4 + \not{p}_4\gamma^\mu\not{p}_4) \\
 & \quad + C_{11}(2\not{p}_3p_3^\mu + 2\not{p}_4p_4^\mu) + C_{12}(-2\not{p}_4p_3^\mu - 2\not{p}_3p_4^\mu) + C_{00}2\gamma^\mu
 \end{aligned} \tag{A.48}$$

Putting this back in (A.43) and summing over ρ we get factors of D . When we write $D = 4 - 2\epsilon$. We get terms that are proportional to ϵ^0 and ϵ^1 . Naively one could think that all terms proportional to ϵ just drop out, because in the end we send $\epsilon \rightarrow 0$. But it is important to be careful, because there are scalar functions that are proportional to $\frac{1}{\epsilon}$. It holds $\epsilon \times B_0 = 1$ and $\epsilon \times C_{00} = \frac{1}{4}$. With this we get:

$$\begin{aligned}
 M_{\text{Vector}}^\mu & = (-4(C_0 + 2C_1)(p_4 \cdot p_4) + 2B_0 - 4C_{00} + 8C_1m_e^2 + 1)\bar{u}(p_3)\gamma^\mu v(p_4) \\
 & \quad - 4m_e(C_1 + C_{11} + C_{12})(p_3^\mu - p_4^\mu)(\bar{u}(p_3)v(p_4))
 \end{aligned} \tag{A.49}$$

It is now useful to define $P = p_3 + p_4$. Then $(p_3 \cdot p_4) = -m_e^2 + \frac{P^2}{2}$. With the Gordon-identity:

$$\bar{\psi}(p') \frac{(p' + p)^\mu}{2m} \psi(p) = \bar{\psi} \left[\gamma^\mu - i \frac{\sigma^{\mu\nu} (p' - p)_\nu}{2m} \right] \psi(p) \quad (\text{A.50})$$

we can write $M_{\text{Vector}}^\mu + M_{\text{Counter}}^\mu$ as:

$$M_{\text{R}}^\mu = \underbrace{(2B_0 + 4m_e^2(C_0 + 2C_1 + 2C_{11} - 2C_{12}) - 2P^2(C_0 + 2C_1) - 4C_{00} + 1 - \delta_2)}_{F_1} \bar{u}(p_3) \gamma^\mu v(p_4) \\ - \underbrace{8m_e^2(C_1 + C_{11} + C_{12})}_{F_2} (\bar{u}(p_3) \frac{i\sigma^{\mu\nu} (p_3 + p_4)_\nu}{2m_e} v(p_4)) \quad (\text{A.51})$$

Now by putting in the B and C functions one finds the well-known renormalized formfactors up to second order in e , that were previously calculated in [43]. Now it is useful to define:

$$\theta = -\frac{1 - \sqrt{1 - \frac{4m_e^2}{P^2}}}{1 - \sqrt{1 + \frac{4m_e^2}{P^2}}}, \quad x = \frac{1 - \sqrt{1 - \frac{4m_e^2}{P^2}}}{1 - \sqrt{1 + \frac{4m_e^2}{P^2}}}. \quad (\text{A.52})$$

For $P^2 < 0$ we get:

$$F_1(\theta) = -\log \frac{\lambda}{m_e} \left(1 + \frac{1 + \theta^2}{1 - \theta^2} \log \theta \right) - 1 - \frac{3\theta^2 + 2\theta + 3}{4(1 - \theta^2)} \log \theta \\ + \frac{1 + \theta^2}{1 - \theta^2} \left(-\frac{1}{4} \log^2 \theta + \frac{1}{2} \zeta(2) + \text{Li}_2(-\theta) + \log \theta \log(1 + \theta) \right), \quad (\text{A.53})$$

$$F_2(\theta) = -\frac{\theta}{1 - \theta^2} \log \theta. \quad (\text{A.54})$$

For $P^2 \geq 4m_e^2$ we get:

$$F_1(x) = -\log \frac{\lambda}{m_e} \left[1 + \frac{1 + x^2}{1 - x^2} (\log x + i\pi) \right] - 1 - \frac{3x^2 - 2x + 3}{4(1 - x^2)} \log x \\ + \frac{1 + x^2}{1 - x^2} \left(-\frac{1}{4} \log^2 x + 2\zeta(2) + \text{Li}_2(x) + \log(x) \log(1 - x) \right) \quad (\text{A.55})$$

$$+ i\pi \left[-\frac{3x^2 - 2x + 3}{4(1 - x^2)} + \frac{1 + x^2}{1 - x^2} \left(\log(1 - x) - \frac{1}{2} \log x \right) \right], \\ F_2(x) = \frac{x}{1 - x^2} (\log x + i\pi) \quad (\text{A.56})$$

The area $0 < P^2 < 4m_e^2$ is kinematically forbidden.

A.5.2 Axial current

Now it is left to calculate the axial part. The part that is proportional to g_A . For simplicity, we drop the factor of $-g_A e^2 \frac{4G_F}{\sqrt{2}}$:

$$M_\mu^{\text{Axial}} = \bar{u}(p_3) \gamma^\rho \int_w \frac{(\psi + \not{p}_3 + m_e) \gamma_\mu \gamma^5 (\psi - \not{p}_4 + m_e)}{[w^2 - \lambda^2 + i\epsilon][(w + p_3)^2 - m_e^2 + i\epsilon][(w - p_4)^2 - m_e^2 + i\epsilon]} \gamma_\rho v(p_4) . \quad (\text{A.57})$$

The calculation is the same as for the vector part and we get the final result:

$$M_{\text{Axial,R}}^\mu = (F_1 - F_2) \bar{u}(p_3) \gamma^\mu \gamma^5 v(p_4) + \underbrace{4m_e(C_1 - C_{11} + C_{12})}_{F_P} \bar{u}(p_3) (p_3^\mu + p_4^\mu) \gamma^5 v(p_4) , \quad (\text{A.58})$$

where F_P is the pseudo scalar form factor, but this is not relevant for our calculation, because in the part of this form factor we would have a trace with less than three γ -matrices and a γ^5 which then just drops out. We can therefore for this work only use the $(F_1 - F_2) \bar{u}(p_3) \gamma^\mu \gamma^5 v(p_4)$ part.

Appendix B

Further Details

B.1 Use of AI tools

AI-Tool	Used for	Why	Where
ChatGPT	\LaTeX , C-code	\LaTeX: Grammar and spell checking, translation C-code: Troubleshooting of shorter code snippets	In the \LaTeX -document of this thesis In the code for the numerical evaluation
Writefull	\LaTeX	Grammar and spell checking	In the \LaTeX -document of this thesis
Overleaf error assist	\LaTeX	Errors in the \LaTeX code	In the \LaTeX -document of this thesis

B.2 Useful integrals

The following integrals have been numerically checked.

X-integrals

$$\begin{aligned}
 \int_0^1 dx \frac{1}{x^2 P^2 - x P^2 + m_e^2} &= 2 \frac{\beta}{|P^2|} \operatorname{arctanh} \left(\frac{2\beta}{\beta^2 + 1} \right) = X_0^{P^2 < 0} \\
 \int_0^1 dx \frac{1}{x^2 (4m_e^2 - P^2) - x (4m_e^2 - P^2) + m_e^2} &= \frac{\beta}{|P^2|} \operatorname{arctanh} \left(\frac{1}{\beta} \right) = X_0^{P^2 > 0} \\
 \int_0^1 dx \frac{x}{x^2 P^2 - x P^2 + m_e^2} &= \frac{\beta}{|P^2|} \operatorname{arctanh} \left(\frac{2\beta}{\beta^2 + 1} \right) = X_1^{P^2 < 0} \\
 \int_0^1 dx \frac{x}{x^2 (4m_e^2 - P^2) - x (4m_e^2 - P^2) + m_e^2} &= 2 \frac{\beta}{|P^2|} \operatorname{arctanh} \left(\frac{1}{\beta} \right) = X_1^{P^2 > 0} \\
 \int_0^1 dx \frac{x^2}{x^2 P^2 - x P^2 + m_e^2} &= \frac{-\beta (P^2 - 2m_e^2) \operatorname{arctanh} \left(\frac{2\beta}{\beta^2 + 1} \right) + P^2}{P^4} = X_2^{P^2 < 0} \\
 \int_0^1 dx \frac{x^2}{x^2 (4m_e^2 - P^2) - x (4m_e^2 - P^2) + m_e^2} &= \frac{2 \frac{1}{\beta} (P^2 - 2m_e^2) \operatorname{arctanh} \left(\frac{1}{\beta} \right) + 4m_e^2 - P^2}{(P^2 - 4m_e^2)^2} = X_2^{P^2 < 0}
 \end{aligned}$$

Cos-integrals

$$\begin{aligned}
 \int_{-1}^1 d \cos \theta \frac{1}{(\pm Q_0 - \mathbf{Q} \cos \theta)^2} &= \frac{2}{Q^2} = G_0 \\
 \int_{-1}^1 d \cos \theta \frac{\cos \theta}{(\pm Q_0 - Q \cos \theta)^2} &= \pm \frac{2 \left(\frac{\mathbf{Q} Q_0}{Q^2} - \operatorname{arctanh} \left(\frac{Q}{Q_0} \right) \right)}{Q^2} = \pm G_1 \\
 \int_{-1}^1 d \cos(\theta) \frac{\cos^2 \theta}{(\pm Q_0 - \mathbf{Q} \cos(\theta))^2} &= \frac{2 \left(\frac{\mathbf{Q}(Q^2 + Q_0^2)}{Q^2} - 2Q_0 \operatorname{arctanh} \left(\frac{Q}{Q_0} \right) \right)}{Q^3} = G_2
 \end{aligned}$$

w-integrals

$$\begin{aligned}
 \int_{\Delta E}^{\infty} d\mathbf{w} f_B(\mathbf{w}) &= \Delta E - T \ln \left(e^{\frac{\Delta E}{T}} - 1 \right) = T_0 \\
 \int_{\Delta E}^{\infty} d\mathbf{w} f_B(\mathbf{w}) \mathbf{w} &= T \left(T \operatorname{Li}_2 \left(e^{-\frac{\Delta E}{T}} \right) - \Delta E \log \left(1 - e^{-\frac{\Delta E}{T}} \right) \right) = T_1
 \end{aligned}$$

B.3 KMS relation

The Kubo–Martin–Schwinger relation is a very useful relation for thermal field theory that originates from the cyclic property of the trace. For a general thermal correlation function of

two operators $\hat{\mathcal{O}}_1$ and $\hat{\mathcal{O}}_2$, with an equilibrium density matrix, the following can be shown [33]:

$$\begin{aligned}
 \langle \hat{\mathcal{O}}_1(t) \hat{\mathcal{O}}_2(t') \rangle_\beta &= \frac{\text{Tr} \left[\hat{\rho}(\beta) \hat{\mathcal{O}}_1(t) \hat{\mathcal{O}}_2(t') \right]}{Z(\beta)} \\
 &= \frac{\text{Tr} \left[\exp(-\beta \hat{H}) \hat{\mathcal{O}}_1(t) \exp(\beta \hat{H}) \exp(-\beta \hat{H}) \hat{\mathcal{O}}_2(t') \right]}{Z(\beta)} \\
 &= \frac{\text{Tr} \left[\hat{\mathcal{O}}_1(t + i\beta) \exp(-\beta \hat{H}) \hat{\mathcal{O}}_2(t') \right]}{Z(\beta)} \\
 &= \frac{\text{Tr} \left[\hat{\rho}(\beta) \hat{\mathcal{O}}_2(t') \hat{\mathcal{O}}_1(t + i\beta) \right]}{Z(\beta)} \\
 &= \langle \hat{\mathcal{O}}_2(t') \hat{\mathcal{O}}_1(t + i\beta) \rangle_\beta .
 \end{aligned} \tag{B.1}$$

B.4 Lagrangian in Fermi theory

The calculation of the weak interaction rate is only important around the decoupling temperature $t_d \approx 1.3$ MeV, which is much smaller than the masses of the W^\pm and Z^0 bosons, which are bigger than 80 GeV. Therefore, it is possible to integrate out the W^\pm and Z^0 propagators, then we get the following effective terms [17, 37]:

$$\mathcal{L}_Z = \frac{i4G_F}{\sqrt{2}} [\bar{\psi}_{\nu_\alpha} \gamma^\mu P_L \psi_{\nu_\alpha}] [\bar{\psi}_e \gamma_\mu (P_L g'_L + P_R g_R)] \tag{B.2}$$

$$\mathcal{L}_W = \frac{i4G_F}{\sqrt{2}} \delta^{\alpha e} [\bar{\psi}_{\nu_\alpha} \gamma^\mu P_L \psi_e] [\bar{\psi}_e \gamma_\mu P_L \psi_{\nu_\alpha}] . \tag{B.3}$$

Here $G_F = \frac{\sqrt{2}g^2}{8m_W^2}$ is the Fermi constant. In addition P_L and P_R are right- or left-handed projectors, respectively, with their prefactors $g'_L = -\frac{1}{2} + \sin^2 \theta_W$ and $g_R = \sin^2 \theta_W$. The Fierz identity [53] can then be used

$$[\bar{\psi}_1 \gamma^\mu P_L \psi_2] [\bar{\psi}_3 \gamma_\mu P_L \psi_4] = [\bar{\psi}_1 \gamma^\mu P_L \psi_4] [\bar{\psi}_3 \gamma_\mu P_L \psi_2] \tag{B.4}$$

to fuse the two terms. We define $g_L^\alpha = g'_L + \delta^{\alpha e}$, which now depends on the species.

$$\mathcal{L}_{4GF} = \frac{i4G_F}{\sqrt{2}} [\bar{\psi}_{\nu_\alpha} \gamma_\mu P_L \psi_{\nu_\alpha}] [\bar{\psi}_e \gamma_\mu (P_L g_L^\alpha + P_R g_R) \psi_e] \tag{B.5}$$

This is now written in left- and right-handed couplings. Sometimes, it is also insightful to use vector and axial couplings $g_{V,A}^\alpha = \frac{1}{2}(g_L^\alpha \pm g_R)$.

B.5 Finite temperature self-energy of the photon and resummed photon propagator

The finite temperature self-energy of the photon at one-loop order reads

$$\Pi_{ab}^{\mu\nu} = (P) = (-1)^{a+b} i e^2 \int \frac{d^4 w}{(2\pi)^4} \text{Tr} \left[i S_e^{ab}(w) \gamma^\mu i S_e^{ba}(k-P) \gamma^\nu \right]. \quad (\text{B.6})$$

We first note that we can connect the contributions with different CTP-indices. It holds for the diagonal components that $(\Pi_{22}^{\mu\nu})^* = -\Pi_{11}^{\mu\nu}$ and further we can use the KMS-relation for the off-diagonal components to find $\Pi_{21}^{\mu\nu} = \exp(\frac{P_0}{T}) \Pi_{12}^{\mu\nu}$. So we note that we only have to calculate $\Pi_{11}^{\mu\nu}$ and $\Pi_{12}^{\mu\nu}$. The diagonal part can be split into a vacuum and a thermal part. The vacuum part reads

$$\Pi_{\text{vac}}^{\mu\nu} = i e^2 \int_w \frac{i}{k^2 - m_e^2 + i\epsilon} \frac{i}{(k+P)^2 - m_e^2 + i\epsilon} \text{Tr} \left[(\not{k} + m_e) \gamma^\mu (\not{k} + \not{P} + m_e) \gamma^\nu \right]. \quad (\text{B.7})$$

The calculation is well known, and in $\overline{\text{MS}}$ -scheme the result is written

$$\begin{aligned} \Pi_{\text{vac}}^{\mu\nu} = \frac{\alpha_{\text{em}}}{\pi} (P^2 \eta^{\mu\nu} - P^\mu P^\nu) & \left[\frac{2}{3} \ln \left(\frac{\mu}{m_e} \right) + \frac{5}{9} + \frac{4m_e^2}{3P^2} \right. \\ & \left. + \frac{1}{3} \left(1 + \frac{\tau}{2} \right) \sqrt{1 - \frac{4m_e^2}{P^2}} \ln \left(\frac{\sqrt{1 - \frac{4m_e^2}{P^2}} - 1}{\sqrt{1 - \frac{4m_e^2}{P^2}} + 1} \right) \right]. \end{aligned} \quad (\text{B.8})$$

To calculate the thermal parts, we split the self-energy into a longitudinal and a transversal part

$$\Pi_{ab}^{\mu\nu} = \Pi_{ab}^L P_L^{\mu\nu} + \Pi_{ab}^T P_T^{\mu\nu}, \quad (\text{B.9})$$

where the projectors for the longitudinal and transverse part are defined as

$$P_T^{00} = P_T^{0i} = P_T^{i0} = 0 \quad (\text{B.10})$$

$$P_T^{ij} = -\delta^{ij} + \hat{P}^i \hat{P}^j \quad (\text{B.11})$$

$$P_L^{\mu\nu} = g^{\mu\nu} - \frac{P^\mu P^\nu}{P^2}. \quad (\text{B.12})$$

We can then use the thermal integrals

$$K^\mu(P) = 2g^2 \int \frac{d^4 k}{(2\pi)^3} k^\mu \frac{\delta(k^2 - m^2) f_D(|k^0|)}{(P+k)^2 - m^2 + i\epsilon} \quad (\text{B.13})$$

$$K^{\mu\nu}(P) = 2g^2 \int \frac{d^4 k}{(2\pi)^3} k^\mu k^\nu \frac{\delta(k^2 - m^2) f_D(|k^0|)}{(P+k)^2 - m^2 + i\epsilon}. \quad (\text{B.14})$$

These were evaluated in [13]. For the vector integral, we get the following results

$$K^0 = \frac{g^2}{8\pi^2\mathbf{P}} \int_m^\infty dk_0 k_0 l_2(k_0, P) f_D(k_0) \quad (\text{B.15})$$

$$K^i = P^i \frac{g^2}{(4\pi)^2\mathbf{P}^3} \int_m^\infty dk_0 [P^2 l_1(k_0, P) + 2k_0 P_0 l_2(k_0, P) - 8\mathbf{k}\mathbf{P}] f_D(k_0) . \quad (\text{B.16})$$

Here we have defined

$$l_1(k_0, P) = \ln \left| \frac{(P^2 + 2\mathbf{k}\mathbf{P})^2 - 4P_0^2 k_0^2}{(P^2 - 2\mathbf{k}\mathbf{P})^2 - 4P_0^2 k_0^2} \right| \quad (\text{B.17})$$

$$l_2(k_0, P) = \ln \left| \frac{P^4 - 4(P_0 k_0 + \mathbf{P}\mathbf{k})^2}{P^4 - 4(P_0 k_0 - \mathbf{P}\mathbf{k})^2} \right| . \quad (\text{B.18})$$

Where the energy of k is just $k_0 = \sqrt{\mathbf{k}^2 + m^2}$, this is due to the delta-distribution $\delta(k^2 - m^2)$ which forces k to be on-shell. The tensor integral is calculated to give

$$K^{00} = \frac{g^2}{8\pi^2\mathbf{P}} \int_m^\infty dk_0 k_0^2 l_1(k_0, P) f_D(k_0) \quad (\text{B.19})$$

$$K^{0i} = \frac{g^2 P^i}{(4\pi)^2\mathbf{P}} \int_m^\infty dk_0 k_0 [2P_0 k_0 l_1(k_0, P) + P^2 l_2(k_0, P)] f_D(k_0) \quad (\text{B.20})$$

$$K^{ij} = I_1 \frac{P^i P^j}{\mathbf{P}^2} + \left(\delta^{ij} - \frac{P^i P^j}{\mathbf{P}^2} \right) \left(\frac{I_2 - I_1}{2} \right) . \quad (\text{B.21})$$

with the two function I_1 and I_2

$$I_1 = \frac{g^2}{2(2\pi)^2\mathbf{P}^3} \int_m^\infty dk_0 [(P^4 + 4P_0^2 + k_0^2) l_1(k_0, P) + 4P^2 P_0 k_0 l_2(k_0, P) - 8\mathbf{P}\mathbf{k}P^2] f_D(k_0) \quad (\text{B.22})$$

$$I_2 = \frac{g^2}{(4\pi)^2\mathbf{P}} \int_m^\infty dk_0 \mathbf{k}^2 l_1(k_0, P) f_D(k_0) \quad (\text{B.23})$$

The diagonal part can then be written, by using the thermal integrals

$$\text{Re}\Pi_{11, T \neq 0}^{\mu\nu} = 4(-\eta^{\mu\nu} (K \cdot P) + 2K^{\mu\nu} + K^\mu P^\nu + K^\nu P^\mu) . \quad (\text{B.24})$$

Inserting the thermal integrals and splitting the self-energy into a longitudinal and a transversal part we get the result:

$$\text{Re}\Pi_{11, T \neq 0}^L = \frac{\alpha_{\text{em}} P^2}{\pi\mathbf{P}^3} \int_{m_e}^\infty dk_0 [8\mathbf{k}\mathbf{P} - l_1(k_0, P)(P^2 + 4k_0^2) - 4l_2(k_0, P)P_0 k_0] f_D(k_0) \quad (\text{B.25})$$

$$\begin{aligned} \text{Re}\Pi_{11, T \neq 0}^T = & \frac{\alpha_{\text{em}}}{\pi\mathbf{P}^3} \int_{m_e}^\infty dk_0 \left[2l_2(k_0, P)P_0 P^2 k_0 - 4\mathbf{k}\mathbf{P}(P_0^2 + \mathbf{P}^2) \right. \\ & \left. + l_1(k_0, P) \left(\mathbf{P}^2 P^2 + 2P_0^2 k_0^2 - 2\mathbf{k}^2 \mathbf{P}^2 + \frac{1}{2} P^4 \right) \right] \quad (\text{B.26}) \end{aligned}$$

For the purely imaginary off-diagonal component we get the following result:

$$\begin{aligned} \text{Re}\Pi_{12,T\neq 0}^L &= -i\frac{2\alpha_{\text{em}}}{\mathbf{P}} \int_{m_e}^{\infty} dk_0 \sum_{\pm} \left[\theta \left(1 - \left| \frac{P^2 \pm 2k_0 P_0}{2\mathbf{kP}} \right| \right) (f_D(k_0) - \theta(\pm k_0)) \right. \\ &\quad \left. \cdot (f_D(|\pm k_0 + P_0|)) - \theta(\mp k_0 - P_0) \right] \times \left(\frac{P^2}{2} - \frac{P^2}{2\mathbf{P}^2} (P_0 \pm 2k_0)^2 \right) \end{aligned} \quad (\text{B.27})$$

$$\begin{aligned} \text{Re}\Pi_{12,T\neq 0}^L &= -i\frac{2\alpha_{\text{em}}}{\mathbf{P}} \int_{m_e}^{\infty} dk_0 \sum_{\pm} \left[\theta \left(1 - \left| \frac{P^2 \pm 2k_0 P_0}{2\mathbf{kP}} \right| \right) (f_D(k_0) - \theta(\pm k_0)) \right. \\ &\quad \left. \cdot (f_D(|\pm k_0 + P_0|)) - \theta(\mp k_0 - P_0) \right] \times \left(\frac{P^2}{2} - \mathbf{k}^2 \left(1 - \left(\frac{P^2 \pm 2k_0 P_0}{2\mathbf{kP}} \right)^2 \right) \right) \end{aligned} \quad (\text{B.28})$$

With these self-energys one can calculate the retarded and advanced self-energy by using

$$\Pi_{R/A}^{T/L} = \Pi_{11}^{T/L} + \Pi_{12/21}^{T/L} = \text{Re}\Pi_{11}^{T/L} \pm \frac{1}{2} \left(\Pi_{12}^{T/L} - \Pi_{21}^{T/L} \right) . \quad (\text{B.29})$$

The resummed photon propagator can be calculated by solving the Dyson-Schwinger equation (3.42) which can be written in terms of retarded and advanced self-energys as

$$\bar{D}_{\mu\nu}^{R/A} = D_{\mu\nu}^{R/A} + D_{\mu\alpha}^{R/A} (\Pi^{\alpha\beta})^{R/A} \bar{D}_{\beta\nu}^{R/A} . \quad (\text{B.30})$$

Solving this yields the resummed photon propagator at one loop level

$$\bar{D}_{11}^{L/T} = \frac{\Omega_{L,T}}{\Omega_{L,T}^2 + \Gamma_{L,T}^2} - i[1 - 2f_B(|P_0|)]\text{sgn}(P_0) \frac{\Gamma_{L,T}}{\Omega_{L,T}^2 + \Gamma_{L,T}^2} \quad (\text{B.31})$$

$$\text{with } \Omega_{L,T} = P^2 + \text{Re}\Pi_R^{L/T} , \quad \Gamma_{L,T} = \text{Im}\Pi_R^{L/T} \quad (\text{B.32})$$

Note that the photon essentially gets a thermal mass, which can act as a regulator for infrared divergences.

The calculation of this section was first and in more detail done in [13].

B.6 Connection of rates with different CPT indices

The rate of the Baseball diagram is the sum over the thermal indices and can be written as follows:

$$\begin{aligned}
 \Gamma_{\text{Baseball}} &= (-1)^{a+b+c+d+1} (ie)^2 \left(\frac{i4G_F}{\sqrt{2}} \right)^2 \\
 &\times \int_{l,q,w} \underbrace{\text{Tr} \left[\not{p} \gamma^\rho P_L iS_{\nu_\alpha}^{12}(l) \gamma^\sigma P_L \right]}_{\text{Tr}_\nu} iD_{\mu\nu}^{cd}(w) \\
 &\times \underbrace{\text{Tr} \left[iS_e^{d2}(u+w) \gamma_\mu iS_e^{1d}(u) \gamma_\sigma (P_L g_L + P_R g_R) iS_e^{c1}(q) \gamma_\nu iS_e^{2c}(q+w) \gamma_\rho (P_L g_L + P_R g_R) \right]}_{\text{Tr}_{\text{QED}}}
 \end{aligned} \tag{B.33}$$

It is now possible to find a relation between the 11/12 and 22/21 elements. We start by investigating Tr_ν^* .

$$\begin{aligned}
 (\text{Tr}_{\nu, \sigma\rho})^* &= \text{Tr} \left[P_L^\dagger (\gamma^\sigma)^\dagger (iS_{\nu_\alpha}^{12}(l))^\dagger P_L^\dagger (\gamma^\rho)^\dagger \not{p}^\dagger \right] \\
 &\quad \text{[Inserting } \gamma^0 \text{]} \\
 &= \text{Tr} \left[P_R \gamma^\sigma (iS_{\nu_\alpha}^{12}(l)) P_R \gamma^\rho \not{p} \right] \\
 &= \text{Tr} \left[\not{p} \gamma^\sigma P_L (iS_{\nu_\alpha}^{12}(l)) \gamma^\rho P_L \right] \\
 &= \text{Tr}_{\nu, \rho\sigma}
 \end{aligned}$$

We can see that taking the complex conjugate of $\text{Tr}_{\nu, \sigma\rho}$ is the same as exchanging the Lorenz indices. We are now going to do the same calculation for Tr_{QED} , but here we have to specify the indices c and d . We first start with the $c = d = 1$ part.

$$\begin{aligned}
 & (\text{Tr}_{\text{QED}, \sigma\rho}^{11})^* (iD_{\mu\nu}^{11}(w))^* \\
 &= \text{Tr} \left[iS_e^{12}(u+w) \gamma_\mu iS_e^{11}(u) \gamma_\sigma (P_{LGL} + P_{RGR}) iS_e^{11}(q) \gamma_\nu iS_e^{21}(q+w) \gamma_\rho (P_{LGL} + P_{RGR}) \right]^* \\
 & \quad \times (iD_{\mu\nu}^{11}(w))^* \\
 &= \text{Tr} \left[(P_{LGL} + P_{RGR})^\dagger \gamma_\rho^\dagger (iS_e^{21}(q+w))^\dagger \gamma_\nu^\dagger (iS_e^{11}(q))^\dagger (P_{LGL} + P_{RGR})^\dagger \gamma_\sigma^\dagger \right. \\
 & \quad \left. \times (iS_e^{11}(u))^\dagger \gamma_\mu^\dagger (iS_e^{12}(u+w))^\dagger \right] D_{\mu\nu}^{22}(w) \\
 & \quad \text{|Insert } \gamma_0 \text{ use } \gamma_0 \gamma_\mu^\dagger \gamma_0 = \gamma_\mu, \gamma_0 (iS_e^{11}(p))^\dagger \gamma_0 = (iS_e^{22}(p)), \gamma_0 (iS_e^{12}(p))^\dagger \gamma_0 = (iS_e^{12}(p)) \\
 &= \text{Tr} \left[(P_{LGL} + P_{RGR}) \gamma_0 \gamma_\rho iS_e^{21}(q+w) \gamma_\nu iS_e^{22}(q) \gamma_0 (P_{LGL} + P_{RGR}) \gamma_0 \gamma_\sigma \right. \\
 & \quad \left. \times iS_e^{22}(u) \gamma_\mu iS_e^{12}(u+w) \gamma_0 \right] iD_{\mu\nu}^{22}(w) \\
 &= \text{Tr} \left[\gamma_\rho (P_{LGL} + P_{RGR}) iS_e^{21}(q+w) \gamma_\nu iS_e^{22}(q) \gamma_\sigma (P_{LGL} + P_{RGR}) iS_e^{22}(u) \gamma_\mu iS_e^{12}(u+w) \right] iD_{\mu\nu}^{22}(w) \\
 &= \text{Tr} \left[iS_e^{22}(u) \gamma_\mu iS_e^{12}(u+w) \gamma_\rho (P_{LGL} + P_{RGR}) iS_e^{21}(q+w) \gamma_\nu iS_e^{22}(q) \gamma_\sigma (P_{LGL} + P_{RGR}) \right] iD_{\mu\nu}^{22}(w) \\
 & \quad \text{|Substitute } q+w \rightarrow q, w \rightarrow -w \\
 &= \text{Tr} \left[iS_e^{22}(u+w) \gamma_\mu iS_e^{12}(u) \gamma_\rho (P_{LGL} + P_{RGR}) iS_e^{21}(q) \gamma_\nu iS_e^{22}(q+w) \gamma_\sigma (P_{LGL} + P_{RGR}) \right] iD_{\mu\nu}^{22}(-w) \\
 &= \text{Tr} \left[iS_e^{22}(u+w) \gamma_\mu iS_e^{12}(u) \gamma_\rho (P_{LGL} + P_{RGR}) iS_e^{21}(q) \gamma_\nu iS_e^{22}(q+w) \gamma_\sigma (P_{LGL} + P_{RGR}) \right] iD_{\mu\nu}^{22}(w) \\
 &= \text{Tr}_{\text{QED}, \rho\sigma}^{22} iD_{\mu\nu}^{22}(w) \tag{B.34}
 \end{aligned}$$

Note that we got the same change in $\sigma\rho$ as we got for Tr_ν . Now performing the same calculation for the 12 part we will see the same connection the the 21 part.

$$\begin{aligned}
 & (\text{Tr}_{\text{QED}, \sigma\rho}^{12})^* (iD_{\mu\nu}^{12}(w))^* \\
 &= \text{Tr} \left[iS_e^{22}(u+w) \gamma_\mu iS_e^{12}(u) \gamma_\sigma (P_{LGL} + P_{RGR}) iS_e^{11}(q) \gamma_\nu iS_e^{21}(q+w) \gamma_\rho (P_{LGL} + P_{RGR}) \right]^* \\
 & \quad \times (iD_{\mu\nu}^{12}(w))^* \\
 &= \text{Tr} \left[(P_{LGL} + P_{RGR})^\dagger \gamma_\rho^\dagger (iS_e^{21}(q+w))^\dagger \gamma_\nu^\dagger (iS_e^{11}(q))^\dagger (P_{LGL} + P_{RGR})^\dagger \gamma_\sigma^\dagger (iS_e^{12}(u))^\dagger \gamma_\mu^\dagger \right. \\
 & \quad \left. \times (iS_e^{22}(u+w))^\dagger \right] D_{\mu\nu}^{12}(w) \\
 & \quad \text{|Insert } \gamma_0 \text{ use } \gamma_0 \gamma_\mu^\dagger \gamma_0 = \gamma_\mu, \gamma_0 (iS_e^{11}(p))^\dagger \gamma_0 = (iS_e^{22}(p)), \gamma_0 (iS_e^{12}(p))^\dagger \gamma_0 = (iS_e^{12}(p)) \\
 &= \text{Tr} \left[\gamma_\rho (P_{LGL} + P_{RGR}) iS_e^{21}(q+w) \gamma_\nu iS_e^{22}(q) \gamma_\sigma (P_{LGL} + P_{RGR}) iS_e^{12}(u) \gamma_\mu iS_e^{11}(u+w) \right] D_{\mu\nu}^{12}(w) \\
 &= \text{Tr} \left[iS_e^{12}(u) \gamma_\mu iS_e^{11}(u+w) \gamma_\rho (P_{LGL} + P_{RGR}) iS_e^{21}(q+w) \gamma_\nu iS_e^{22}(q) \gamma_\sigma (P_{LGL} + P_{RGR}) \right] D_{\mu\nu}^{12}(w) \\
 & \quad \text{|Substitute } q+w \rightarrow q, w \rightarrow -w \\
 &= \text{Tr} \left[iS_e^{12}(u+w) \gamma_\mu iS_e^{11}(u) \gamma_\rho (P_{LGL} + P_{RGR}) iS_e^{21}(q) \gamma_\nu iS_e^{22}(q+w) \gamma_\sigma (P_{LGL} + P_{RGR}) \right] D_{\mu\nu}^{12}(w) \\
 &= \text{Tr}_{\text{QED}, \rho\sigma}^{21} iD_{\mu\nu}^{21}(w) \tag{B.35}
 \end{aligned}$$

Therefore it holds that:

$$\Gamma = 2\text{Re}(\Gamma^{22} + \Gamma^{21}) . \tag{B.36}$$

Bibliography

- [1] N. Schöneberg, *The 2024 BBN baryon abundance update*, *JCAP* **06** (2024) 006 [2401.15054].
- [2] G. Mangano and P.D. Serpico, *A robust upper limit on N_{eff} from BBN, circa 2011*, *Phys. Lett. B* **701** (2011) 296 [1103.1261].
- [3] V. Barger, J.P. Kneller, H.-S. Lee, D. Marfatia and G. Steigman, *Effective number of neutrinos and baryon asymmetry from BBN and WMAP*, *Phys. Lett. B* **566** (2003) 8 [hep-ph/0305075].
- [4] Z. Hou, R. Keisler, L. Knox, M. Millea and C. Reichardt, *How Massless Neutrinos Affect the Cosmic Microwave Background Damping Tail*, *Phys. Rev. D* **87** (2013) 083008 [1104.2333].
- [5] M. Escudero, *Neutrino decoupling beyond the Standard Model: CMB constraints on the Dark Matter mass with a fast and precise N_{eff} evaluation*, *JCAP* **02** (2019) 007 [1812.05605].
- [6] TOPICAL CONVENERS: K.N. ABAZAJIAN, J.E. CARLSTROM, A.T. LEE collaboration, *Neutrino Physics from the Cosmic Microwave Background and Large Scale Structure*, *Astropart. Phys.* **63** (2015) 66 [1309.5383].
- [7] R. Barbieri and A. Dolgov, *Neutrino oscillations in the early universe*, *Nucl. Phys. B* **349** (1991) 743.
- [8] A.M. Abdullahi et al., *The present and future status of heavy neutral leptons*, *J. Phys. G* **50** (2023) 020501 [2203.08039].
- [9] F. D’Eramo, F. Hajkarim and S. Yun, *Thermal QCD Axions across Thresholds*, *JHEP* **10** (2021) 224 [2108.05371].
- [10] S. Gariazzo, P. de Salas and S. Pastor, *Thermalisation of sterile neutrinos in the early universe in the 3+1 scheme with full mixing matrix*, *Journal of Cosmology and Astroparticle Physics* **2019** (2019) 014–014.

-
- [11] J.J. Bennett, G. Buldgen, M. Drewes and Y.Y.Y. Wong, *Towards a precision calculation of the effective number of neutrinos N_{eff} in the Standard Model I: the QED equation of state*, *JCAP* **03** (2020) 003 [1911.04504].
- [12] J.J. Bennett, G. Buldgen, P.F. De Salas, M. Drewes, S. Gariazzo, S. Pastor et al., *Towards a precision calculation of N_{eff} in the Standard Model II: Neutrino decoupling in the presence of flavour oscillations and finite-temperature QED*, *JCAP* **04** (2021) 073 [2012.02726].
- [13] M. Drewes, Y. Georis, M. Klasen, L.P. Wiggering and Y.Y.Y. Wong, *Towards a precision calculation of N_{eff} in the Standard Model. Part III. Improved estimate of NLO contributions to the collision integral*, *JCAP* **06** (2024) 032 [2402.18481].
- [14] T. Binder, M. Drewes, Y. Georis, M. Klasen, G. Pierobon and Y.Y.Y. Wong, *Towards a precision calculation of N_{eff} in the Standard Model IV: Impact of positronium formation*, 2411.14091.
- [15] PLANCK collaboration, *Planck 2018 results. VI. Cosmological parameters*, *Astron. Astrophys.* **641** (2020) A6 [1807.06209].
- [16] M. Cielo, M. Escudero, G. Mangano and O. Pisanti, *N_{eff} in the Standard Model at NLO is 3.043*, *Phys. Rev. D* **108** (2023) L121301 [2306.05460].
- [17] L.P. Wiggering, *Precise Theoretical Predictions for the Dark Matter Relic Density and Neutrino Dynamics in the Early Universe*, Ph.D. thesis, Munster U., 2024.
- [18] G. Jackson and M. Laine, *QED corrections to the thermal neutrino interaction rate*, *JHEP* **05** (2024) 089 [2312.07015].
- [19] G. Jackson and M. Laine, *$\nu\nu$ production, annihilation, and scattering at MeV temperatures and NLO accuracy*, *JCAP* **05** (2025) 054 [2412.03958].
- [20] S. Esposito, G. Mangano, G. Miele, I. Picardi and O. Pisanti, *Neutrino energy loss rate in a stellar plasma*, *Nucl. Phys. B* **658** (2003) 217 [astro-ph/0301438].
- [21] J.R. Bade, *Dark matter freeze-in from non-equilibrium quantum field theory: Treatment of real intermediate states*, .
- [22] J. Lesgourgues, G. Mangano, G. Miele and S. Pastor, *Neutrino Cosmology*, Cambridge University Press (2, 2013).
- [23] G. Mangano, G. Miele, S. Pastor and M. Peloso, *A Precision calculation of the effective number of cosmological neutrinos*, *Phys. Lett. B* **534** (2002) 8 [astro-ph/0111408].
- [24] V. Mukhanov, *Physical Foundations of Cosmology*, Cambridge University Press, Oxford (2005), 10.1017/CBO9780511790553.

-
- [25] D. Baumann, *Cosmology*, Cambridge University Press (7, 2022), 10.1017/9781108937092.
- [26] S. Weinberg, *Cosmology*, Oxford University Press (2008).
- [27] T. Matsubara, *A New approach to quantum statistical mechanics*, *Prog. Theor. Phys.* **14** (1955) 351.
- [28] M. Chala and G. Guedes, *The High-Temperature Limit of the SM(EFT)*, 2503.20016.
- [29] L.V. Keldysh, *Diagram technique for nonequilibrium processes*, *Zh. Eksp. Teor. Fiz.* **47** (1964) 1515.
- [30] J. Schwinger, *Brownian motion of a quantum oscillator*, *Journal of Mathematical Physics* **2** (1961) 407 [https://pubs.aip.org/aip/jmp/article-pdf/2/3/407/19046507/407_1_online.pdf].
- [31] M.L. Bellac, *Thermal Field Theory*, Cambridge Monographs on Mathematical Physics, Cambridge University Press (3, 2011), 10.1017/CBO9780511721700.
- [32] A.K. Das, *Field theory: A Path integral approach*, vol. 52 (1993).
- [33] A.K. Das, *Finite Temperature Field Theory*, World Scientific, New York (1997).
- [34] J.I. Kapusta and C. Gale, *Finite-temperature field theory: Principles and applications*, Cambridge Monographs on Mathematical Physics, Cambridge University Press (2011), 10.1017/CBO9780511535130.
- [35] M.G. Mustafa, *An introduction to thermal field theory and some of its application*, *Eur. Phys. J. ST* **232** (2023) 1369 [2207.00534].
- [36] M.E. Peskin and D.V. Schroeder, *An Introduction to quantum field theory*, Addison-Wesley, Reading, USA (1995), 10.1201/9780429503559.
- [37] M.D. Schwartz, *Quantum Field Theory and the Standard Model*, Cambridge University Press (2013).
- [38] N. Landsman and C. van Weert, *Real- and imaginary-time field theory at finite temperature and density*, *Physics Reports* **145** (1987) 141.
- [39] H. Groenewold, *On the principles of elementary quantum mechanics*, *Physica* **12** (1946) 405.
- [40] T. Kinoshita, *Mass singularities of Feynman amplitudes*, *J. Math. Phys.* **3** (1962) 650.
- [41] H.A. Weldon, *Cancellation of infrared divergences in thermal QED*, *Nucl. Phys. A* **566** (1994) 581C [hep-ph/9308249].

-
- [42] T. Altherr and T. Grandou, *Thermal field theory and infinite statistics*, *Nucl. Phys. B* **402** (1993) 195 [[hep-th/9206065](#)].
- [43] R. Barbieri, J.A. Mignaco and E. Remiddi, *Electron form-factors up to fourth order. 1.*, *Nuovo Cim. A* **11** (1972) 824.
- [44] O. Tomalak and R.J. Hill, *Theory of elastic neutrino-electron scattering*, *Physical Review D* **101** (2020) .
- [45] T. Hahn, *Loop calculations with FeynArts, FormCalc, and LoopTools*, *Acta Phys. Polon. B* **30** (1999) 3469 [[hep-ph/9910227](#)].
- [46] T. Hahn, *CUBA: A Library for multidimensional numerical integration*, *Comput. Phys. Commun.* **168** (2005) 78 [[hep-ph/0404043](#)].
- [47] PARTICLE DATA GROUP collaboration, *Review of particle physics*, *Phys. Rev. D* **110** (2024) 030001.
- [48] R.P. Feynman, *Space - time approach to quantum electrodynamics*, *Phys. Rev.* **76** (1949) 769.
- [49] G. 't Hooft and M.J.G. Veltman, *Regularization and Renormalization of Gauge Fields*, *Nucl. Phys. B* **44** (1972) 189.
- [50] H. B elusca-Ma ito, A. Ilakovac, M. Mador-Bo zinovi c and D. St ockinger, *Dimensional regularization and Breitenlohner-Maison/'t Hooft-Veltman scheme for γ_5 applied to chiral YM theories: full one-loop counterterm and RGE structure*, *JHEP* **08** (2020) 024 [[2004.14398](#)].
- [51] G. Passarino and M.J.G. Veltman, *One Loop Corrections for $e^+ e^-$ Annihilation Into $\mu^+ \mu^-$ in the Weinberg Model*, *Nucl. Phys. B* **160** (1979) 151.
- [52] K. Kovařík, *Hitchhiker's guide to Renormalization*, private notes.
- [53] P.B. Pal, *Representation-independent manipulations with Dirac spinors*, [physics/0703214](#).

Acknowledgments

First, I would like to thank Michael Klasen for his guidance on physics-related questions and for his support on the summer schools that i attended. I am also grateful to him for the opportunity to work on my master's thesis topic, which allowed me to collaborate with Yvonne Wong, Marco Drewes, Yannis Georis, Yuan-Zhen Li, and Luca Wiggering. I would like to thank all of you for the enjoyable conversations both about physics and beyond. A special thanks goes to Prof. Wong for kindly serving as my second examiner. Furthermore, I would like to give thanks to Yannis Georis and Yuan-Zhen Li for verifying some of the analytical results.

To Luca Wiggering, Jan Ravi Bade, Jannis Brirup, and Noah Mozgovykh: thank you for reading parts of my thesis and helping me polish it. I'm also incredibly lucky to have shared an office with Tim Huesmann, Jan Ravi Bade, Jannis Brirup, Daniel Woitaschek, and Luca Wiggering—you made every day at the office enjoyable.

Last but not least, I would like to thank Luca Wiggering for his mentorship throughout my thesis. Honestly, I'm not sure there's enough Coca-Cola Zero in the world to thank you properly.

Declaration of Academic Integrity

Declaration of Academic Integrity I hereby confirm that this thesis, entitled **precision calculation of the effective number of neutrino species**, is solely my own work and that I have used no sources or aids other than the ones stated. All passages in my thesis for which other sources, including electronic media, have been used, be it direct quotes or content references, have been acknowledged as such and the sources cited. I am aware that plagiarism is considered an act of deception which can result in sanction in accordance with the examination regulations. I confirm that I am aware that my work may be cross-checked with other texts to identify possible similarities and that it may be stored in a database for this purpose. I confirm that I have not submitted the following thesis in part or whole as an examination paper before.

Münster, 20. July 2025